Biogas valorization for chemical industries via catalytic process

Aqeel Ahmad Taimoor

▶ To cite this version:

Aqeel Ahmad Taimoor. Biogas valorization for chemical industries via catalytic process. Food and Nutrition. Université Claude Bernard - Lyon I, 2010. English. NNT : 2010LYO10243 . tel-00881030

HAL Id: tel-00881030
https://theses.hal.science/tel-00881030

Submitted on 7 Nov 2013

N° d'ordre 243-2010   Année 2010

THESE DE L'UNIVERSITE DE LYON

Délivrée par

L'UNIVERSITE CLAUDE BERNARD LYON 1

ECOLE DOCTORALE

DIPLOME DE DOCTORAT

(arrêté du 7 août 2006)

soutenue publiquement le (15 Novembre 2010)

par

M. TAIMOOR Aqeel Ahmad

<u>TITRE</u> : Biogas Valorization for Chemical Industries via Catalytic process

JURY :

Mme EPRON COGNET Florence	: Rapporteur
M PAUL Sébastien	: Rapporteur
M KADDOURI Abdel Hakim	
M TRABLY Eric	
M MEUNIER Frédéric	
Mme MEILLE Valérie	
Mme PITAULT Isabelle	

UNIVERSITE CLAUDE BERNARD - LYON 1

Président de l'Université   **M. le Professeur L. Collet**

Vice-président du Conseil Scientifique   M. le Professeur J-F. Mornex

Vice-président du Conseil d'Administration   M. le Professeur G. Annat

Vice-président du Conseil des Etudes et de la Vie Universitaire   M. le Professeur D. Simon

Secrétaire Général   M. G. Gay

COMPOSANTES SANTE

Faculté de Médecine Lyon Est – Claude Bernard   Directeur : M. le Professeur J. Etienne

Faculté de Médecine et de Maïeutique Lyon Sud – Charles Directeur : M. le Professeur F-N. Gilly
Mérieux

UFR d'Odontologie   Directeur : M. le Professeur D. Bourgeois

Institut des Sciences Pharmaceutiques et Biologiques   Directeur : M. le Professeur F. Locher

Institut des Sciences et Techniques de la Réadaptation   Directeur : M. le Professeur Y. Matillon

Département de formation et Centre de Recherche en Biologie Directeur : M. le Professeur P. Farge
Humaine

COMPOSANTES ET DEPARTEMENTS DE SCIENCES ET TECHNOLOGIE

Faculté des Sciences et Technologies   Directeur : M. le Professeur F. Gieres
Département Biologie   Directeur : M. le Professeur F. Fleury
Département Chimie Biochimie   Directeur : Mme le Professeur H. Parrot
Département GEP   Directeur : M. N. Siauve
Département Informatique   Directeur : M. le Professeur S. Akkouche
Département Mathématiques   Directeur : M. le Professeur A. Goldman
Département Mécanique   Directeur : M. le Professeur H. Ben Hadid
Département Physique   Directeur : Mme S. Fleck
Département Sciences de la Terre   Directeur : Mme le Professeur I. Daniel
UFR Sciences et Techniques des Activités Physiques et Sportives Directeur : M. C. Collignon
Observatoire de Lyon   Directeur : M. B. Guiderdoni
Ecole Polytechnique Universitaire de Lyon 1   Directeur : M. P. Fournier
Institut Universitaire de Technologie de Lyon 1   Directeur : M. le Professeur C. Coulet
Institut de Science Financière et d'Assurances   Directeur : M. le Professeur J-C. Augros
Institut Universitaire de Formation des Maîtres   Directeur : M. R. Bernard

This thesis is dedicated to those who understand the vastness of love.

He who does not thank men can not thank God.

Muhammad

ACKNOWLEDGEMENT

Contents

List of Figures

List of Tables

Investigation after declaration of submission leads astray.

Wasif Ali Wasif

1
INTRODUCTION

By the end of this century, share of hydrogen as an energy source is predicted or wished to be 50 % of the total joules required by world because of several advantages [1]. Primarily due to 141.9 MJ/kg of energy liberated by hydrogen complete oxidation, which is far higher than methane giving 55.5 MJ/kg. Moreover hydrogen burns to water, thus having no negative effect on the environment because of the green house gases emission, only if its enough production does not lead to any pollutants.

The hydrogen potential production from various resources is shown in Figure 1.1. Except for hydrolysis (electrical or thermal), all other methods do not produce pure hydrogen (usually accompanying CO_2 but sometimes also NO_x and SO_x) and require imperative purifying processes. Choice among these methods in near future demands environmental and energy aspects evaluations.

A number of investigations have been or are being conducted to utilise hydrogen either as an energy source (fuel cells and hydrogen fired combined cycles) or an intermediate reactant for high valued products (fertilizers, crude oil hydro-alkylation, hydro-desulphurisation and hydro-cracking and reducing ores). Currently industrial hydrogen production is realised through various processes as i) steam reforming and thermal cracking of methane, ii) partial oxidation of heavier hydrocarbons and iii) coal gasification.

All of them use non-renewable fossil fuels as feedstocks and are not pollutant free. Thus, their continuation does not result in de-carbonization of the energy sources. Global warming concerns, on the other hand, cannot tolerate this to continue. A historical trend for carbon dioxide emission is shown in Figure 1.2. If half of the fuel burned is replaced by renewable hydrogen energy source by 2100 then it will only kill the sharp slope of CO_2 production statistics and absolutely no green house gas reduction occurs. Moreover these processes are not actually conceived for hydrogen production as an energy source, rather they are applied for the high value products manufacturing or potential refining. Furthermore they eliminate the basic hydrogen environmentally friendly feature of no carbon dioxide emission. Also scarcity of the feed stocks used in the above mentioned processes does not provide future security. This necessitates the exploration of clean fuel free from green house gasses. Hydrogen is immaculate in this regard but renewable clean ways of its enough production should be formulated to full fill subsequent needs.
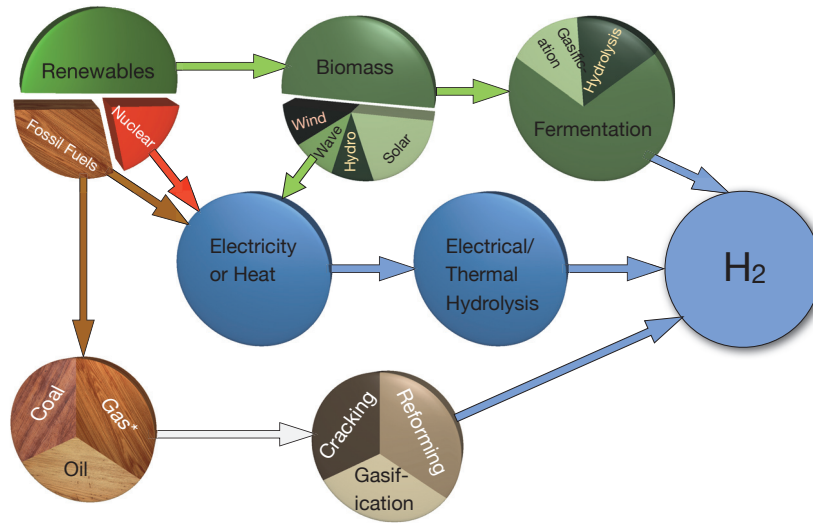
Figure 1.1: Potential hydrogen production by various sources [2]
*Hydrogen may exist as natural gas component naturally

As hydrogen production from the fossil fuels is not a sustainable option and nuclear source has its own disadvantages, so renewable energy sources are prime future entities to be valorized. Generally the production of hydrogen by renewable resources is categorized as i) water electrolysis, ii) thermo-chemical, iii) radiolytic and iv) biological processes

Electricity is an efficient form of energy and is required for water electrolysis. Clean renewable ways of producing electricity are currently widely investigated. However this is mainly done to either replace thermal and nuclear power plants or at least shift the balance in favour of renewables. Apart from expensive water treatment, clean water scarcity for many nations around the globe is another aspect hindering vast application of water electrolysis. Similarly thermo-chemical and radiolytic processes do have their own implications and they are not essentially pollutant free. Perspective of hydrogen production from very low value wastes by biological processes is vastly studied to valorize its potential with energy crops, agriculture and various other wastes as feed stocks [4]. Energy crops are widely criticised because of food scarcity. On the other hand whether other wastes and forests are in sufficient quantities to meet Terra Joules required by the world or can their hydrogen potential balance the equation of providing reduction environment for industrial usage?

Thermal gasification of biomass results in high value products and is studied to realise biorefineries [5]. However huge amount of energy required for their valorization in this manner may have very small positive or even negative impact on overall energy balance. Therefore natural ways of biomass treatment are being explored.

Nature does have its own way of handling the wastes, for this purpose a life chain exists. The waste having low energy not enough to support complex life structure of higher organisms is decomposed by the lower ones. This process is termed as biodegradation. The workhorses for biodegradation are mostly the single cell organisms mainly bacteria. If
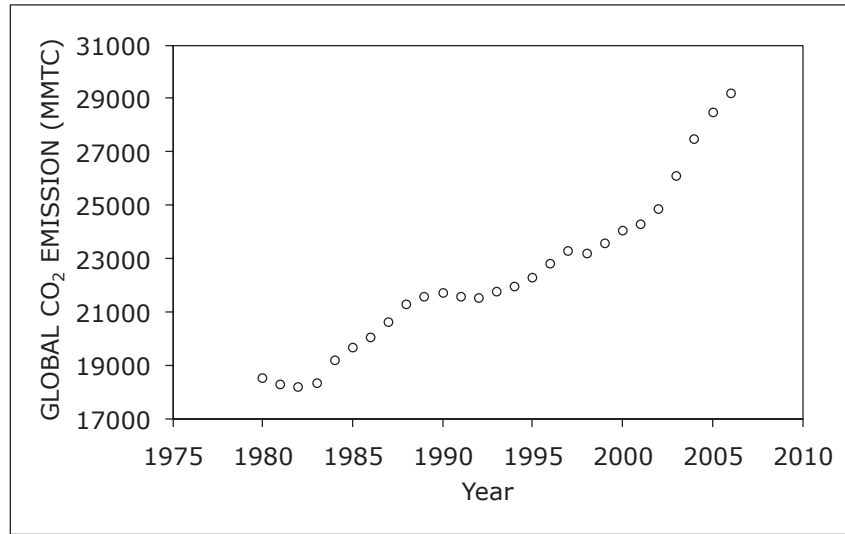
Figure 1.2: Carbon dioxide emission trend, data by courtesy of Energy Information Administration [3]

degradation/fermentation is conducted under special conditions maintained in a bioreactor, the resulting compounds may be of our interest.

Fermentation is known to man since ancient times and bacteria often *Lactobacillus* in combination with yeasts and moulds, have been used for thousands of years in the preparation of fermented foods such as cheese, pickles, soy sauce, sauerkraut, vinegar, wine, beer and yoghurt.

A comparatively new method of controlled dark-fermentation may produce hydrogen as bio-gas component (in some cases up to 74 %[1]), expending less energy compared to gasification, while the carbon dioxide produced is part of natural life cycle so, virtually 0 % pollution add up. This is elucidated in Figure 1.3. Digester or fermentor may produce biogas containing H_2/CO_2 rather CH_4/CO_2 if conditions are well monitored.

The biogas (H_2 or CH_4) produced from digester or fermenter poses a couple of disadvantages:

1. If this gas is used to run combined cycle then biogas dilution with carbon dioxide lowers overall process efficiency.

2. The biogas contains various waste or poisonous gases such as H_2S and NH_3. So, if burnt as such it will produce NO_x and SO_x pollutants in flue gas.

In wake of above pre-processing of the biogas is required. However, the overall benefits become inadequate (huge capital investments), if the process is not designed intelligently. Hydrogen, although having high heating value, cannot be compressed or liquefied without huge energy consumption for general purpose use thus having large volume; requiring high

---

[1]depends upon the type of waste treated and conditions.
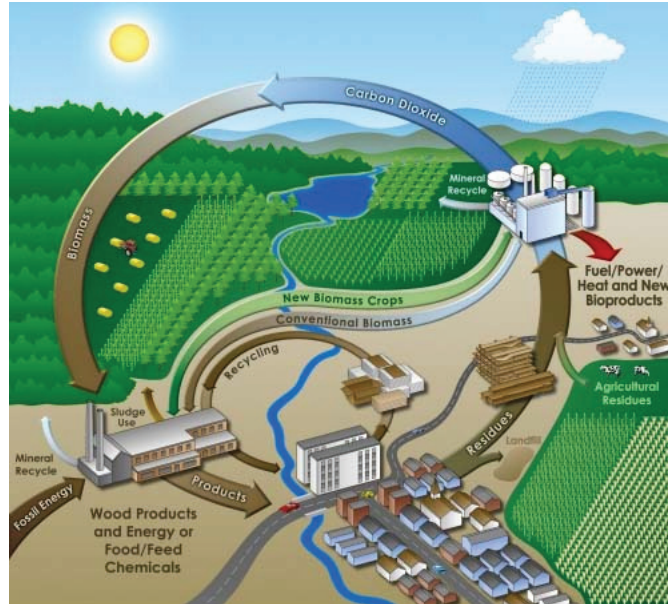
Figure 1.3: Biomass Life cycle [6]

energy for transportation and is of limited interest for mobile users tanks. Also burning of biogas rich in hydrogen to lowest form of energy i.e. heat will probably be the last option for its exploitation as production of methane rather hydrogen from biomass may serve this purpose well. Therefore how to valorize this hydrogen (energy or high value product manufacturing), how much energy is used in the process, how much of this can be captured with thermodynamic limitations in place, what are the advantages gained other than simple burning and overall environmental benefits of the green process? or should we abandon this way? are the main areas studied. Thus the objective of this thesis is

> *'The coupling of a catalytic reactor with fermenter to use raw or partially pre-*
> *processed biogas (H_2/CO_2 mix) to valorize its potential with minimum energy*
> *requirements by either producing/processing high value products or appropriate*
> *storage for mobile energy usage in an environmental friendly manner'*

For sake of better unfolding of our research this dissertation is structured in four parts. First the bio-processes potential to produce hydrogen is discussed according to the available literature review. It includes various fermentation processes along their key conditions, detailed evaluation of dark fermentation and bio-reactors constraints. A comparison of present/classical biogas usage is also discussed.

Next part relate to the possibility of using biogas (H_2/CO_2) in a chemical reaction instead of pure hydrogen via catalytic hydrogenation. For this purpose aromatic hydrogenation with toluene is taken as test reaction molecule. Based on a detailed literature

survey of toluene hydrogenation, effect of CO_2 on hydrogenation is experimentally investigated. Experiments are done over various catalysts with and with no CO_2 and mechanisms are detailed.

The second reaction i.e. carboxylic acids (low value abundant reactant) hydrogenation to high value product is subsequently discussed. Similarly literature review and mechanistic details already published are given. Our findings come subsequently with detailed analysis.

The final chapter includes the combination of the literature review and our findings to develop a workable process of valorization. Process is devised with an overall energy feasibility analysis and is optimised.

The ground's generosity takes in our compost and grows beauty. Be like the ground!

Rumi

2

BIO GAS PRODUCTION

Before I evaluated the use of H_2/CO_2 mixture for catalytic hydrogenation, I have showed the capacity of a digester to produce hydrogen in terms of flow rate and biogas composition. In this area, literature being wide , I focused my review only on H_2 production.

2.1 MICROBIAL METABOLISMS

Metabolism of various anaerobes, aerobes, cyanobacteria, photosynthetic bacteria and algae can produce hydrogen while working under certain conditions [7]. In contrast to higher organisms, bacteria exhibit an extremely wide variety of metabolism types. Bacterial metabolism is classified on the basis of three major criteria:

1. kind of energy used for growth

2. source of carbon

3. electron donor used for bacterial growth

An additional criterion of respiratory micro organisms are the electron acceptors used thus, differentiating between aerobic and anaerobic respiration.

Carbon metabolism in bacteria is either heterotrophic, where organic carbon compounds are used as carbon sources, or autotrophic, meaning that cellular carbon is obtained by fixing carbon dioxide. In general chemotrophic bacteria use chemical substances for energy, which are mostly oxidised at the expense of oxygen or alternative electron acceptors (aerobic/anaerobic respiration).

These bacteria are further divided into lithotrophs that use inorganic electron donors and organotrophs that use organic compounds as electron donors. Chemotrophic organisms use the respective electron donors for energy conservation and biosynthetic reactions (e.g. carbon dioxide fixation). Respiratory organisms use chemical compounds as a source of energy by taking electrons from the reduced substrate and transferring them to a terminal electron acceptor in a redox reaction. This reaction releases energy that can be used to synthesise adenosine triphosphate (ATP) and drive metabolism. In aerobic organisms,

oxygen is used as the electron acceptor. In anaerobic organisms, other inorganic compounds such as nitrate, sulfate or carbon dioxide are used as electron acceptors.

2.2 BIO-PERSECTIVE FOR H_2

According to the main objective a brief classification of various biological processes producing hydrogen is given by Das and Veziroğlu [7] :

1. Biophotolysis of Water.

2. Photosynthetic bacterial decomposition

3. Fermentative decomposition

4. Hybrid processes.

2.2.1 BIOPHOTOLYSIS OF WATER

There are two ways for water Bio-Photolysis: direct and indirect.

Direct water Bio-Photolysis is its decomposition via photo-enzymatic reaction, simply shown by equation (2.1)

$$2H_2O \xrightarrow{Light\ Energy} 2H_2 + O_2 \tag{2.1}$$

Incubation of micro-green eukaryote in anaerobic conditions with temperature usually below $30\,^\circ$C induces an enzyme *hydrogenase* capable of realizing this reaction [8] which is absent in higher green plants so they only reduce CO_2 [9]. However, even traces of oxygen will inhibit hydrogen production. So this reaction is divided in two phases to separate the production of oxygen and hydrogen [10].

Indirect biophotolysis works on the principle of photosynthesis. The process includes the reduction of CO_2 and splitting of water to produce H_2 and O_2 as described by following equations:(2.2)&(2.3)

$$6H_2O + 6CO_2 \xrightarrow{Light\ Energy} Glucose \tag{2.2}$$

$$C_6H_{12}O_6 + 6H_2O \xrightarrow{Light\ Energy} 12H_2 + 6CO_2 \tag{2.3}$$
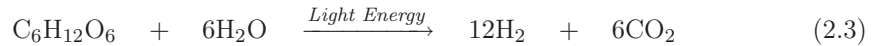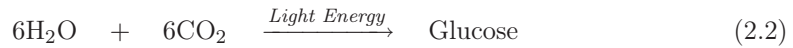
There are three important types of enzymes present in cyanobacterium (hydrogen producers via photolysis) that effectuate hydrogen production:

1. nitrogenase $\Rightarrow$ This enzyme produces hydrogen as a by-product in nitrogen reduction to ammonia.

2. uptake hydrogenase $\Rightarrow$ This enzyme oxidises hydrogen produced by nitrogenase.

3. bi-directional hydrogenase $\Rightarrow$ It is able to both produce and consume hydrogen.

The hydrogen production rate and yield from biophotolysis is lowest but the conversion efficiency is the highest among H_2 processes, thus is not very significant.

2.2.2 PHOTOSYNTHETIC BACTERIAL/LIGHT FERMENTATION

Photosynthetic bacteria contain all the chemical formulation to catalyse following reaction (2.4) thus providing hydrogen at the expense of solar energy and an electron donor.

$$(CH_2O)_2 \underset{ATP}{\longrightarrow} Ferredoxin \underset{ATP}{\longrightarrow} Nitrogenase \rightarrow H_2 \qquad (2.4)$$
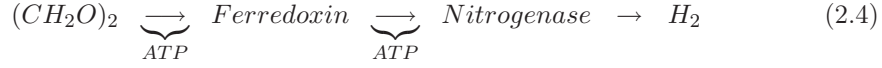
In fact they only produce hydrogen by equation (2.3) contrary to indirect photolysis of water. However a consumable nitrogen supply is required for the activity of nitrogenase enzyme embedded in these kind of bacteria and the choice of an effective source is particularly important in order to get maximum hydrogen yield from biomass [11]. The activity of nitrogenase can also be inhibited by the nitrogen source quantity [12]. Molecular nitrogen inhibits the hydrogen production thus, cannot be used [13]. This type of metabolism requires absolute anaerobic conditions and any ingress of oxygen will destroy the nitrogenase enzyme thus, prohibiting hydrogen production.

Presence of hydrogenase enzyme for photosynthetic fermentation is not necessary. A simplified diagram (Figure 2.1) for understanding the metabolic pathway is provided by Koku et al. [13].
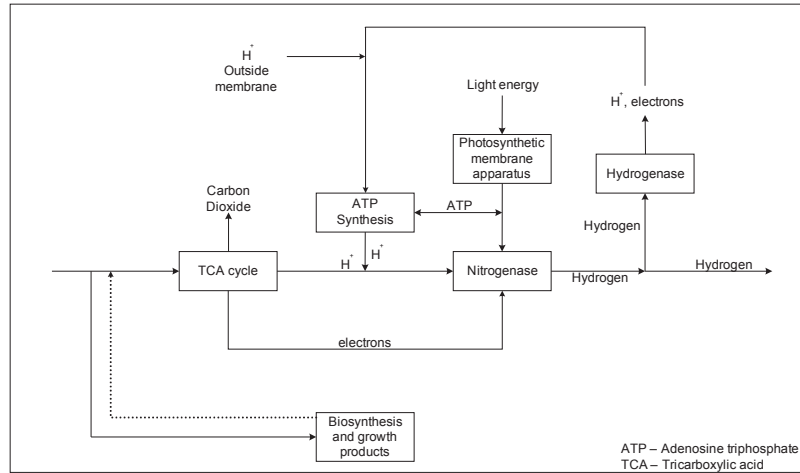
Figure 2.1: Overall scheme of hydrogen production by *Rhodobactor Sphaeroides* [13]

Rate of hydrogen producing metabolism increases with the intensity of light and after reaching maximum stabilizes [11, 14, 15]. This is in fact the key factor to design the bioreactor used for such kind of hydrogen generation as dense culture growth hinders light penetration. Furthermore usually each type of bacteria works on specific band of light wavelengths (infra-red) [16].

Carbon dioxide is usually the only co-product found along with hydrogen, so theoretically and practically photosynthetic bacteria give high hydrogen yield defined as $\frac{\text{moles of hydrogen produced}}{\text{theoretical moles of hydrogen can be produced}} \times 100$. Generally various factors influence hydrogen production including hydraulic retention time for the reactor and substrate type, its pre-

treatment, its carbon to nitrogen ratio and potential metabolic pathways. Activity of some photosynthetic bacteria for hydrogen production is shown in Table 2.1

Microbe Type	Biomass used	Hydrogen yield% [a]	Nitrogen source	Ref	Remarks
Rhodobacter capsulatus	Lactate	49.2	Na-glutamate	[14]	
	DL malate	77	Ethanol amine	[11]	3.5mM Ethanol amine
	DL malate	77	L-glutamate	[11]	7mM L-glutamate
	D-glucose	70	L-glutamate	[11]	7mM L-glutamate
	D-xylose	73	L-glutamate	[11]	7mM L-glutamate
	Acetate 56.6% Propionate 20.4% Butyrate 23%	55.5	$(NH_4)_2SO_4$	[17]	
Purple Non-sulphur[b]	Sugar	13.5	NH_3	[12]	
Rhodopseud-monas SP	Acetate	72.8	Na-glutamate	[18]	
Rhodopseud-monas Plastrus	Butyrate	48	Na-glutamate	[19]	
R.sphaeroides & C.butyricum	Glucose	0.6 $\frac{ml}{ml-medium}$	Glutamate	[20]	

[a]Depends on various conditions like temperature and light penetration etc.
[b]CSTR (continuous process), for else it is batch reactor

Table 2.1: Comparison of various Bio-Photosynthetic Bacterial activity

2.2.3 BIOMASS FERMENTATION

Chemotrophic process in the absence of possible electron acceptors like oxygen is termed as fermentation, where electrons taken from the reduced substrates are transferred to oxidise intermediates to generate reduced fermentation products (e. g. lactate, ethanol, hydrogen, butyrate). Fermentation is possible because the energy content of the substrates is higher than that of the products, which allows the organisms to synthesise adenosine triphosphate (ATP - energy packet molecule for organisms releasing energy at cell level) and drive their metabolism.

Bacteria, often Lactobacillus although not producing H_2 in combination with yeasts and molds, have been used for thousands of years in the preparation of fermented food but hydrogen production from fermentation has been studied recently.

Production of hydrogen is theoretically represented by equations: (2.5) and (2.6) where the glucose is transformed into acids or acetates, while the detailed metabolic pathway is represented by Figure 2.2.

$$C_6H_{12}O_6 \quad + \quad 2H_2O \quad \longrightarrow \quad 2CH_3COOH \quad + \quad 2CO_2 \quad + \quad 4H_2 \quad \quad (2.5)$$

$$C_6H_{12}O_6 \quad \longrightarrow \quad CH_3CH_2CH_2COOH \quad + \quad 2CO_2 \quad + \quad 2H_2 \quad \quad (2.6)$$
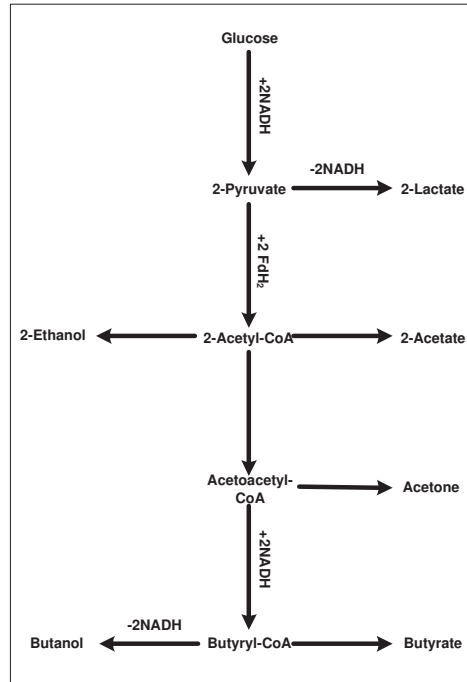
Figure 2.2: General schematic of Biomass degradation Pathway [21]

Butyrates and acetates are usually found the most abundant Volatile Fatty Acids (VFAs) present after fermentation [22, 28]. However there exists two different metabolic path ways for the production of two, by bacteria in dark fermentation. This makes the final pH of

Acidogen Type	Reactor Type	Biomass used	H_2 Yield or Production (H_2 molar % / Time h)	Non-gaseous Products (relative mole %)	Ref
Clostridium	Batch	Glucose	16 $\frac{ml}{g\ VSS.h}$ (80 ml / 72)	HPr, HBu, HVa, HAc (9.1, 79.2, 0, 11.7)	[22]
	Batch	Sucrose	5.4 $\frac{ml}{g\ VSS.h}$	HAc, HPr, HBu (31.4, 9.6, 63.1)	[23]
Clostridium butyricum W5	Batch	Glucose	7.61 $\frac{mmol}{l.h}$	HLa, HAc, HBu (92, 3.9, 4.1)	[24]
Clostridium acetobutylicum	Batch	Glucose	2 $\frac{molH_2}{mol_{Glucose}}$	HAc, HBu	[21]
Clostridium acetobutylicum ATCC 824	Trickle Bed	Glucose	220 $\frac{ml}{h.l}$ (80 / 40)	HAc, HBu (70.6, 29.4)	[25]
Clostridium thermolacticum	Continuous	Lactose	2.58 $\frac{mmol}{l.h}$ (85.7 / 0.19)	HAc, HLa, Ethanol	[26]
Clostridium thermocellum	Continuous	α-Cellulose	6.54 $\frac{ml}{g\ VSS.h}$ (43.6 /24)	HAc, HLa, HFa Ethanol (69.8, 5.2, 10.3, 14.7)	[27]
Mixed Culture	CSTR	Glucose	212 $\frac{ml}{g\ VSS.h}$ (60 / 6)	HBu, HAc, HPr, Lactate, Caproate, Ethanol (40.5, 36.9, 3.6, 5.8, 0.6, 12.6)	[28]
Thermoanaero-bacteriaceae	Batch	Starch	15.21 $\frac{ml}{g\ VSS.h}$	HAc, HBu, HPr Ethanol, Methanol (46.3, 35.6, 1.1, 7.9, 2.1)	[29]
Enterobacter aero genes	Continuous	Molasses	3.5 $\frac{mol}{mol\ sugar}$	HLa, HBu, HAc	[30]
Cladanaerobacter subterraneus	Batch	Glucose	172.9 $\frac{ml}{g\ VSS.h}$	HAc, HLa, Ethanol Alanine (72.5, 2, 6.4, 19.1)	[31]

Table 2.2: Comparison of various Dark-Fermentative Bacterial activity

waste water acidic after fermentation i.e. 4 - 4.6 [29]. During fermentation pH is usually controlled by converting these acids into salts (acetates). Almost all of the organic loading can be converted to VFAs [32]. Generally the exponential growth of the microbes favours hydrogen production but shifts in favour of VFAs at latter stages. Carbohydrates are reported as the most efficient hydrogen producing substrates than protein and fat rich biomass [33, 34].

Rate of hydrogen production is highest by dark fermentation. A comparison of various hydrogen cultures, production rates and VFAs produced is provided in Table 2.2 This comparison is not complete mainly due to the lack of data in respective articles.

2.2.4 "COUPLED" PROCESSES

Combination of above processes photo and dark fermentation to maximize the hydrogen yield falls under this category. e.g. photolysis of water and photosynthetic bacterial fermentation cannot work during night (when sunlight is considered as an energy source) as they require light for their inbuilt processes of fermentation to work. However they can degrade the left over low molecular weight organic acids (dark fermentation), thus maximizing the hydrogen yield [12, 19, 35]. Such a combination will also help in cutting down the light requirement of photosynthetic bacteria working on raw biomass. However the Volatile Fatty Acids (VFAs) are not completely degraded by bacteria and the conversion efficiency decreases with increase in molecular weight of these acids [36].

Argun et al. [37] have studied this process and concluded that a ratio of 1 to 7 for biomass treated by Dark and Photo fermentation is optimum. This may adjust the microbe culture ratio between acidogens and photosynthetic bacteria to maximum hydrogen production rate. This modus operandi may result in more hydrogen production per hour than each of the individual processes.

The effluents of dark fermentation are comprised of fatty acids so, the final pH will be on lower side usually ≈ 4 (generally pH regulated at 5.5 - 6). However the second stage of hybrid process i.e. photosynthetic fermentation stops to produce below 6.5 [20]. Therefore, pH adjustment between the two is required.

Theoretically all of the biomass should convert into hydrogen and carbon dioxide by photo fermentation [18] but experimental studies show that some methane is also produced during the run.

Microbial electrolysis cell (MEC) is another technique to enhance hydrogen production. External voltage is provided through electrodes to ease the transfer of electrons for microbes metabolism. Lu et al. [38] have concluded that only 1.12 kWh electrical energy is required to yield 1 m^3 of hydrogen in a hybrid process combining dark fermentation with MEC, which is far less than the power required for water electrolysis (5.6 kWh$\cdot$m^{-3}). However the biological life in the cell is highly sensitive to pH. Control of voltage is also required as higher than optimum will result in methane production.

Other processes include the production of methane in second stage. This is the most rapid process available for biomass fermentation. A schematic of various hybrid processes is shown in Figure 2.3.

The coupling of two processes may be achieved by combining various bacteria cultures (dark and Photo Fermentation) in same fermenter [39]. However the ratio of two cultures should be adjusted as carboxylic acids form dark cultures may produce at faster rate compared to their consumption by Photo bacteria culture. On the other hand this feature may further be exploited to design an energy feasible down stream process.
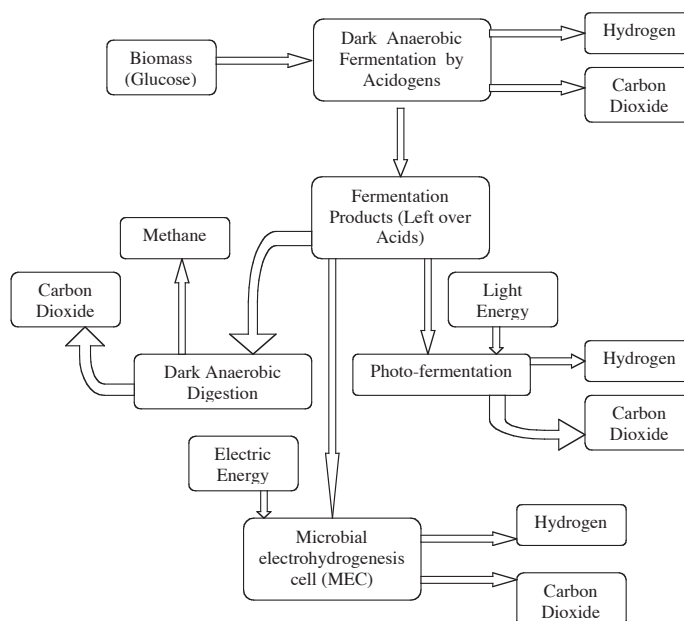
Figure 2.3: Hybrid processes

It is evident from the literature survey that biomass has great potential for hydrogen and is environmentally friendly. Photofermentation if not supported by external light source other than sun, has an inbuilt gas supply surge depending upon light intensity. Batch dark fermentation processes are also of very limited use in this regard. Continuous bioreactors although sustain the non stop production but at the cost of low overall yield. An intelligent combination of dark continuous process with left overs treatment via photo fermentation and MEC cells may serve the process needs well for aromatic hydrogenation. For carboxylic acids as feed stock, only dark fermentation is envisaged.

2.3 BIOREACTORS FOR BIOMASS FERMENTATION

According to IUPAC, bio-reactor may refer to any device or system that supports a biologically active environment. However bioreactor processes need more stringent control than simple chemical reactors. Certain conditions like pretreatment, pH, temperature and microbe type etc. should be adjusted to produce desired product.

2.3.1 BIOMASS or SEED SLUDGE PRE-TREATMENT

The treatment of either biomass or seed sludge will serve the basic cause of enhancing hydrogen yield by suppressing the bio-activity of methanogens (methane producing bacteria). This is usually done for dark fermentation processes.

Different processes reported in literature for pre-treatment of microbes or substrates are listed below:

1. pH treatment

2. Heat shock treatment

3. Freezing and thawing

4. Aeration

5. Chloroform treatment

6. Treatment with 2-bromoethanesulonate/2-bromoethanesulfonic acid

7. Iodopropane treatment

Production of hydrogen from waste water poses a serious challenge as it contains various types of microbes and if not pre-treated, can promote hydrogen consuming bacteria [40]. The heat treatment of the biomass to truncate the growth of non-hydrogen producing bacteria, is most widely studied to enhance hydrogen production [41]. Argun et al. [42] has concluded it as the most efficient. However it is not always the effective one [43]. Treatment by heating and thawing require lot of energy thus making bio-hydrogen producing processes energetically infeasible.

There is a lack of consensus between the researchers over the best pre-treatment method but treatment by heat shock is widely used (80%). A hybrid pH control technique for both inoculum and main reacting mass is proposed by Chen et al. [22]. This feature is also exploited by Ferchichi et al. [60] by adjusting initial pH of the Biomass. A radical analysis of the various techniques employed is tabulated as in Table 2.3. It is very difficult to conclude the best method for our process and my competence in this area is fairly limited.

2.3.2 FERMENTERS OPERATING CONDITIONS

An intelligently chosen set of operating conditions will result in high hydrogen production by squashing hydrogen consuming microbes mainly methanogens [22, 61]. These conditions change with type of substrate being processed [23]. Wang and Wan [62] provide a review of various kinetic models to describe the effect of different conditions affecting fermentation. Such models may provide an insight over hydrogen production mechanism.

Fermentative processes are generally affected by following factors:

1. pH

2. Hydraulic retention time

3. Temperature

4. Carbon to nitrogen ratio of substrates (photosynthetic fermentation)

5. Substrate concentration

6. Microbe type

7. Substrate specification and inflow rate

Pretreatment type	Seed	Pretreatment methods	Substrate	Max Hydrogen yield $\frac{molH_2}{molsub}$	Ref
Thermal	Digested sludge	Boiled at 100 °C for 15min	Glucose	1.78	[43]
	Anaerobic sludge	Baked at 104 °C for 2h	Glucose	0.968	[44]
	Anaerobic sludge	Heated in Boiling water for 30min	Glucose	1.1	[45]
	Anaerobic sludge	Boiled fro 15min	Rice	134 $\frac{ml}{g-VS}$	[33]
	Soil	Dried at 104 °C for 2h	Glucose	0.92	[46]
	Soil	Dried at 105 °C for 2h	Glucose	1.8	[47]
	Cow dung compost	Baked at $100-105$ °C for 2h	Sucrose	2.24	[48]
	Digested sludge	Boiled for 20min	Sucrose	3.18	[49]
	Anaerobic sludge	Heated at 102 °C for 90min	Sucrose	4.0	[50]
	Soil	Dried at 104 °C for 2h	Sucrose	1.8	[46]
	Cracked cereals	Baked for 2h and then boiled for 30min	Sucrose	2.73	[51]
	Activated sludge	Heated at 100 °C for 45min	Sucrose	3.43	[52]
	Activated sludge	Heated at 100 °C for 45min	Sucrose	0.0015	[53]
	Activated sludge	Heated at 100 °C for 45min	Sucrose	4.8	[54]
	Activated sludge	Heated at 100 °C for 45min	Sucrose	1.84	[55]
Acid or base	Digested sludge	Pretreated at pH 3 for 24h	Glucose	0.80	[43]
	Sewage sludge	Pretreated at pH 3 for 24h	Glucose	1.0	[22]
	Activated sludge	Pretreated at pH 3-4 for 24h	Sucrose	2.8	[56]
	Anaerobic sludge	Pretreated at pH 3 for 24h	Glucose	0.72	[45]
	Digested sludge	Pretreated at pH 3 for 30min	Sucrose	3.1	[49]
	Anaerobic sludge	Pretreated at pH 3-4 for 24h	Sucrose	2.6	[50]
	Digested sludge	Pretreated at pH 10 for 24h	Glucose	1.09	[43]
	Sewage sludge	Pretreated at pH 10 for 24h	Glucose	0.58	[22]
	Digested sludge	Pretreated at pH 10 for 30min	Sucrose	6.12	[49]
	Anaerobic sludge	Pretreated at pH 12 for 24h	Sucrose	0.96	[50]
	Activated sludge	Pretreated at pH for 24h	Sucrose	4.5	[57]
Chloroform	Digested sludge	Pretreated by 2% chloroform	Glucose	0.69	[43]
	Anaerobic sludge	Pretreated by 0.1% chloroform	Glucose	1.17	[45]
	Anaerobic sludge	Pretreated by chloroform	Glucose	0.005	[58]
Aeration	Digested sludge	Aerated with air for 24h	Glucose	0.86	[43]
	Sludge compost	Pretreated under aerobic condition for 3 days	Glucose	2.1	[59]
	Digested sludge	Flushed with air for 30min	Sucrose	4.84	[49]
Halogens	Digested sludge	Pretreated for 30min by 2-bromoethanesulfonic acid	Sucrose	5.28	[49]
	Digested sludge	Pretreated for 30min by iodopropane	Sucrose	5.64	[49]

Table 2.3: Various studies conducted on Pretreatment methods

8. Hydrogen partial pressure

9. Oxidation and reduction potential of substrate

10. Reactor configuration (design)

For photosynthetic bacterial fermentation, pH is usually kept between 6.4-6.9 and below 6.4 production of hydrogen stops [11,14,15]. However fermentative type of bio-hydrogen production prevails at much lower pH [32,61,63]. In fact pH greatly influences the metabolism of the microbes, so its control is crucial for producing desired product.

Hydraulic Retention Time (HRT), defined as $\frac{\text{Bioreactor volume}}{\text{In flow rate}}$, is another important factor for hydrogen production rate. The gaseous as well as leftover bio-mass product by dark fermentation can be adjusted through this parameter. Low retention time leads in higher hydrogen production rate but low yield or vice versa. Hydraulic retention time should not be confused with the total time spent by microbial growth and fermentation. Furthermore optimum microbial growth in reactor is crucial for its stable process and high hydrogen production rate.

Temperature control of the bio-reactor is vital for an effective hydrogen production. This depends upon the type of microbe being used. High temperature usually supports hydrogen production. It is reported that hydrogen producing bacteria prefer high temperature than Methanogens. Zhang et al. [29,64] have given a comparison between $37\,°C$ and $55\,°C$ and concluded latter as a better option. Levin et al. [10,65] define the temperature ranges based upon biological culture as:

1. Mesophilic ($25\,°C$ - $40\,°C$)

2. Thermophilic ($40\,°C$ - $65\,°C$)

3. Extreme thermophilic ($65\,°C$ - $80\,°C$)

4. Hyper thermophilic ($> 80\,°C$)

However logically the minimum temperature of the reactor suits overall thermal efficiency of the process and a slight miss management can shift the balance and diminishes the industrial interest. On the other hand if it is possible to find enough waste heat during the process it can be valorized through temperature adjustment of the bioreactor. Table 2.4 provide the various conditions against the hydrogen yield.

A metabolic pathway shift of specific bacteria by defining the carbon to nitrogen ratio of the biomass feed is observed by Lin and Lay [54,59] and an optimum choice will result in high hydrogen production for photo-fermenters. On the other hand Koku et al. [71] has reported the effect of inoculum age on hydrogen production. According to them availability of vitamins for bacterial colonies is necessary, if not provided will weaken the bio-life and thus limiting hydrogen production.

High substrate loading in dark fermentation processes will result in large quantity of Volatile Fatty Acids ((2.5) & (2.6)) thus decreasing reactor pH [72]. This is known as reactor soaring. As described earlier that the control of pH is vital in hydrogen production [1], so substrate loading rate poses a serious constraint for bio-reactors [23,67,70]. Shen et al. [73] have reported that the optimum substrate loading rate is close to the threshold

---

[1]pH should be regulated by some means because for pH lower than 4.5 bacteria metabolism shifts to solventogenesis i.e. production of ethanal, acetone and butanol with no H_2 production

Reactor type	Substrate	pH	Temperature °C	HRT h	Hydrogen $\frac{molH_2}{molsubstrate}$	Ref
Batch	Sucrose	5.0-5.5	22	?	4.3	[66]
Batch	Dairy Waste Water	4.2-5.6	26-30	23	0.0491 $\frac{mmol}{gCOD}$	[67]
Batch	Glucose	5.5	30	96	21.6 % yield	[32]
Batch	Sucrose	5.5	33.5	45	3.7	[23]
Continuous	Glucose	5.2	35	24	0.78	[68]
Fixed Bed	Sucrose	?	35	0.5	3.03	[69]
Fluidized Bed	Sucrose	5.8-6.8	35	2	2.67	[41]
CSTR	Glucose	5.5	36	6	2	[28]
Continuous	Starch	5.5	36-38	5	2.8 $\frac{l}{g.biomass.day}$	[63]
Batch	Glucose	?	41	24	1.67	[64]
Batch	Starch	6	55	120	17 % yield	[29]
Batch	POME[a]	?	60	9.2	1.62	[59]
Batch	CREST[b]	?	60	28.3	1.44	[59]
Batch	Glucose	?	75	72	3.32	[31]
ASBR	Sucrose	4.9	?	16	2.53	[61]
Batch	Cheese whey	6	?	50-52	2.56	[60]
Batch	Xylose	6.5	?	76	2.6	[70]

[a]Palm oil mil effluent

[b]Municipal waste

Table 2.4: Effect of various conditions on Bio-Activity in Dark Fermentation

limit causing soaring while below this, hydrogen yield is proportional to substrate loadings. In order to overcome this problem, often bio-recator is split in two parts i.e. one used to harvest hydrogen in lower pH while other producing methane [68, 74].

Removal of gaseous product from the reactor must be spontaneous as an increase in hydrogen partial pressure results in diminution of its production rate. However, hydrogen pressure build up having positive effect on its production is also reported [66].

The processes involving photo-bacterial metabolism should be done in a vessel designed to give high inside distribution of light intensity. [15]. The spectrum of light is also a key factor in evaluating hydrogen production and thus contributes to an effective bioreactor design [16]. Uneven distribution of light bands within the reactor poses serious reduction in light energy consumption efficiency by the metabolic reaction. The maximum reported conversion efficiency of light energy to hydrogen is 7.9%. [75]

2.3.3 BIO-REACTORS YIELD POTENTIAL

In Table 2.5, Levin et al. [10] compared the bioreactors volumes necessary to produce power from fuel cell operated on bio-hydrogen. In their analysis dark fermentation processes look very promising to generate enough hydrogen but the problem of purity is posed. Contrary to bio-photolysis, hydrogen by dark fermentation is not pure and requires pre-treatment before using in fuel cell.

Bio Hydrogen System	Size of Bioreactor (m^3)			
	1 KW	1.5 KW	2.5 KW	5 KW
Direct Photolysis	34.1	51.2	85.6	171
Indirect Photolysis	67.3	101	169	337
Photo-fermentation	149	224	374	758
Dark Fermentation				
Mesophilic, pure strain	1.14	1.71	2.85	5.70
Mesophilic, undefined	0.371	0.557	0.929	1.86
Mesophilic, undefined	0.198	0.297	0.495	0.989
Thermophilic, undefined	2.91	4.38	731	14.6
Extreme thermophilic, undefined	2.85	4.28	7.13	14.3

Table 2.5: Volume of Bioreactors Vs Power generated [10]

2.3.4 OPERATION MANAGEMENT

Batch or continuous both types of reactors can be used to generate hydrogen. However for any further coupling of bio-reactor, continuous operation is preferred because in batch operation hydrogen output does not remain same [12, 61]. Also the fast removal of VFAs from the reactor is crucial as their higher concentration inhibits bio-hydrogen production [33]. Furthermore studies have shown not only the good stability of continuous reactor but also its quick recovery from any external shock [27]. A comparison between various bio-reactors studied in published writings is shown in Table 2.6. These reactors are usually combination of intelligent compromise between hydrogen yield and operation facilitation. For instance fixed bed type reactors are easy to operate but transfer resistances and choking probability are very high. Also continuous reactors limit the hydrogen yield as effluents also wash out the percentage of microbe cultures.

An economical balance should be done to adjust the optimum yield, H_2/CO_2 ratio and production rate as these factor conclude the capital and running cost of the reactor. Sometimes high hydrogen yield is not economically feasible [65].

Generally there are two systems of having microbe culture in the reactor i.e.

1. Attached (Microbe cultures are grown over support)

2. Suspended (Microbe cultures are in suspension)

Usually attached growth type is preferred for hydrogen generation [10, 76]. However such type of system is more prone to the development of methanogens thus requiring pre-treatment of the feed used [65].

Reactor	Main Features	Advantages	Ref
Anaerobic Sequencing Batch Reactor (ASBR)	⇒Work in four phases: ∗ Feeding ∗ Reaction ∗ Settling ∗ Decanting	⇒ A homogeneous mixture of biomass and microbes is obtained ⇒ Can work to produce continuous hydrogen ⇒Each sequence time can be adjusted thus, optimizing hydrogen production	[61] [67]
Carrier-Induced Granular Sludge Bioreactor (CIGSB)	⇒Fixed bed type filled with carrier support. ⇒ Biofilms are present on support ⇒ Continuous operation ⇒ Highly porous (> 90 %)	⇒ Stable operations at extremely low HRT ⇒ Maintain high biomass concentration ⇒ High hydrogen production rate ⇒ Small volume reactor ⇒ Immobilized culture media	[69] [65]
Fluidized Bed Reactor	⇒ Filled with support embedded with bio-culture Substrate is used to fluidize the bed	⇒ High porosity ⇒ Low HRT ⇒ Adaptable with change in substrate concentration ⇒ Less prone to choking than CIGSB	[41] [77]
Continuous Stirred Tank Reactor (CSTR)	⇒ Usually equipped with a mixing device	⇒ Provides complete homogeneity of biomass and culture ⇒ Quick removal of product gas	[65]
Anaerobic Membrane Bioreactor (MBR)	⇒ Equipped with a cross flow membrane ⇒ Pumping system is required to overcome ∆P across membrane ⇒ Cleaning system to keep membrane free from fouling	⇒ Retain large amount of bacteria in reactor ⇒ High organic removal rates ⇒ Relatively small reactor volume ⇒ Low rate of sludge production ⇒ Produces high quality effluent	[78]
Trickle Bed	⇒ Packed with beads ⇒ Require a cleaning/backwashing system to avoid choking	⇒ Low resistance to gas ensuring rapid hydrogen evolution	[25]

Table 2.6: Comparison of various bio-reactors

2.4 CURRENT H$_2$/CO$_2$ VALORISATION

In this part, I tried to explain the possible ways of valorization of a mixture H$_2$/CO$_2$ to generate energy (mainly electricity). Currently this biogas is planned to be used to generate energy via:

1. Combined cycle.

2. Fuel cell.

2.4.1 COMBINED CYCLE

Gas turbines are classical engines to drive electric generator device. These turbines are highly adaptive to various harsh conditions and usually work on variety of fuels including pulverised coal. These turbines efficiency is however very low and usually they have waste heat boiler (HRSG) at their downstream. Their efficiency is mainly compromised because of combustion chamber metallurgy (Temperature range 1000 - 1700 °C). Excess air to burners is usually adjusted to keep temperature within limits [79]. Furthermore very high temperature also results in high NOx in the turbine exhaust which is usually monitored by environmental agencies. A comparison between pure hydrogen and biogases used as gas turbine fuel is done via a simple simulation package and is presented in Table 2.7. Process efficiency of the gas turbine working on biogas comprised of methane is highest. This does not justify the production of hydrogen containing biogas at first hand, as methane containing biogas is relatively easy to produce and provides high output. Furthermore this biogas may contain H$_2$S and NH$_3$ and if burnt without further treatment will result in NOx and SOx, thus ruining environmentally friendly aspects of this green emergent process.

2.4.2 FUEL CELL

Fuel cell is an electrochemical device used to generate electrical energy continuously through the process of electrolysis. The working of fuel cell is schematically shown in Figure 2.4. The hydrogen is dissociated by the help of catalyst present after anode and transfer of proton to cathode is realised through an electrolyte. By completing the circuit electric current starts to flow. These fuel cells are usually categorised on the basis of electrolyte used. Effect of accompanying CO$_2$ (along hydrogen) on different types of fuel cells along with their comparison is provided in Table 2.8 .

Generally fuel cells at low temperature are not CO$_2$ tolerant. This however is not true for PAFC type cells, although having same catalyst as that of other low temperature cells. Cells operating above 600 °C use low grade catalysts as hydrogen dissociation kinetics is compensated by high temperature augmentation. Therefore they are less affected by CO$_2$. Fuel cell technology is currently under full swing research, and yet their potential to handle biogas is to be thoroughly investigated. Hydrogen produced by reforming is also accompanied by CO$_2$ and may be used in fuel cells [80]. However high temperature along corrosive materials limits the use of these cells. In contrast to gas turbines these cells are of low operating times and need to be replaced periodically (typical operating hours for AFC is 8000 h).

Basis $= 1\text{kgmol·h}^{-1}$ $H_2 = 286\text{kJ·mol}^{-1}$, Combustion chamber temperature $= 1700\,°C$
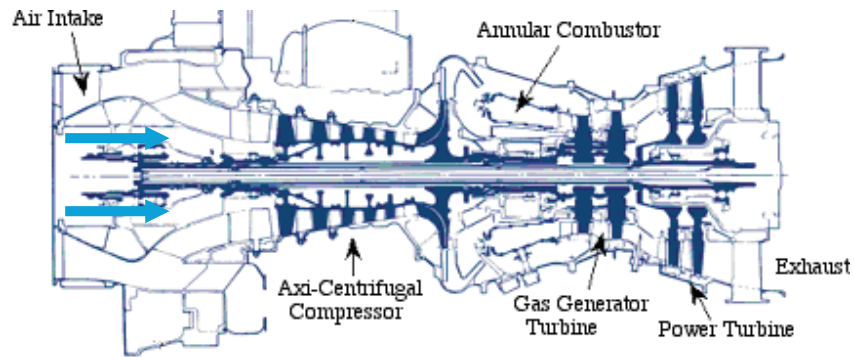
Parameter	Units	Pure H_2	H_2/CO_2	CH_4/CO_2
Air in take	kgmol·h^{-1}	5.121	3.277	4.183
Compressor Power	kW	20.95	13.41	19.69
Fuel in take	kgmol·h^{-1}	1 (100% H_2)	2 (50% H_2)	0.644 (50% CH_4)
Fuel Compression	kW	4.162	7.658	2.339
Heat capacity (hot gas)	kJ·kgmol^{-1}·K^{-1}	42.3	46.83	43.08
Turbine out put	kW	63.52	61.24	64.73
Net power available	kW	38.41	40.18	42.7
Process Efficiency	%	48.6	50.9	54.5

Table 2.7: Process comparison of gas turbine working on different fuel mixtures. *Simulation done by HYSYS*
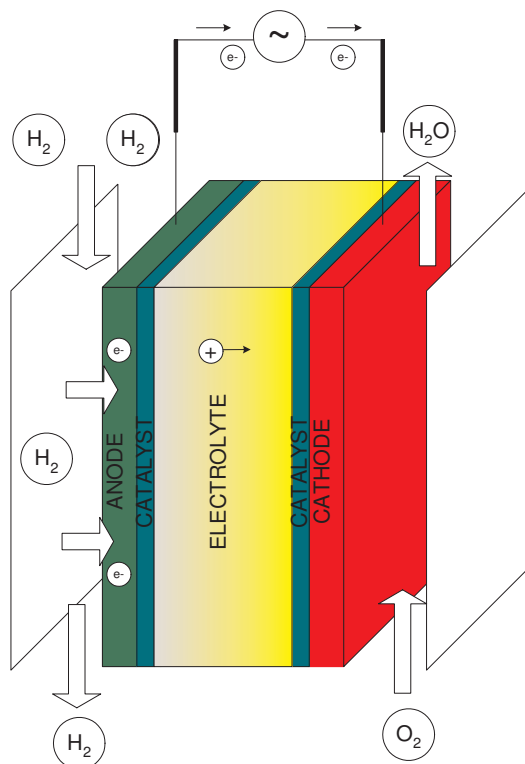
Figure 2.4: Working of Fuel Cell

Temperature and pressure conditions as explained in chapter 3, fall close to those for PEM fuel cell type. CO_2 does have an inhibitory effect assumed to be because of reverse water gas shift reaction under these conditions [82]. As fuel cell circuit is completed by hydrogen atom transfer through some media so activity depends on the rate of hydrogen dissociation. Such dissociation is inhibited by CO_2 but no complete loss is observed by the researchers. On the other hand dissociation of hydrogen in aromatic hydrogenation kinetics is not rate limiting (section:3.1.3) so such inhibition may not be either observed in catalytic hydrogenation of feed stocks via biogas or it may not be that severe .

Currently alkanolamines (MDEA, DMEA) [84] and potassium carbonate (Benfield and Catacarb) [85, 86] processes are being used industrially for separating acidic gases and are very effective for CO_2 removal. Relatively new emerging technologies are membrane separation and pressure shift molecular sieve processes. Existing processes require certain investment but result in almost CO_2 free hydrogen, at the expense of high energy as they involve stripping and regeneration steps. New technologies do have their own constraints like small capacity and relatively high vulnerability to surge shocks.

2.5 CONCLUSION

In wake of above discussion and limitations described, an intermediate process should be devised to secure hydrogen based future. A coupling of bio-reactor with catalytic one (immune to CO_2) is conceived to realise this objective. This will not only store hydrogen in
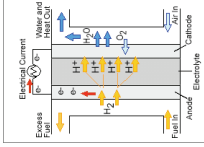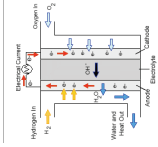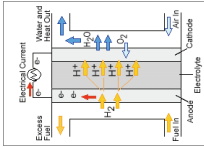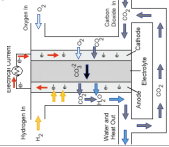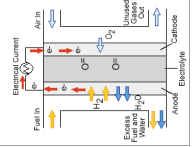
Fuel Cell Type	Electrolyte used	Operating Temperature °C	Catalyst used	Salient features	Effect of CO_2	Schematic
Polymer Electrolyte Membrane (PEM)	Solid organic	50-100	Nobel metals Typically Pt	⇒ high power density ⇒ equipped with porous carbon electrodes ⇒ do not require any corrosive fluids ⇒ quick start ⇒ typically used in mobile users	Inhibiting [81,82]	
Alkaline Fuel cells (AFC)	KOH_{aq} soaked in a matrix	90-100	Non-precious	⇒ high cost ⇒ low stable operation time ⇒ historically being used in remote locations ⇒ high performance because of fast kinetics ⇒ Variety of catalyst can be used	Poisoned	
Phosphoric Acid Fuel cell (PAFC)	Liquid Phosphoric acid soaked in a matrix	150-200	Pt	⇒ stationary power generation ⇒ low power density ⇒ very expensive ⇒ tolerant to impurities	Tolerant	
Molten Carbonate Fuel cell (MCFC)	Li/Na and/or KCO_3 soaked in a matrix	600-700	non-precious metals	⇒ high efficiency ⇒ insitu reforming to produce hydrogen ⇒ can use variety of catalysts ⇒ corrosive agents involved at high temperature	Completely tolerant	
Solid Oxide Fuel cell (SOFC)	Yttria stabilised zirconia	600-1000	non-precious metals	⇒ internal fuel reforming is possible ⇒ can use variety of catalysts ⇒ electrolyte management is relatively easy ⇒high temperature restricts mobility	Completely tolerant	

Table 2.8: Comparison of various fuel cells and effect of CO_2 on the catalyst *(courtesy of US department of energy)* [83]

liquid form bonded in an organic structure but also require 0 % pretreatment ideally. Also another option for converting this low value biomass to high valued product i.e. post fermentation reaction of fermented products is also considered. These products thus produced may also serve as energy reservoirs. However a must meet condition is low pressure drop to avoid biogas accumulation over bio-reactor as it is fatal for organic life.

This concept differs from bio-refinery, as latter incorporates various separation techniques after biological reaction through selected bacterial strains and usually requires biomass gasification. Also generally bio-reactor contains copious amount of water; necessitating in high energy requirements for isolating the valuables. On the other hand this work focuses on the use of raw biogas to saturate various industrial substrates in an independent reactor, thus culminating to high value products. These substrates may be of fermentation origin that are comparatively easy to separate from fermenting mass.

The dissection of further research bifurcates in three parts. In first saturation of aromatics is considered while, in second part organic acids are consider as an alternate option. However third part chew over the process feasibility and overall energy balance of the system. The evaluation will be based on the work of Gavala et al. [65] who investigated the production of hydrogen from continuous fermentation process (see section:5.2.1).

The thing we tell of can never be found by seeking. Yet only seekers can find it.

Bayazid Bistami

3
AROMATICS HYDROGENATION

It has been concluded in previous part that the biogas (H_2/CO_2) may only be used for heat or electricity production via fuel cell. But H_2 is widely used in chemical industry to hydrogenate organic compounds. Depending upon catalysts, some pollutants inhibiting the hydrogenation such as H_2S and CO are well known. On the other hand effects of CO_2 are not clearly described, therefore we have studied its effects on two types of reactions i.e. hydrocarbon hydrogenation and carboxylic acids conversion.

3.1 STATE OF ART OF AROMATICS HYDROGENATION

In this work, toluene hydrogenation is considered as a test case reaction because of multiple reasons including availability of vast published literature and its close relevance with benzene, yet less toxic than its counterpart. [87]. Furthermore its hydrogenation is used to test catalyst surface activity and researchers [88–91] validate their catalyst manufacturing techniques or characterisation by comparing toluene hydrogenation results to the established activities. Toluene by hydrogenation to methycyclohexane may also be used to store hydrogen for their usage in mobile consumers and for transportation as both of these compounds are liquid at ambient temperature [92]. Moreover it is easy to handle and cheaper compared to unsaturated lighter hydrocarbons, while methylcyclohexane the sole product reported has very limited possibility of polymerisation.

Hydrogenation of aromatics remains a concern for many researchers in developing variety of processes for their valorisation and toluene is an important member of the family.

Hydrogenation of aromatics is commercially important because:

1. Stringent limits to the fuel quality are the direct result of the environmental concerns, requiring decrease in amount of aromatics present in fuel by hydrogenation [93].

2. Coal liquids, obtained through coal processing, also contain significant amount of aromatic compounds and usually require dearomatisation before its usage as an alternate fuel. This may be achieved through distillation requiring huge energy. Other possible way is through hydrogenation of these components.

3. Uneven burning and smoke emission by aromatics present in diesel oil should be addressed thus, augmentation in cetane number of the diesel fuel requires saturation of the aromatics; making their hydrogenation commercially useful [94].

4. Increase in demand of light alkenes results in the consideration of aromatics as possible feed stock but their prior hydrogenation is required.

3.1.1 THERMODYNAMICS

Hydrogenation of toluene is exothermic in nature and the overall reaction equation can be written as in equation (3.1).

$$\text{(toluene)} + 3H_2 \rightleftharpoons \text{(methylcyclohexane)} \qquad \Delta H = \text{-}206 kJ \cdot mol^{-1} \quad (3.1)$$
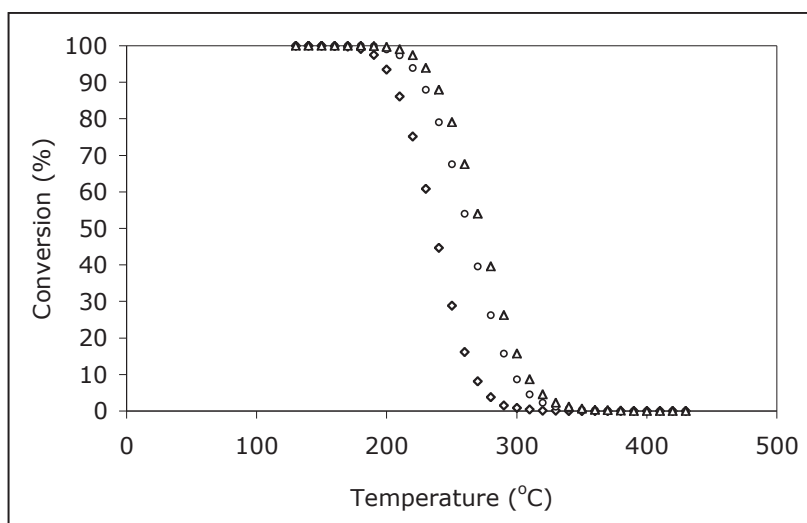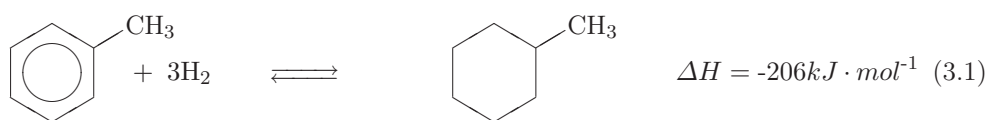
Figure 3.1: Equilibirum conversion of toluene at different pressures $\frac{H_2}{N_2} = 1$, Tol = 10%, $\diamond$ P = 1bar, $\circ$ P= 2bar, $\triangle$ P = 3bar (*Equilibrium data computed by Aspen HYSYS*)

Effect of resonance in hydrogenation of aromatics becomes evident by comparing the heat generated by hydrogenation of benzene i.e. -206 kJ/mol with that of same hypothetical molecule without resonance i.e. -359kJ.mol^{-1} [95]. This implies that the energy of resonance is about 153 kJ.mol^{-1}. The hydrogenation of toluene is also coupled with the resonance effect of the benzene ring. Therefore there are many similarities in hydrogenation of the

two molecules [96–98]. As a general rule the hydrogenation of benzene is much easier than alkyl benzene over pure metal catalyst [99–101]. However results of some researchers show that under certain conditions hydrogenation follows the opposite rule [88, 91, 95].

The maximum achievable conversion for this reaction at any temperature is shown in Figure 3.1. Low temperature and high pressure favour toluene conversion contrary to low pressure. However, the objective of this thesis is to utilize biogas without any prior treatment and this biogas exits at atmospheric conditions so, pressure of 1 bar is selected. Hence the temperature of the reactor is maintained below $150\,°C$ not only to avoid any thermodynamic limitation but also to curtail energy usage.

3.1.2 CATALYSIS

Almost all elements of period 8-10 in periodic table (pure metal + mixture of two or more metals or non-metals) may be used as catalyst to hydrogenate toluene but the base metals and palladium (sometimes even ranked below nickel and iron) are the least active. The mixing of two catalytic effect-bearing metals might result in increased catalytic activity of the resulting catalyst [91]. It is not prudent to provide exact values for the Turn Over Frequency (TOF) because sometimes it become misleading with respect to the conditions chosen by each of researcher. However a general trend can be summarised as shown in Table 3.1.

3.1.3 REACTION REGIME AND KINETICS

Toluene hydrogenation kinetics is an extensively studied chemical process. It includes investigations of how differently experimental conditions can influence the speed of a chemical reaction and yield. Information about the reactions mechanism and transition states results in the construction of mathematical models that can describe the characteristics of a chemical reaction. Such models are essential not only to predict process behaviour but also a key to reactor design (regarded as process heart).

These models are established for kinetic regime because conversion beyond the limits dictated by chemical kinetic regime can not be governed by rate laws, rather they are controlled by various other constraints including equilibrium.

3.1.3.1 INTERNAL AND EXTERNAL TRANSFER RESISTANCES

There is consensus between various researchers over the absence of internal and external diffusional resistances for toluene hydrogenation reaction in gaseous phase [88,91,97,99,100, 103, 104]. External diffusion resistance can be avoided by selecting a reasonable residence time in the reactor. For internal resistance calculations will be done to check its existence. Heat transfer resistances can also be neglected as reactor thickness (used in experiments) is reasonably small and temperature is controlled at the core of reactor.

3.1.3.2 INTERMEDIATES PRODUCTS

Hydrogenation of toluene and benzene thermodynamically hinders the production of intermediates e.g. energy liberated by hydrogenation of cyclohexadiene (an intermediate of benzene hydrogenation reaction) is -232 $kJ \cdot mol^{-1}$ in comparison to -206 $kJ \cdot mol^{-1}$: energy associated with benzene hydrogenation. This value confirms that the formation of

Rh > Ru > Pt > Ir > Pd > Ni > Co			
Ir	Pd	Pt	Rh
Ir/Al_2O_3 > Ir/Al_2O_3 3%Cl > Ir/Al_2O_3 3%F [91]	Pd/SiO_2 - Al_2O_3 > Pd/TiO_2 > Pd/Al_2O_3 > Pd/SiO_2 > Pd/MgO [98]	Pt/SiO_2 - Al_2O_3 > Pt/TiO_2 > Pt/Al_2O_3 = Pt/SiO_2 [97]	Rh/Al_2O_3 > Rh/Al_2O_3 3%F > Rh/Al_2O_3 3%Cl [91]
$Pt-Ir/Al_2O_3$ 3%Cl = $Pt-Ir/Al_2O_3$ 3%F > $Pt-Ir/Al_2O_3$ [91]	Pt 100% > Pd17%Pt83% > Pd100% > Pd65%Pt35% [89]		$Rh-Ni/Al_2O_3$ > $Rh-Co/Al_2O_3$ > $Rh-Fe/Al_2O_3$ > Rh/Al_2O_3 > $Rh-Pd/Al_2O_3$ [102]
		PtRh > PtRe > PtIr > Pt > PtU [91]	
		Pt/Al_2O_3 3%F > Pt/Al_2O_3 1%F > Pt/Al_2O_3 6%F [91]	
		$Pt-Re/Al_2O_3$ 3%Cl > $Pt-Re/Al_2O_3$ 1%Cl > $Pt-Re/Al_2O_3$ 6%Cl [91]	
		Pt/Al_2O_3 > Pt/Al_2O_3 3%Cl > Pt/Al_2O_3 3%F [91]	
		$Pt-Rh/Al_2O_3$ > $Pt-Rh/Al_2O_3$ 3%Cl > $Pt-Re/Al_2O_3$ 3%F [91]	

Table 3.1: Comparison of various catalysts used for toluene hydrogenation

such compounds is endothermic in nature thus reaction is self-inhibiting to its intermediates [87, 89, 96, 100].

3.1.3.3 ADSORPTION

Heterogeneous catalytic reactions commence by adsorption of the reactants over catalyst surface. Such adsorption may be of chemical or physical in nature. The understanding of this surface phenomenon is first step towards any reaction investigation. As the role of hydrogen, toluene and methylcyclohexane is vital in this reaction, so their behaviour is discussed as follow:

HYDROGEN ADSORPTION: Hydrogen adsorption usually depends upon the surface coverage and this reaction is sensitive to its pressure as order of reaction for hydrogen is greater than toluene [100, 103, 105, 106]. Hydrogen adsorption enthalpy is usually regarded as thermoneutral [96]. Another phenomenon of hydrogen spillover is also reported by various researchers (arguable). Hydrogen spillover arises in hydrogen-catalysed reactions on supported metal catalysts. Dihydrogen molecules dissociate on the metal part of the catalyst. Some hydrogen atoms remain attached to the metal, whilst others diffuse to the support and are assumed to be spillover. Spillover hydrogen has often been inferred from hydrogen adsorption and reactivity studies. Acidic supports might contribute the same effect that is why enhanced reaction rate was observed over the catalyst with such supports [91, 97, 104, 107, 108]. The same was observed with n-type semiconductor. On the other hand, no effect with basic diluent was shown [90]. Another positive effect of hydrogen spillover is conversion of coke deposits on catalyst surface into harmless alkanes thus initiating self-regeneration of catalyst [104]. On contrary hydrogen spillover may be just the reaction between adjacent hydrogen adsorbed on metal surface and the toluene adsorbed on the catalyst support.

TOLUENE ADSORPTION: Toluene is an electron donor, so more the metal surface is electron deficient as metals with acidic supports, the adsorption of toluene is enhanced e.g. in case of platinum-zirconium catalyst the Engel-Brewer theory comes into play and zirconium attracts the electrons of metal thus making it more electron deficient and hence, making platinum surface more vulnerable to toluene adsorption [88]. This is also strengthened by the fact of using zeolite base catalyst to modify the structure of toluene. The reaction order for toluene in its hydrogenation is usually on lower side with high toluene surface coverage than hydrogen [103]. This may require optimization of the catalyst as if more of toluene will be adsorbed over a catalyst it will hinder the adsorption of hydrogen and hence the overall reaction rate.

METHYLCYCLOHEXANE ADSORPTION: Methylcyclohexane desorption, after its formation, is reported rapid and does not hinder the reaction rate [91, 96].

3.1.3.4 TEMPERATURE EFFECTS

The rate is often observed to pass through a temperature maxima [87, 89, 96, 97, 103, 107]. However this maximum rate temperature conversion for some catalysts may not be attributed to equilibrium approach [99–101, 105, 106]. This fact can be observed by comparing equilibrium curve with experimental conversion data reported in literature for different

catalysts. According to some researchers this corresponds to the escape of catalytically active hydrogen from the surface of the catalyst at high temperatures. This is argued by the fact that the decrease in hydrogen partial pressure will result in shifting of T_{max} to lower value [99, 105]. Another possible reason may be that although the rate constant for reaction increases with temperature whereas its inverse effect on adsorption constants overcompensates the augmentation in reaction rate [100, 109].

3.1.3.5 MECHANISM

Many researchers established toluene hydrogenation reaction rate law based upon some mechanism. Saeys et al. [96] have proposed same mechanism for toluene as for benzene hydrogenation as shown in Figure 3.2. It shows the dominant path for the reaction to proceed and logically the rate limiting step is the addition of fifth hydrogen as it requires the most energy (respective energies are shown on the arrows).
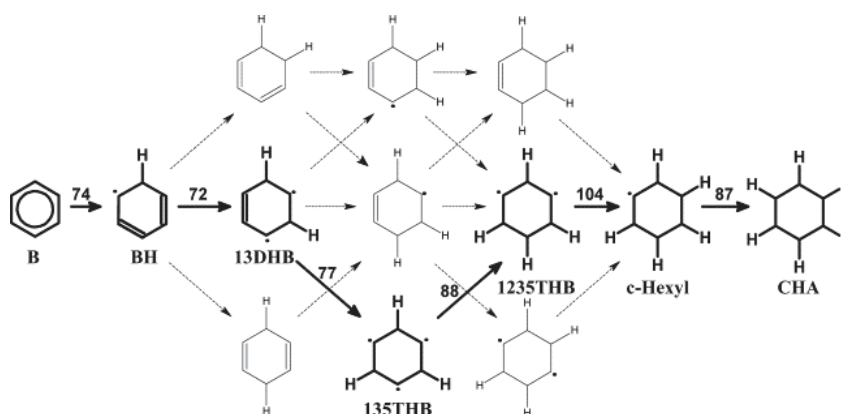
Figure 3.2: Proposed reaction mechanism for benzene hydrogenation. Bold lines show the dominant path. [96]

3.1.3.6 RATE LAWS

Kinetic laws based upon the reaction mechanism of toluene hydrogenation with a rate-determining step while other steps are considered in quasi-state equilibrium, are extensively described in the literature. Generally these laws differ according to assumptions related to their mechanism including: i) dissociative or non-dissociative adsorption of hydrogen, ii) competitive or non-competitive adsorption of aromatics and hydrogen over catalyst surface, iii) rate determining step (RDS), iv) kinetic dependence on the support (i.e. Strong Metal Support Interaction SMSI) and v) sequential or simultaneous hydrogen addition.

Mode of hydrogen adsorption causes slight disparity among reported rate laws. A model based upon non-dissociative type hydrogen adsorption is proposed by Lindfors et al. [106]. They further reported that this character has only minor effect and it is impossible to draw conclusion of true form of hydrogen adsorption via experimentally measured hydrogen kinetics. Non-dissociative hydrogen adsorption approach is reckoned as if hydrogen adsorbs dissociatively, then it forms strong bonds with the surface of catalyst metal; while, according to Gaidai et al. [110, 111] the only hydrogen that takes part into the reaction for Pt base catalysts is loosely bonded. Such behaviour is also used to explain the decrease in hydrogenation rate when reduction temperature of the catalyst is increased. This may lead to hydrogen adsorption as molecules. However majority of researchers have argued otherwise i.e. dissociative adsorption of hydrogen and derive their mechanism based on it [96–98, 103, 112, 113].

Competitive or non-competitive adsorption behaviour of hydrogen and aromatics for active sites of catalyst also contribute to the variety of kinetic models. If toluene molecule adsorbs linearly over the catalyst surface, then geometrically it leaves space for hydrogen to adsorb thus confirming non competitive adsorption [97, 98, 112, 113]. However Saeys et al. [96] have assumed otherwise: at high temperature, hydrogen competitive adsorption capacity against aromatic decreases thus reducing hydrogen adsorption resulting in overall reaction rate diminution. It is also elucidated by decrease in reaction rate after temperature maxima which should not be dictated by thermodynamic equilibrium.

The main cause behind multiplicity of kinetic models is the choice of rate determining step. Saeys et al. [96] have reported thermodynamically, the addition of fifth hydrogen as a rate-limiting step. However, first hydrogen addition to the aromatic ring is also considered to be rate limiting [97] as resonance energy is higher than that of any single hydrogen addition step [95, 99], which is related to first hydrogen addition or toluene adsorption. On the other hand some researchers [98, 110, 111] concluded the addition of second hydrogen as rate limiting. Lindfords and Salmi [105] have also considered addition of all six hydrogen atoms as rate determining. Other considered different steps as rate limiting with sequential and simultaneous addition assumptions based upon the best fit equation according to their data [103, 105, 106].

Strong metal support interactions (SMSI) deal with the hydrogenation of the aromatics adsorbed on the support. Support itself cannot initiate the hydrogenation step as hydrogen does not adsorb on the support surface. This phenomenon is closely coupled with hydrogen spillover. With some supports like TiO_2, $SiO_2 - TiO_2$, the reaction rate depends upon the temperature at which the catalyst is reduced. Increase in reduction temperature results in the curtail of reaction rate. Rahman and Vannice [98, 113] argued that Brønsted or acidic sites on support increase the hydrogenation reaction but after reduction at high temperatures, such sites were removed thus decreasing the activity. According to Gaidai et al. [110, 111], the strongly bonded hydrogen adsorbed on surface because of catalyst reduction at high temperature is responsible for the decrease in reaction rate. It may decrease the spillover hydrogen responsible for the hydrogenation of toluene adsorbed on the support material. Both the groups gave their models based on the premises stated above. Former added another reaction term with the RDS assumption for the support, while the latter only changed the kinetic parameters according to the reduction temperatures stating SMSI has no effect on the kinetic law of the reaction.

With such variety of assumptions, number of Langmuir-Hinshelwood-Hougen-Watson (LHHW) type models were proposed (Table 3.2).

Catalyst	Reactor/ 'Activity Loss'	P. Press H$_2$ kPa	P. Press. Tol kPa	Temp °C	Kinetic Laws	Ref	Remarks
Pt/TiO$_2$	Diff 'yes'	$30 - 101$	$0.2 - 4$	$130 - 180$	$\dfrac{kP_{H_2}{}^2 P_b}{(P_{H_2}^{0.5}+K_{H_2}P_{H_2}+K_TP_T)^2}$	[110]	⇒RDS=Second hydrogen addition. ⇒Best fit=130 − 160°C.
Pt/SiO$_2$	Diff 'yes'	$35 - 94$	$7 - 19$	$130 - 180$	$\dfrac{kP_{H_2}P_b}{P_{H_2}^{0.5}+K_{H_2}P_{H_2}+K_bP_b}$	[111]	⇒Equation based upon benzene hydrogenation.
Pd/SiO$_2$ −Al$_2$O$_3$ Pd/TiO$_2$	Fixed bed 'yes'	$14 - 94$	$10 - 0.7$	$100 - 150$	$\dfrac{k_{Pd}KK_{H_2}P_{H_2}K_TP_T}{1+K_TP_T}$ $+$ $\dfrac{kK'K_{H_2}P_{H_2}K_T'P_T}{1+K_T'P_T}$	[98] [113]	⇒Hydrogen spillover to the support surface results in the second term of the rate law. ⇒Non-competitive and dissociative adsorption. ⇒RDS=Second hydrogen addition.
Pt/SiO$_2$ Pt/Al$_2$O$_3$ Pt/SiO$_2$ −Al$_2$O$_3$ Pt/TiO$_2$	Diff 'yes'	95	7	$60 - 100$	$\dfrac{kK_{H_2}P_{H_2}K_TP_T}{1+K_{H_2}P_{H_2}+K_dK_TP_T}$	[97] [112]	⇒RDS=First hydrogen addition. ⇒Non-competitive and dissociative hydrogen adsorption. ⇒No SMSI effect.
Pt/SiO$_2$ Pt/Al$_2$O$_3$ Pt/SiO$_2$ −Al$_2$O$_3$ Pt/TiO$_2$	Diff 'yes'	95	7	$60 - 100$	$\dfrac{kK_S{}^2 P_T P_{H_2}}{1+K_TP_T+K_SK_TP_TP_{H_2}^{\frac{1}{2}}}$	[97] [112]	⇒ Rate law for support reaction ⇒ RDS=hydrogen transfer from metal to support i.e. hydrogen spillover

Table 3.2: Various rate laws presented in literature-Gas phase toluene hydrogenation

Catalyst	Reactor 'Act. Loss'	P. Press H_2 kPa	P. Press. Tol kPa	Temp °C	Kinetic Laws	Ref	Remarks
Pt/SiO$_2$	Diff 'yes'	95	7	60 − 100	$\dfrac{kK_TK_S{}^2K_{H_2}P_TP_{H_2}}{1+K_Sk(K_{H_2}P_{H_2})^{\frac{1}{2}}} \cdot \dfrac{1}{K_S(K_{H_2}P_{H_2})^{\frac{1}{2}}+K_dK_TP_T}$	[97]	⇒ Rate law for support reaction
Pt/Al$_2$O$_3$						[112]	⇒ RDS=second hydrogen addition
Pt/SiO$_2$ –Al$_2$O$_3$ Pt/TiO$_2$							⇒This rate is an additive to reactions occurring on metal
Ni/Si$_2$	Fixed bed 'no'	19 − 97	1 − 6	120 − 150	$kP_T^mP_{H_2}^n$ $m = \frac{(-872\pm38)}{T+273} + 2.2 \pm 0.1$ $n = \frac{-2553\pm69}{T+273} + 7.1 \pm 0.2$	[100]	⇒Empirical relation
Ni/Al$_2$O$_3$ Non-Commercial	Fixed bed '?'	40 − 82	12 − 32	120 − 200	$kP_T^mP_{H_2}^n$ $m = -0.3 \sim 0$ $n = 0.3 \sim 1.9$	[106]	⇒Empirical relation
Ni/Al$_2$O$_3$ Non-Commercial	Fixed bed '?'	40 − 82	12 − 32	120 − 200	$\dfrac{kK_TK_{H_2}{}^3P_TP_{H_2}{}^3}{(K_TP_T+(K_{H_2}P_{H_2})^{\frac{1}{2}})+1)^7}$	[105]	⇒Competitive and dissociative hydrogen adsorption RDS=simultaneous addition of all six hydrogens
Ni/Al$_2$O$_3$	Fixed bed '?'	40 − 82	12 − 32	120 − 200	$\dfrac{kK_TK_{H_2}P_TP_{H_2}}{(3K_TP_T+(K_{H_2}P_{H_2})^{\frac{1}{2}})+1)^3}$	[105]	⇒RDS=sequential addition of all six hydrogens
Ni/Al$_2$O$_3$ Commercial	Fixed bed '?'	18 − 68	15 − 50	150 − 210	$kP_T^mP_{H_2}^n$ $m = -0.67 \sim -1.64$ $n = 1.27 \sim 3.28$	[105]	Empirical relation

Table 3.3: Various rate laws presented in literature-Gas phase toluene hydrogenation continue...

Catalyst	Reactor 'Act. Loss'	P. Press H_2 kPa	P. Press Tol kPa	Temp °C	Kinetic Laws	Ref	Remarks
Ni/Al$_2$O$_3$ Commercial	Fixed bed '?'	$18-68$	$15-50$	$150-210$	$\frac{kK_TK_{H_2}P_TP_{H_2}}{(K_TP_T+(K_{H_2}P_{H_2})^{\frac{1}{2}})+1)^2}$	[106]	⇒ Competitive and non-dissociative hydrogen adsorption ⇒Sequential hydrogen addition
Pt/ZSM-22	CSTR 'yes'	$100-300$	$10-60$	$150-225$	$kP_T^mP_{H_2}^{\ n}$ $m=-0.2\sim0.3$ $n=0.6\sim1.3$	[103]	⇒Empirical relation
Pt/ZSM-22	CSTR 'yes'	$100-300$	$10-60$	$150-225$	$\frac{C_TK_S(B^3K_TP_T(K_{H_2}P_{H_2})^{\frac{1}{2}}X}{(X(1+(K_{H_2}P_{H_2})^{\frac{1}{2}})+K_TP_TY)^2}$	[103]	⇒Competitive adsorption ⇒RDS=first four hydrogen addition
Pt/ZSM-22	CSTR 'yes'	$100-300$	$10-60$	$150-225$	$\frac{C_Tk_i(\sum_{j=1}^i k_j)K_TP_T(K_{H_2}P_{H_2})^{\frac{i}{2}}}{(1+K_TP_T+(K_{H_2}P_{H_2})^{\frac{1}{2}})^2}$	[103]	⇒Competitive and dissociative adsorption RDS=third or fourth hydrogen addition i.e. i=3 or 4
Pt/ZSM-22	CSTR 'yes'	$100-300$	$10-60$	$150-225$	$\frac{C_Tk_i(\sum_{j=4}^i k_j)K_TP_T(K_{H_2}P_{H_2})^{\frac{5}{2}}}{(1+K_TP_T+(K_{H_2}P_{H_2})^{\frac{1}{2}})^2}$	[96]	⇒Competitive and dissociative adsorption RDS=fifth hydrogen addition

Table 3.4: Various rate laws presented in literature-Gas phase toluene hydrogenation continue..

3.1.4 DEACTIVATION

Any fall in activity of the catalyst is termed as deactivation or catalyst decay. It is usually a chemical reaction (not always) having inverse effect over the catalyst surface. Deactivation is generally divided into six types [114].

1. Poisoning

2. Thermal degradation

3. Vapour compound formation

4. Vapour-solid/ or solid-solid reaction

5. Fouling

6. Crushing/attrition

Last two are of mechanical in their nature whereas rest are chemical in their action.

3.1.4.1 POISONING

It is the strong chemisorption of the chemical substance including reactants, products or impurities on the sites that are responsible for catalysis. Therefore it is dictated by adsorption phenomenon. Such chemisorption may induce i) strong surface bonds with the poison, ii) electronical modification of neighbouring catalysis sites, iii) catalyst surface restructuring, iv) forming a protective layer among the adsorbed reactants and v) augmenting surface diffusion resistance for the reactants. Examples are metal poisoning by sulphur or arsenic, neutralisation of acid sites by amines and oxidation of iron by water, CO_2, CO and oxygen in ammonia synthesis. If rate of poisoning is linear with respect to poison concentration it is termed as non-selective poisoning while preferential adsorption of poison is termed as selective poisoning.

3.1.4.2 FOULING

Coke formation over various crude oil processing catalyst falls under this category. It is a mechanical type deposition of any poison blocking active catalyst sites thus inhibiting reactants diffusion into the catalyst pores. Fouling by carbon deposition is mostly discussed in literature usually requiring high temperature depending upon the catalyst type. Deactivation by polymerisation also comes under the same category.

3.1.4.3 THERMAL DEGRADATION/SINTERING

It is also termed as independent deactivation because it is independent of the components present in the feed. It is usually caused by the structural modification of the catalyst surface because of exposure to extreme thermal conditions. Thermal shocks may result in i) crystalline structure modification of the catalysts, ii) loss of surface area due to support or pore collapse and/or iii) change in catalyst state from active to non-active. Sintering is aggravated if reactor and catalyst are not physically designed to dissipate heat, depending upon the reaction. Such reaction may be between reactants or of poisoning type thus combining two types of deactivation.

3.1.4.4 VAPOUR COMPOUND FORMATION

It concerns the physical loss of the catalyst by its conversion to vapours via reacting with some poison or the reactant it self. Typical example is the formation of nickel carbonyl in presence of CO over nickel catalysts. Amount of loss is usually insignificant but high temperature and low pressure may result in appreciable loss. This is therefore not exactly the catalyst deactivation. Sometimes etching and pitting because of catalyst loss may also physically hinder the neighbouring sites.

3.1.4.5 VAPOUR-SOLID/ OR SOLID-SOLID REACTION

Solid catalyst support diffusion to the catalyst surface and then reacting or just depositing to foul the catalyst may come under this heading. A typical example is the catalyst promoters inhibition by catalyst support as in case of ammonia synthesis. Potassium may react with alumina, diffused to the surface, to produce potassium alumina complex-an example of iron base catalyst promoters inactivation.

3.1.4.6 CRUSHING OR ATTRITION

As the name suggests this is mechanical failure of the catalyst because of process pressure surges or physical induced stresses. It will not only result in crushing of pores but also augments the pressure drop across the reactor-a closely monitored feature for industrial reactors.

3.1.4.7 TRANSITION PERIOD/CATALYST STABILISATION

This is not really a type of deactivation; rather it is catalyst surface transition because of its exposure to feed at reaction conditions, just after activation. This is usually attributed to adsorption of various reactants, products or even reaction intermediates. This should not be confused with rate limiting step because of slow kinetics as described through Langmuir-Hinshelwood-Hougen-Watson-mecahnism (LHHW), instead it is the time required for the

catalyst to achieve the condition of quasi state equilibrium for adsorption of reactants and desorption of products. Generally it is very fast with just few seconds, however occasionally depending on the reaction conditions, it may rest for days.

3.1.4.8 TOLUENE HYDROGENATION & FALL OF ACTIVITY

Although some of the researchers observed catalysts deactivation [89,91,112] and have used the bracketing technique (catalyst regenerated between two experiments) to regenerate the catalyst between two sample experiments however none of them have considered it in their rate laws. As the temperature of the said reaction is low compared to the temperature required for carbon link breakage therefore no role of sintering may be considered. Adsorption type deactivation of the catalyst may be accounted for determining kinetic models. It has also been shown that the activity of platinum is far better than that of palladium base catalyst but deactivation of later is reported slow compared to the former [87, 107]. On the other hand with nickel-silica catalyst carbon link breakage is important even at room temperature thus coking may occur over this catalyst [87].

3.2 BIOGAS EFFECTS ANALYSIS: LITERATURE SURVEY

Due to lack of information about CO_2 effect on toluene hydrogenation at low temperature and low pressure, we tried to estimate its effect using the literature on reactions that can occur between H_2 and CO_2 under those conditions over catalyst. The by-reactions over reduced catalyst we found are shown in equations (3.2) to (3.6).

$$CO_2 \quad + \quad H_2 \quad \rightleftharpoons \quad CO \quad + \quad H_2O \qquad \Delta H = 42 kJ \cdot mol^{-1} \qquad (3.2)$$

$$CO_2 \quad + \quad 4H_2 \quad \rightleftharpoons \quad CH_4 \quad + \quad 2H_2O \qquad \Delta H = \text{-}165 kJ \cdot mol^{-1} \quad (3.3)$$

$$CO_2 \quad + \quad 3H_2 \quad \rightleftharpoons \quad CH_3OH \quad + \quad H_2O \qquad \Delta H = \text{-}50 kJ \cdot mol^{-1} \quad (3.4)$$

$$CH_4 \quad + \quad 3CO_2 \quad \rightleftharpoons \quad 4CO \quad + \quad 2H_2O \qquad \Delta H = 330 kJ \cdot mol^{-1} \quad (3.5)$$

$$CH_4 \quad + \quad CO_2 \quad \rightleftharpoons \quad 2CO \quad + \quad 2H_2 \qquad \Delta H = 248 kJ \cdot mol^{-1} \quad (3.6)$$
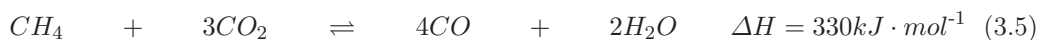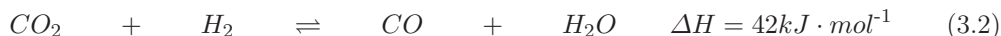
3.2.1 REVERSE WATER GAS SHIFT

CO_2 is usually considered as an inert molecule, but it can lead to carbon monoxide through the reverse water gas shift reaction (RWGS) (3.2) when an appropriate catalyst such as a Pt-group metal is used [115, 116]. This reaction usually propagates at temperature above 250 °C. Below this, kinetics is hindered by the equilibrium i.e. high temperature favours hydrogenation of carbon dioxide to carbon monoxide as demonstrated by the equilibrium curve shown in Figure 3.3. This reaction can easily adjust carbon monoxide to hydrogen ratio compared to methane reforming(3.6) [117].

Figure 3.3: Equilibirum conversion of carbon dioxide to carbon monoxide, P = 1 bar, $\frac{H_2}{CO_2}$ = 1 (*Equilibrium data computed by Aspen HYSYS*)

3.2.2 CO POISONING

The concentration of CO produced is small at low temperatures. Primarily because of thermodynamic limitations and secondly, because the reaction rates are minute below 250 °C for catalysts based on Pt [118–120]. However even if the CO concentrations formed are low and possibly not detectable in the reactor effluent, CO traces may lead to a dramatic change of Pt-group metals activity. The dissociative chemisorption energy of H_2 on the Pt(111) surface is typically comprised between 68 and 80 kJ/mol [121–123], while the CO binding energy on the same surface ranges from 144 to 173 kJ/mol [124]. Therefore, CO molecules bind more strongly to the Pt atoms than dissociating H atoms and block the sites required for hydrogen adsorption and strongly decrease the hydrogenation rate. The poisoning effect will be worse if the molecule to be hydrogenated can only adsorb on the metal sites, hence in competition with CO. Note that the adsorption enthalpy of toluene on Pt(111) is about 65 kJ/mol [96].

The poisoning of Pt catalysts by CO formed from CO_2 was actually reported by several authors. Brugen et al. [125] showed by in situ IR spectroscopy that Pt, Ru, Rh and Pd were all gradually covered with carbonyl species under 90 bars of supercritical CO_2 (scCO_2) in the presence of 1 % H_2 at 50 °C, with the Pt-based sample displaying the highest rate of carbonyl formation. They had reported earlier on the deactivation and low activity of a 5 wt.% Pt/Al_2O_3 in scCO_2 at ca. 35 °C during ethyl pyruvate hydrogenation, which was ascribed to the reduction of CO_2 to CO, the latter species poisoning the metal surface [126]. Xu et al. [127] have used a CO_2-containing medium for polystyrene ring hydrogenation and reported a deactivation due to CO from the RWGS over a Pd-based catalyst at 150 °C, while the deactivation of a Ni-based catalyst (observed at 180 °C) is due to water formed

from the CO_2 methanation (Equation (3.3)).

The involvement of the RWGS is also noted in the operation of low-temperature fuel cells. Gu et al. [128] have shown that the reformate (i.e. CO_2, N_2, and H_2) used in a proton exchange membrane fuel cell (PEMFC) at 70 °C led to the formation of some CO that poisoned the Pt electrode. Interestingly, it was observed that higher the cell back pressure, higher the formation of CO. However Bruijn et al. [82] have observed that CO_2 reduces the PEMFC efficiency by 30 % but it does not totally deactivate the fuel cell.

3.2.3 CO_2 ADVANTAGES

It must be stressed that beneficial effects due to CO_2 reactivity have also been reported. Wang et al. [129] have reported that CO_2 used as a gas diluent during the dehydrogenation of ethyl benzene to styrene may act as a promoter for the reaction. These authors proposed that ethylbenzene dehydrogenation is coupled with the RWGS, hence the hydrogen formed being effectively scavenged by the CO_2. Note that this coupling is observed at a high temperature, i.e. 550 °C over non-precious transition metals supported on alumina.

Arai et al. [130] reported that both conversion and selectivity increased during the hydrogenation of unsaturated aldehydes to unsaturated alcohols over a 1 wt.% Pt/Al_2O_3 at 50 °C in $scCO_2$ (super critical carbon dioxide). The improvement in activity is suggested to arise from (although no evidence is provided):

1. the change of the dielectric constant of the reaction medium

2. the increased solubility of reagents

3. increased mass transport coefficient

The possible formation of CO is not mentioned. Zhao et al. [131, 132] have used $scCO_2$ medium to enhance selective hydrogenation of nitro aromatics over Pt/C. These authors reported no deactivation and similar conversions as those measured in ethanol are obtained. The reaction in $scCO_2$ is found to be structure insensitive, while the opposite is true in the case of using the ethanol solvent. Again, no clue of a possible role of carbon monoxide on the activity of the sample is mentioned.

The increased reagent solubility and transfer coefficient (via overcoming of the liquid-gas interface) improve catalytic properties while working in scCO2. There seems some controversy on whether CO formation can be effective or induce poisoning for hydrogenation reactions carried out in the presence of CO_2. It seems to inhibit hydrogen dissociation which is not the rate limiting step for aromatic hydrogenation as described earlier, so it is difficult to conclude the exact behaviour of CO_2 from the existing literature. However CO production may also alter the support surface for catalysts such as Pt/Al_2O_3 by forming carbonate complexes [133].

3.2.4 CO_2 CONVERSION TO METHANOL

Conversion of carbon dioxide to methanol by reaction (3.4) is thermodynamically possible at low temperatures as shown in Figure 3.4. However by keeping temperature above 40 °C will greatly reduce its production. Furthermore no adverse effect of methanol on the catalyst is reported in literature.
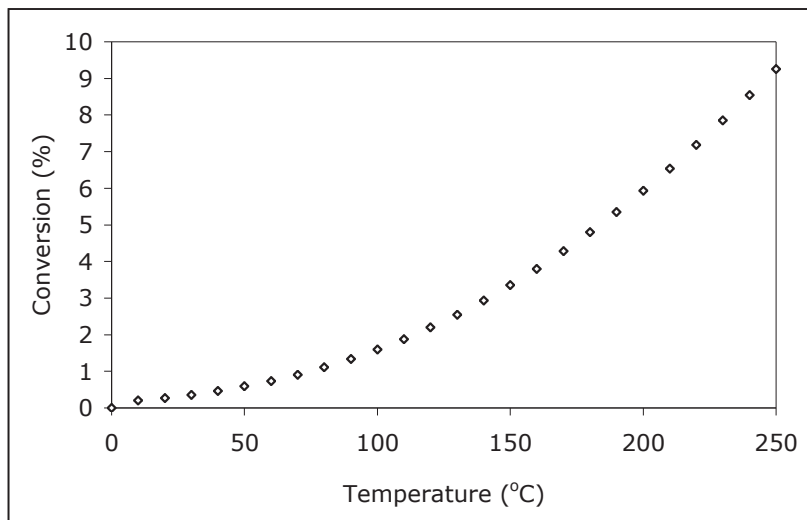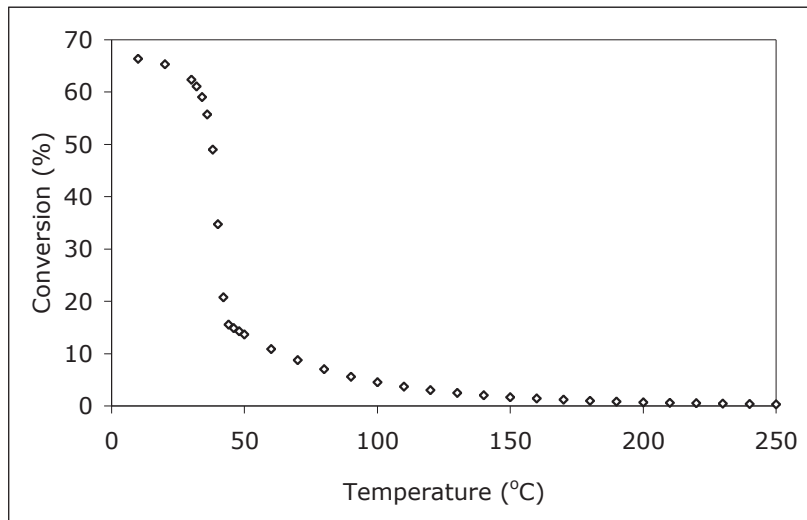
Figure 3.4: Equilibrium conversion of carbon dioxide to methanol, P = 1 bar, $\frac{H_2}{CO_2} = 3$ (*Equilibrium data computed by Aspen HYSYS*)

3.2.5 EFFECT OF METHANE

Methane yield by equation (3.3) from CO_2 is 97 % thermodynamically possible within the given temperature range. Researchers like Mark Saeys et al. [96] have considered methane as an inert for toluene hydrogenation reaction. Furthermore, methane is not present in great quantities in the portion of the biogas to be used in this research work therefore, it does not pose as much problem as that of carbon dioxide. Production of carbon monoxide from methane by equations (3.5) and (3.6) does not commence at the temperature below 200 °C.

3.3 EXPERIMENTAL RESULTS ON TOLUENE HYDRO-GENATION USING BIOGAS

Based on literature survey, and finding none adequate response, we decided to evaluate the possibility to hydrogenate toluene with biogas (H_2/CO_2) on Pt catalyst even if CO_2 could induce low partial activity loss (section: 2.4.2) on hydrogen dissociation.

Experiments are started with Pt/Al_2O_3 - a well known hydrogenation catalyst for toluene with no reported Strong Metal Support Interaction (SMSI) effects [110, 111]. Furthermore it is well studied and is commercially being utilized for aromatic hydrogenation in petroleum industry along with several other applications. The cost of platinum is well compensated by brisk reaction rate. Alumina in addition to its inertness has several other advantages as shown bellow:

1. Hard and wear-resistant.

2. Resists strong acid and alkali attack at elevated temperatures.

3. Good thermal conductivity.

4. Excellent size and shape capability.

5. High strength and stiffness.

6. Available in purity ranges from 94 %, an easily metallizable composition, to 99.5 %
   for the most demanding high temperature applications.

In order to understand and compare the alumina behaviour, two other catalysts have
been tested: Pt/SiO_2 and Pt/SiO_2-TiO_2.

3.3.1 EXPERIMENTAL SETUP, PROCEDURES AND CATALYST
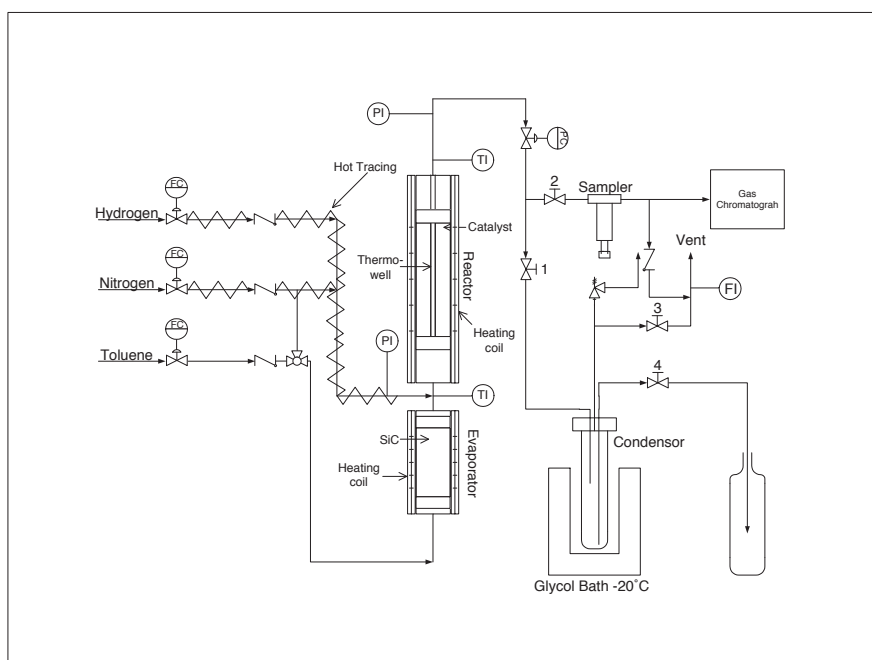
Figure 3.5: Experiment bench for toluene hydrogenation - Process Flow Diagram

The process used was gas phase hydrogenation in a small packed bed reactor provided
with necessary provisions of injection, sampling and analysing (see Figure 3.5). Reactor is
5 cm in height and 0.5 cm in diameter and is filled by 2 g of catalyst between 5 mm of
quartz layers. Particle size for catalyst is about 200 μm. Thus the L/d_p ratio for the reactor
is 250 hence can safely be considered as plug flow reactor. Liquid toluene is vaporised in
a separate evaporator and gas mixtures are premixed and heated before making contact
with the catalyst. Any pulsation or perturbation in toluene flow or irregular evaporation
is minimized via establishment of the saturated equilibrium. This is achieved by adjusting
vapour pressure of the liquid, so that resulting partial pressure of the hydrocarbon becomes

equal to the desired molar composition in the final mixture entering the reactor. This methodology however, only works with pure liquids or azeotropes. Refrigeration set-up is composed of a chillier and a glycol bath to maintain the temperature as minimum as -25 °C. This is low enough to condense almost all of the products from the reactor. The sampler and condenser remain in the bath, thus ensuring complete condensation. Overall material balance is conducted to balance the quantities entering and leaving the reactor. A transparent Teflon line is provided across the evaporator and reactor to assess the process stability. If the liquid toluene level in the evaporator remains constant (determined via level tube) during the sample run, validity of the test is verified. Transition period as well as preliminary samples were rejected to get clean results free from any contamination. Residence time, in wake of literature values, is adjusted to keep diffusion resistances at minimum. Special care is taken with start-up and shut-down procedures to keep the catalyst in stable state.

Catalysts chosen to effectuate this reaction in this part are Pt supported (Pt/Al_2O_3, Pt/SiO_2, Pt/SiO_2-TiO_2).

The catalyst Pt/Al_2O_3 consists of γ-alumina particles impregnated by Pt/ acetyl-acetonate. Size of supported alumina provided by Sasol Chemie was found between 150 -250 mm with an effective specific surface area of 145 - 165 $m^2 \cdot g^{-1}$. 150 g of alumina powder was mixed with 200 ml toluene and 3.13 g of Platinum Acetyl-acetonate. The mixture was stirred for 3 hours at 60 °C. The solvent was then removed by evaporation at 80 °C under reduced pressure. The resulted powder was then dried at 120 °C for one night. This catalyst was then calcined with air at 500 °C for 4 h with an average temperature ramp of 3 °C$\cdot$min^{-1}. After impregnation and drying platinum content on Alumina is about 0.88 % and overall dispersion is about 54 % measured through hydrogen chemisorption. Nitrogen adsorption reveals BET = 147 $m^2 \cdot g^{-1}$ with pore diameter and pore volume equal to 12.3 nm and 0.45 $cm^3 \cdot g^{-1}$ respectively.

For silica based platinum catalyst, 10 g of SiO_2 having particle size of 150 - 250 mm were mixed with 50 ml of toluene and then impregnated by 0.2057 g (0.1 g Pt) of Pt/ acetyl-acetonate. The mixture was stirred for 5 h while temperature was adjusted to 70 °C followed by vacuum evaporation for 2 h at 80 °C. The resulting solid was placed in oven for one night at 120 °C then dried in air at 150 °C for 2 h; temperature was increased with the ramp of 10 °C$\cdot$min^{-1}. For calcination, temperature was programmed to increase at the rate of 4 °C$\cdot$min^{-1} uptill 500 °C thereafter catalyst was kept for 4 h at same temperature. The platinum content is about 0.91 wt% and overall dispersion is found below 5 %.

Pt/SiO_2-TiO_2 catalyst is prepared by coating TiO_2 around SiO_2 200μm diameter. In order to prepare bi-support catalyst the two supports (20 g each) were mixed together in 80 ml water. Mixture was heated to 70 °C for 4 h before vacuum evaporation at 80 °C for 2 h. The resulting mass remained in oven for 2 days at 120 °C before calcination at 500 °C (@4 °C$\cdot$min^{-1}) for 4 h. 20 g of SiO_2-TiO_2 was mixed with 30 ml of Toluene and then impregnated by 0.403 g (0.2 g Pt) of Pt/ acetyl-acetonate. The mixture was stirred for 4 h while temperature was adjusted to 70 °C followed by vacuum evaporation for 2 h at 80 °C. The resulting solid was placed in oven for one night at 120 °C. For calcination, temperature was programmed to increase at the rate of 4 °C$\cdot$min^{-1} uptill 450 °C thereafter catalyst was kept for 4 h at same temperature. The platinum content and overall dispersion measured for this catalyst are 1 wt% and 63.4 % respectively.

In order to evaluate CO_2 effect, toluene hydrogenation was carried out with and with no CO_2. For no CO_2 conditions the flow ratios are adjusted with nitrogen.

The operating procedures, catalyst characterisation and chromatograph analysis scheme

is presented in annexes A to C.

3.3.2 HYDROGENATION WITH NO CO_2 ON Pt/Al_2O_3

3.3.2.1 EFFECT OF TEMPERATURE ON CONVERSION

To highlight the temperature effect on toluene conversion, temperature is varied for different residence times. In experimental results (Figure 3.6(a)) TOF indicates the turn over frequency calculated as $\text{TOF} = \frac{X \cdot F_{tol,o}}{n_{Pt}}$ with units of s^{-1}. The toluene content, pressure and H_2 to N_2 ratio are adjusted to 0.1, 1 bar and 1 respectively. This figure can be divided into two zones i.e. kinetic regime (below $150\,^\circ$C) and equilibrium dictated regime (above $150\,^\circ$C). The existence of temperature maxima for toluene hydrogenation was previously observed in the literature (section:3.1.3.4). The results under kinetic regime are approximately consistent and conversion decreases with decrease in contact time of toluene over the catalyst. However unexpected decrease in conversion is observed after the temperature maxima for $\tau = 130$ kgcat $\cdot$ s $\cdot$ mol^{-1}; not explained by thermodynamics. Before each profile test run, standard experiment at temperature and residence time of $75\,^\circ$C and 50 kgcat $\cdot$ s $\cdot$ mol^{-1} respectively is conducted with an approximate conversion of 55 %, followed by the residence time adjustment. Temperature is then varied during the day to establish the profile conversion values. For all the profiles the standard experiment shows conversion variation between 50 - 60 % with majority of values around 55 %, indicating no deactivation. But the drop in conversion for temperature profile at $\tau = 130$ kgcat $\cdot$ s $\cdot$ mol^{-1} may be because of some kind of activity loss of the catalyst. Keane and Patterson [99] reported the same for nickel based catalyst but they attributed this to surface phenomenon (Deactivation may also be termed as surface phenomenon depending upon its nature). However such type of deactivation is also undetectable by effluent analysis. This reaction is very selective and methylcyclohexane is the only reaction product observed, since there is no ghost peak found in the chromatograph analysis. Same TOF values for 75 and $100\,^\circ$C are plotted in Figure 3.6(b) indicating increase in conversion with increasing residence time for $75\,^\circ$C. However for $100\,^\circ$C the conversion is almost same for various residence times. The decrease in Reynold's number with increasing τ in the reactor can trigger the external diffusion resistance. The factor for such resistance is calculated and found negligible ($f_{ex} << 1$) for lowest velocity i.e. $\tau = 130$ kgcat $\cdot$ s $\cdot$ mol^{-1}. This suggests some drop in catalyst activity.

Sequence Duration (min)	Temp. $^\circ$C	Press. bar	τ kgcat $\cdot$ s $\cdot$ mol^{-1}	Conversion %
0 - 90	75	1	50	72.4
90 - 225	75	1.5	50	88.4
225 - 315	75	1	50	64.2
315 - 375	75	1	50	61.6
		day break		
375 - 485	75	1	50	61.8
485 - 625	150	1	50	99.4
625 - 715	150	1	50	99.8
715 - 810	75	1	50	48

Table 3.5: Activity loss verification tests $\frac{H_2}{N_2} = 1$, $\frac{\text{Toluene}}{(H_2+N_2)} = 0.1$, P = 1 bar
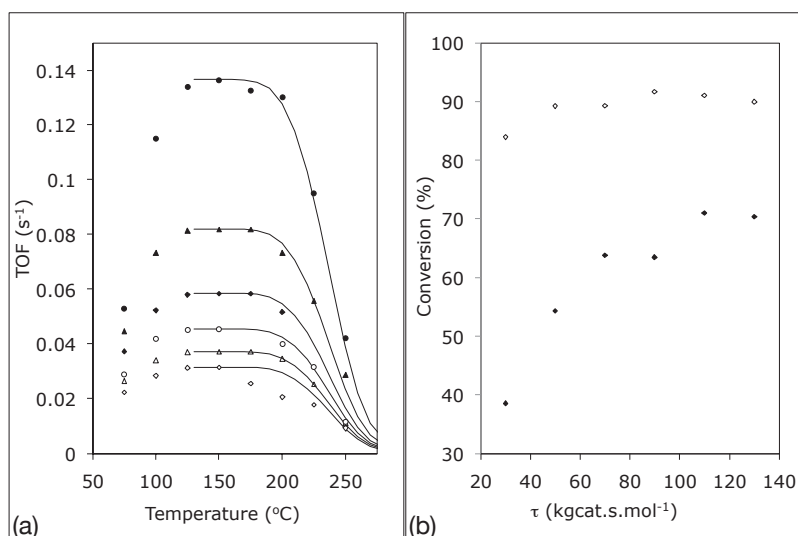
Figure 3.6: (a) - TOF profile on Pt/Al_2O_3 at different temperatures. $\frac{H_2}{N_2} = 1$, $\frac{Toluene}{(H_2+N_2)} = 0.1$, P = 1 bar, $\diamond$ $\tau = 130$ kgcat·s·mol^{-1}, $\triangle$ $\tau = 110$ kgcat·s·mol^{-1}, $\circ$ $\tau = 90$ kgcat·s·mol^{-1}, $\blacklozenge$ $\tau = 70$ kgcat · s · mol^{-1}, $\blacktriangle$ $\tau = 50$ kgcat · s · mol^{-1}, $\bullet$ $\tau = 30$ kgcat · s · mol^{-1}, Solid lines show equilibrium values. (b) - Conversion vs τ at $\blacklozenge = 75\,°C$ and $\diamond = 100\,°C$

3.3.2.2 ACTIVITY LOSS DEMONSTRATION

Some other experiments were planned to demonstrate catalyst activity loss. After reactivation under H_2 the catalyst have been contacted with constant gas mixtures for two days. The sampling duration and conversion are indicated in Table 3.5. It is clearly depicted by the results that catalyst ability to hydrogenate toluene falls during the day. Moreover an increase of temperature for 3.8 h seems to decrease the activity dramatically.

3.3.2.3 PARAMETERS AFFECTING ACTIVITY LOSS

Catalyst deactivation during toluene hydrogenation must be considered as its presence is confirmed via previous experimental run.

With the catalyst as previously used, long duration experiments are carried out varying some conditions such as residence time, temperature and reactant partial pressure. The reaction at 75 °C and 1 bar pressure is taken as standard, to estimate the relative activity of the catalyst with residence time of 50 kgcat·s·mol^{-1} and 10 % (mol) toluene of the total flow while the rest being equal molar mixture of nitrogen and hydrogen (45 % H_2/45 %N_2). These conditions (temperature, pressure and hydrogen to nitrogen molar ratio) generally correspond to the conditions at fermenter downstream, with carbon dioxide replaced by nitrogen. However this time standard reaction is done for relatively long period of time. The time values presented in graph axis represents the duration passed since last catalyst reactivation. Moreover the results take in to account the time toluene remain in contact
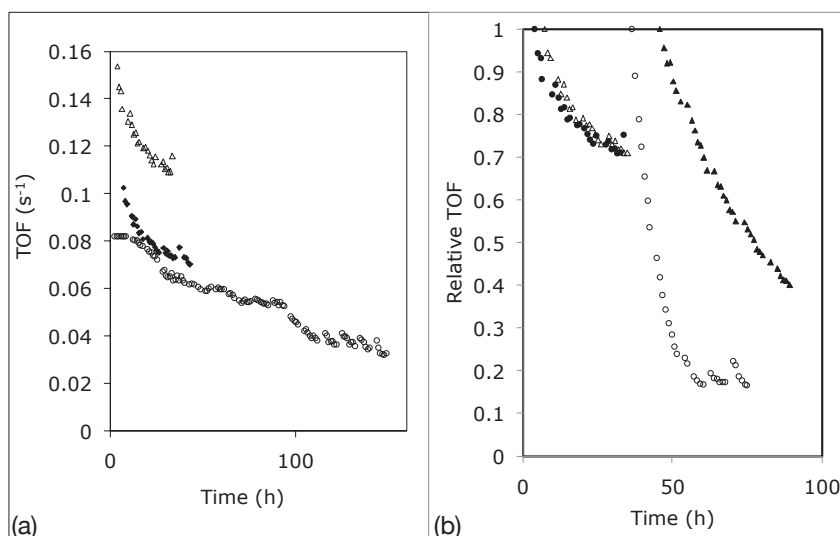
Figure 3.7: Effect of residence time and temperature on activity depletion profile $\frac{H_2}{N_2} = 1$, $\frac{Toluene}{(H_2+N_2)} = 0.1$, P = 1 bar (a) - T=75 °C, $\tau = \circ - 50, \blacklozenge - 30$ *and* $\triangle - 20$ kgcat $\cdot$ s $\cdot$ mol^{-1}, (b) $\tau = 30$ kgcat $\cdot$ s $\cdot$ mol^{-1} & T = $\triangle - 75$ °C, $\blacktriangle - 100$ °C, $\tau = 20$ kgcat $\cdot$ s $\cdot$ mol^{-1} & T = $\bullet - 75$ °C, $\circ - 125$ °C

with the catalyst during transition (i.e. start up and shut down sequence time).

The Figure 3.7a shows the TOF evolution with time keeping the same experimental conditions at the reactor entrance (partial pressure, flow rate and temperature) for different residence times. As elucidated in Figure 3.7b, catalyst activity loss is evident but this loss does not depend upon residence time. About 4-5 % of decrease in conversion is observed per day but the overall reduction is very high and cannot be attributed to sample collection error. Furthermore for every long duration experiments the activity seems to attain stabilisation at some equilibrium point. Feeble reactivation is observed during night, when reactor is pressurized under hydrogen without toluene entrainment. However this cannot be ignored when catalyst tends to stabilize it self, broken lines represent the day breaks and highlight the phenomenon. Furthermore the same activity loss behaviour is observed at different residence times, while catalyst is reactivated between different sets of data. This also confirms the absence of external diffusion limitations. Hydrogenation of toluene over Pt/$\gamma - Al_2O_3$ is coupled with catalyst deactivation.

For experiments shown in Figure 3.7 the catalyst have been reactivated by the same sequence but with hydrogen flow rate of 80 ml·min^{-1}. A remarkable increase in its activity is observed implying the activation dependence on purge rate. This point will be further discussed in later section.

The temperature affects the catalyst activity in two ways, primarily increasing the kinetics (by Arrhenius Law Figure 3.6) and secondly by increasing the activity loss rate (Figure 3.7b). The effects of residence time on activity loss rate being feeble, it is adjusted

($\tau = 30$ kgcat $\cdot$ s $\cdot$ mol^{-1} for T - $100\,^{\circ}$C and $\tau = 20$ kgcat $\cdot$ s $\cdot$ mol^{-1} for T - $125\,^{\circ}$C) to keep conversion in scale. Similarly the final equilibrium point of catalyst activity is dependent on temperature, probably due to adsorption effect. The phenomenon of reactivation during night is observed at $125\,^{\circ}$C as at $75\,^{\circ}$C.
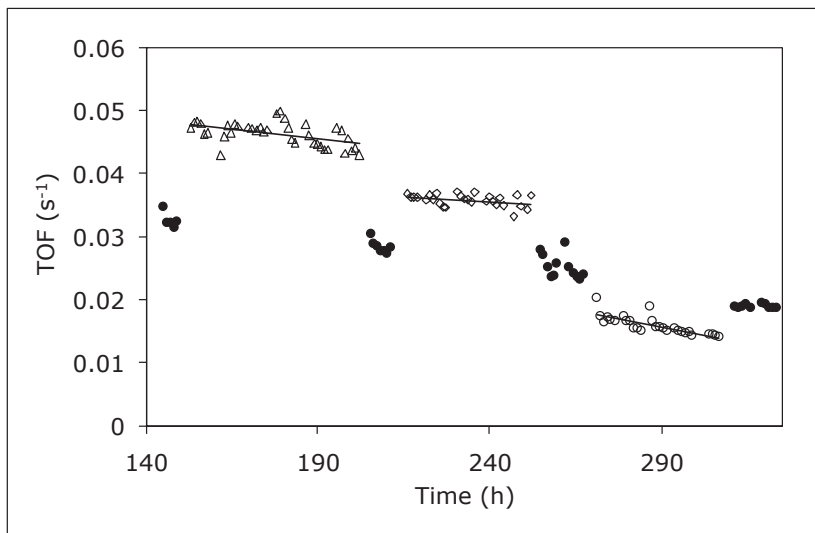
Figure 3.8: Effect of partial pressures on toluene conversion P $= 1$ bar, $\tau = 50$ kgcat $\cdot$ s $\cdot$ mol^{-1}, T $= 75\,^{\circ}$C, $\circ - \frac{H_2}{Tol} = 3$, $\bullet -$ Standard reaction conditions $i.e.$ $\frac{H_2}{Tol} = 4.5$, $\triangle - \frac{H_2}{Tol} = 9$, $\diamond - \frac{H_2}{Tol} = 19$

Reaction rate always increases with augmentation in hydrogen partial pressure while activity loss rate decreases (Figure 3.8). The increase in catalytic activity by increase in hydrogen partial pressure is in accordance with the previous observations made by various researchers [100, 103, 105, 106]. This global fall in activity is not linear with respect to time but a representative rate may be estimated for individual conditions. For a hydrogen to toluene ratio of 3, 9 and 19, the gradients representing the fall in activity are -28$\cdot 10^{-9}$ s^{-2}, -17$\cdot 10^{-9}$ s^{-2} and -8.3$\cdot 10^{-9}$ s^{-2} respectively confirming the positive effect of hydrogen and negative effect of toluene. For standard conditions ($\frac{H_2}{Tol} = 4.5$) in between two different consecutive data sets, reaction activity follows the same activity loss rate e.g. the gradient between 145 h to 210 h is -17$\cdot 10^{-9}$ s^{-2} which is same for hydrogen to toluene ratio of 9. This indicates that no reactivation occurs by changing experimental conditions, only the activity loss rate is more or less rapid.

The TOF values calculated for the toluene hydrogenation are comparable with the published results in literature as shown in Table 3.6.

This transition in catalyst activity or 'deactivation' is reported by various researchers for toluene hydrogenation over various catalysts [96–98, 103, 110–113] but no information regarding the quantification is provided. Their results represent catalyst activity at time $\simeq 0$ as they used bracketing technique (i.e. insertion of hydrogen between different experiments)

to regenerate catalysts. Researchers using Pt/Al_2O_3 have divided opinion. Lin et al. [97, 112] and Rousse et al. [89] observed deactivation while Castano et al. [109] reported otherwise. This may be because the latter group used high hydrogen to toluene ratio and thus might have not triggered this deactivation as elucidated through Figure 3.8 i.e. under $H_2/Tol = 19$ conditions rate of activity loss is negligible. The increase in catalytic activity by increase in hydrogen partial pressure is in accordance to the previous observations made by various researchers. They also report the order for toluene nearly equal to zero [100, 103, 105, 106]. In our case increase of toluene partial pressure with no change of H_2 partial pressure has been difficult to achieve. Consequently activity changes cannot be attributed to hydrogen or toluene.

To highlight the activity loss mechanism, several ways of reactivation have been tested. After the stabilisation of catalyst at its equilibrium point, reactivation sequence is initiated by replacing hydrogen with nitrogen at 350 °C for 4 h. Nitrogen is also fed during temperature ramp period in order to avoid any ingression of other gases that can regenerate the catalyst surface. The catalyst is equally reactivated even with nitrogen as that of hydrogen (see Figure 3.9). Also reactivation is found to be purge rate dependent. As adsorption decreases with increase in temperature so, the adsorbent needed only to be purged out at high temperature. Therefore catalyst can be reactivated by any inert gas like nitrogen at high temperature. This fact rules out the possible coke production by polymerisation or cracking which usually requires burning of carbonaceous material through air at high temperature. On the other hand this observation does not exclude higher molecular weight oligomers only if such light polymers are easily desorbed. Catalyst surface modification may also be rejected in wake of same as hydrogen is generally required in rehabilitation of such alterations.

As described by Chupin et al. [107] a kind of polymerisation to dimers and trimers is possible over Pt/Al_2O_3. Such polymers termed as coke may cause such type of activity loss. But precursor used to prepare catalyst by the said group is $[Pt(NH_3)_4]Cl_2$ making catalyst acidic or basic in nature thus promoting such kind of reaction. Whereas we used Pt/ acetylacetonate to prepare the catalyst, which may or may not promote such oligomerisation. The catalyst activation by simple purging via nitrogen at high temperature may be because of light oligomers adsorption type deactivation and not the coke formation.

Nitrogen is generally considered as an inert. However we have verified its effect on the catalyst under study, investigating its decay. Two sets of experiments are done, each set comprises the same partial pressures of toluene and hydrogen while, total and partial pressure of nitrogen are changed. Also the individual residence time of the reactants is same to nullify any decrease in toluene conversion by change in contact time. The results are shown in Figure 3.10. As the catalyst activity essentially remains the same even the

Conversion %	Temp °C	Press. bar	Pt content wt. %	Dispersion %	Tol/H2	TOF s^{-1}	ref
5	100	2	0.5	84.6	0.11	0.11	[109]
>12	60	1	0.78	$\simeq 1$	0.07	0.037	[97]
	75	1	0.06		0.027	0.12	[89]
75	100	1	0.88	54	0.22	0.1	This study

Table 3.6: TOF values for toluene hydrogenation over Pt/Al_2O_3
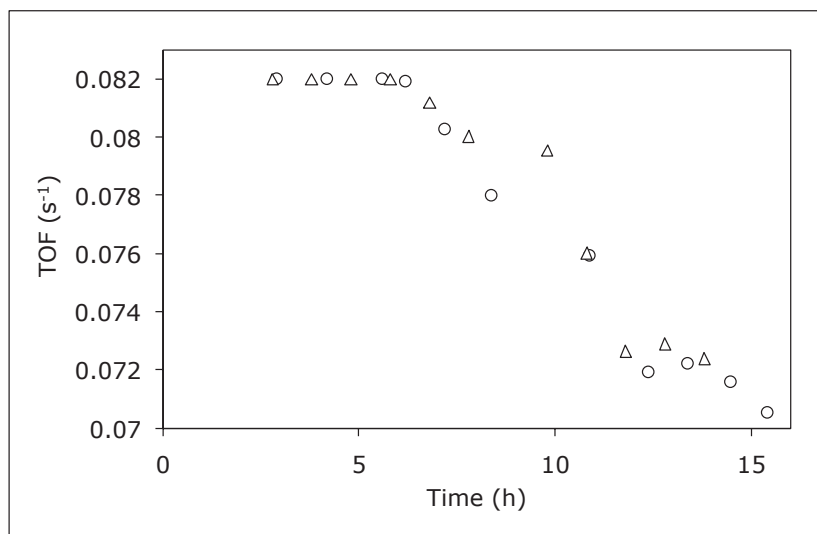
Figure 3.9: Catalyst reactivation. Catalyst activity under standard reaction conditions after reactivation under ∘ − hydrogen, △ − nitrogen

total pressure is increased by increasing the partial pressure of nitrogen so, it can safely be assumed as an inert. The catalyst was stabilised to equilibrium point before conducting this experiment.

As provided in literature [96] and confirmed by chromatography, methylcyclohexane (MCH) is the only product recovered from this reaction (surface species are not considered). So either methylcyclohexane or toluene cause such activity loss or they are reactant to some reaction resulting in such catalyst decay. In order to verify their behaviour two sets of experiments were planned. The time zone selected for this test is with the highest rate of 'deactivation'. In first experiment, after catalyst reactivation, reactor is placed under the same conditions as for standard reaction for 8h with toluene replaced by methylcyclohexane (establishing 100 % toluene conversion condition). The same procedure is repeated for second test with 0 % conversion conditions i.e. toluene and nitrogen are injected in reactor for whole one day shift. The results obtained by standard reaction before and after these 8h are shown in Figure 3.11. It is shown that methylcyclohexane does not incite 'deactivation' and catalyst remain more or less at the same level of activity. On the contrary toluene introduction results in decrease in the catalyst conversion ability. This confirms that activity loss is linked to toluene or some of its surface derivative not present in gas phase in appreciable amounts.

3.3.2.4 OTHER POSSIBLE CAUSES OF ACTIVITY LOSS

Poisoning by any foreign material such as sulphur present in the feed is rejected because of the four observations: i) All reagents used are of laboratory scale purity. Furthermore different grades (laboratory level) of toluene are tested and same rate of deactivation is ob-
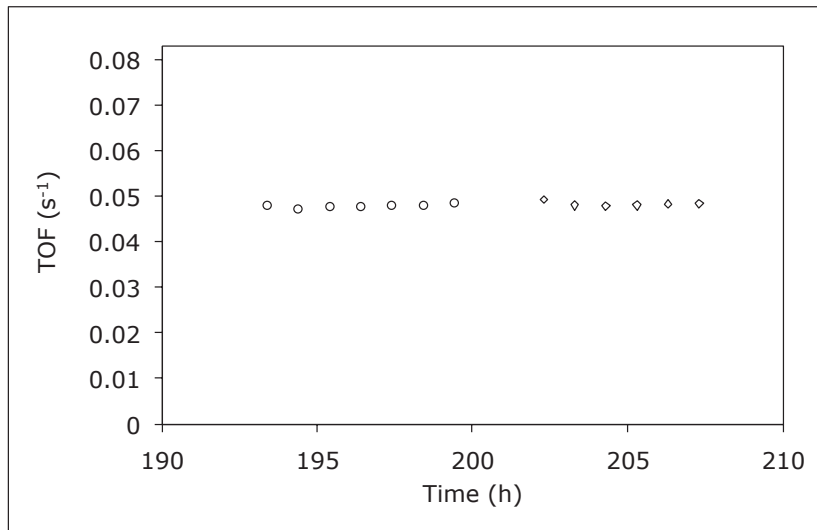
Figure 3.10: Effect of nitrogen on catalyst activity, $P_{H2} = 0.6\,\mathrm{bar}$, $P_{Tol} = 0.1\,\mathrm{bar}$, $\circ - P_{N2} = 0.3\,\mathrm{bar}$, $\tau = 50\,\mathrm{kgcat \cdot s \cdot mol^{-1}}$, $\diamond - P_{N2} = 0.8\,\mathrm{bar}$, $\tau = 33.28\,\mathrm{kgcat \cdot s \cdot mol^{-1}}$

served. Also toluene obtained through the dehydrogenation reaction over same catalyst in a different reactor is also used and the same rate of activity fall is noticed. ii) Deactivation is not linear and dependent on temperature. As if some feed impurity is considered imparting such deactivation then it should decrease as adsorption decreases with temperature (considering no reaction of such impurity with catalyst as confirmed through Figure 3.9). iii) Classical decrease in catalyst activity with increase in residence time and essentially the same deactivation rate i.e. if deactivation is caused by some reagents impurity then deactivation rate should be increased with increase in inlet quantity of reactants as per Figure 3.7b. iv) Catalyst activity does not fall to zero as any poison results in total loss of catalyst activity [134].

In conclusion adsorption type slows deactivation either by toluene or some of its derivative including light oligomers may be responsible for such type of behaviour. Overall Pt/Al_2O_3 is an effective catalyst for toluene hydrogenation even after total activity loss to stabilisation point at low temperature. Enough data is now available with us to determine the effect of CO_2 on this catalyst.

3.3.3 TOLUENE HYDROGENATION WITH CO_2 ON Pt/Al_2O_3

As explained in section 3.2, carbon dioxide can affect platinum catalyst activity at high temperature and can induce a low decay for fuel cell. To highlight CO_2 effects on hydrogenation catalysts, some experiments have been performed using H_2/CO_2 mixtures.

After reactivation and catalyst full activity confirmation, experiments were performed replacing N_2 by CO_2 under standard conditions. Rapid fall in toluene hydrogenation to almost 0 % conversion is observed. Moreover catalyst can not be then reactivated by the
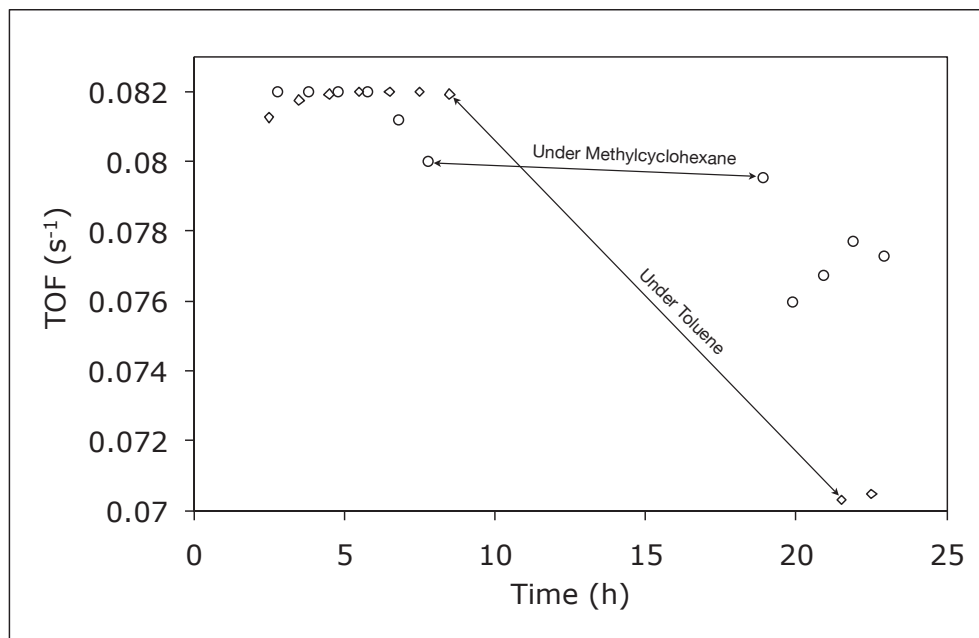
Figure 3.11: Effect of toluene and methylcyclohexane on catalyst activity ∘-Methylcyclohexane ⋄-Toluene

normal routine i.e. heating to $350\,°C$ under hydrogen or nitrogen for 4 h. Regeneration is done by heating the catalyst under air to remove any specie formed by CO_2 on the catalyst surface with subsequent reduction through hydrogen.

To estimate the rate of deactivation, pulses of CO_2 of 10 ml·min^{-1} for approximately 2 s is injected between various samples collected during standard experiments. Results are shown in Figure 3.12a. Rapid deactivation of the catalyst is evident by carbon oxides. The deactivation caused by CO_2 is clearly irreversible at every level in absence of CO_2. Furthermore no CO is detected at $75\,°C$ on the chromatograph.
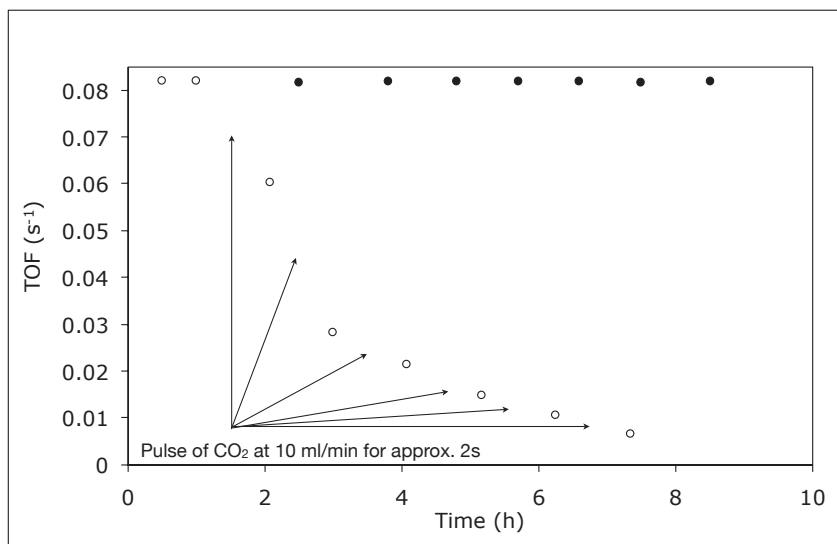
Figure 3.12: ∘ - T=75 °C, Effect of CO_2 on toluene conversion ● - Toluene hydrogenation under no CO_2
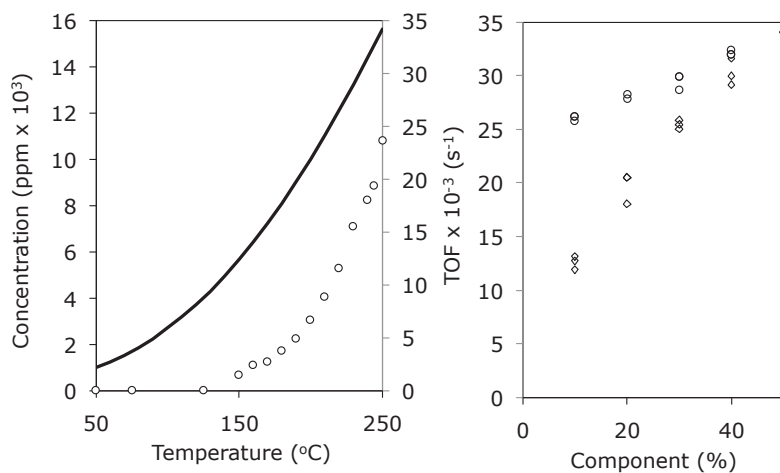
Figure 3.13: P = 1 bar, (a) CO production temperature profile $\frac{H_2}{CO_2} = 1$, Solid lines show the equilibrium TOF (b) Effect of CO_2 and H_2 contents on CO production, ◇ - CO_2, ∘ - H_2

In order to understand the causes of deactivation, an equimolar flow of H_2/CO_2 with no toluene was injected in reactor with increasing temperature. Below $150\,°C$ no change in gas phase composition is detected. But this is not true for temperature above $150\,°C$, where CO is present. However nothing can be said about the surface presence of CO at $75\,°C$.

Figure 3.13a represents the temperature profile of the CO production. The conversion is far less then the equilibrium, thus it is not dictated by thermodynamics but RWGS can't be neglected on this catalyst. The external and internal diffusion resistance factor is calculated and reaction is found to excel in chemical regime.

Effect of carbon dioxide pressure (contrary to toluene) is much more pronounced than that of hydrogen as shown in Figure 3.13b manifesting higher reaction order for CO_2. At $150\,°C$ the CO content in gas phase is 1000 ppm while the detection limit of the chromatograph is approximately 600 ppm. The extrapolation of our results confirms approximately 550 ppm and 150 ppm CO at $125\,°C$ and $50\,°C$ respectively.

In conclusion, Pt/Al_2O_3 is an effective catalyst for toluene hydrogenation as far as it is not subjected to CO_2 flow. CO_2 either itself acts as poison for the said reaction or produces CO, a well known Pt poison, by RWGS. As previously reported [108, 135] toluene hydrogenation depends on support as well as metal counterpart of the catalyst. However as reported through the DRIFTS study conducted by Ferri et al. [133] alumina may form certain type of complexes (carbonates) upon exposure to CO_2. Such carbonates may be the root cause of such rapid deactivation as alumina surface change is expected by CO_2, thus hindering some important step in toluene hydrogenation. In wake of this some other supports are tested with same metallic part i.e. platinum.

3.3.4 SILICA AND TITANIA SUPPORTED PLATINUM CATALYSTS

As CO_2 imparts changes in alumina by altering its surface through CARBONYLS or HYDROXYLS so, the support of the catalyst is changed. Silica based platinum has almost same reported activity as metal deposited on alumina but its inertness towards CO_2 can be exploited (as no study elaborating any effect of CO_2 over silica is found).

Similarly to Pt/Al_2O_3, some toluene hydrogenation experiments with and with no CO_2 have been performed on Pt/SiO_2 and Pt/SiO_2-TiO_2.

As shown in Figure 3.14 catalyst is active under $\frac{H_2}{N_2} = 1$. Pt/SiO_2 TOF is higher compared to Pt/Al_2O_3, however overall activity is far less than that of Pt/Al_2O_3 this is attributed to very low Pt/SiO_2 dispersion ($< 5\,\%$). On the other hand activity drops under $\frac{H_2}{CO_2} = 1$. However selectivity shift is not 100 % and still catalyst can hydrogenate toluene to 11 % of its original activity. This activity loss is not irreversible and catalyst starts to recover as soon as CO_2 is curtailed, although not with exceptional rate. Furthermore contrary to Pt/Al_2O_3, reactivation under hydrogen at $350\,°C$ is enough for total catalyst regeneration.

As conversion is low for Pt/SiO_2, so according to literature, its activity may be enhanced through the addition of titania [97]. Titania powder alone could not be used because of its size being too small resulting in high pressure drop in the reactor.

Accordingly, the activity of this third catalyst is very high in absence of CO_2 but falls to zero in its presence. However the catalyst is regenerated through treatment with hydrogen at $350\,°C$ indicating no surface modification by the acidic gas. It may be concluded for tested Pt based catalysts that the more the catalyst is active in dissociating hydrogen to create drastic conditions for hydrogenating aromatics the more the activity drops with CO_2.
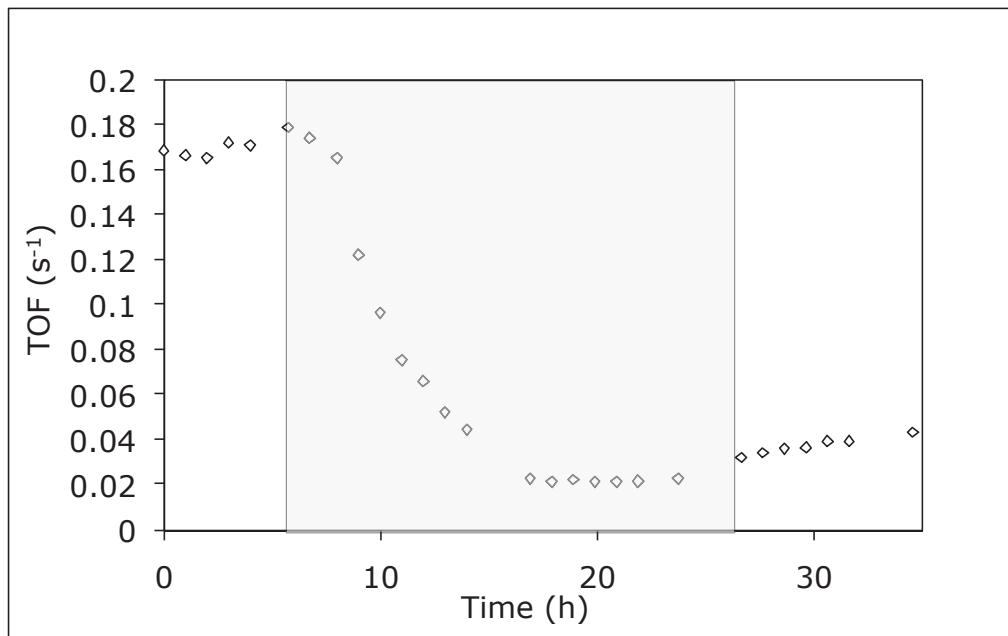
Figure 3.14: Toluene hydrogenation over Pt/SiO_2, Shaded area - $\frac{H_2}{CO_2} = 1$, White area - $\frac{H_2}{N_2}$ = 1, T = 75 °C, τ = 100 kgcat·mol^{-1}·s

For both active catalysts (Pt/Al_2O_3 and $Pt/TiO_2\text{-}SiO_2$), the platinum dispersion is high (54 % and 64 % respectively), whereas the Pt dispersion on Pt/SiO_2 is lower than 5 %. Thus deactivation is probably due to Pt cluster size [116]. This conclusion is in accordance with results on RWGS, where dispersion is an important parameter for catalyst activity. In this case the deactivation could be due to CO formation though no CO is detected with the gas chromatograph for experiments at 75 °C.

Nevertheless the dispersion does not explain why the SiO_2 catalysts are regenerated only with H_2 contrary to Al_2O_3 catalyst. In this case this phenomena is perhaps due to carbonates. In order to confirm our assumptions, some DRIFTS experiments have been performed on Pt/Al_2O_3 and Pt/SiO_2. Some additional results may be seen in chapter 4 where $Pt/SiO_2\text{-}TiO_2$ is used with carboxylic acids hydrogenation in competition with RWGS.

3.4 DRIFTS ANALYSIS

From the hydrogenation results it is evident that platinum based catalysts cannot be used to catalyse toluene hydrogenation in the presence of CO_2. However, further choice of the catalyst remains unclear as logical understanding of the phenomena governing this behaviour is still unknown. Furthermore the mode of activity shift may be because of
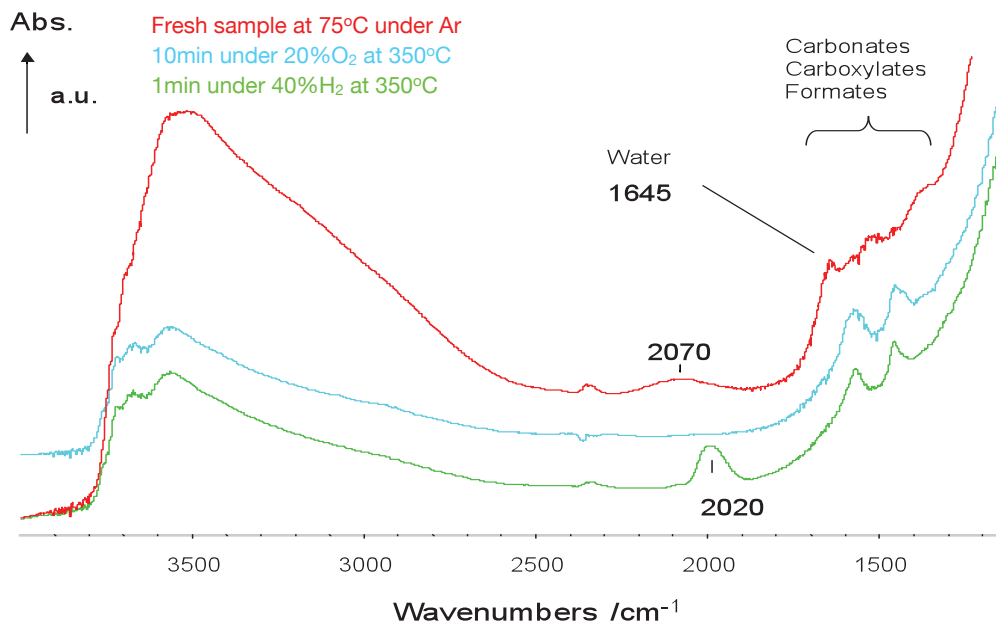
Figure 3.15: In situ DRIFTS spectra of the Pt/Al_2O_3 catalyst: fresh sample (top) under argon at $75\,°C$, sample after 1 min under $40\,\%$ H_2 at $350\,°C$ (bottom), oxidised sample after 10 min under $20\,\%$ O_2 at $350\,°C$ (middle).

several reasons including:

1. Simple competitive adsorption between CO_2 and one of the reactants with toluene.

2. Formation/Mechanism of poisonous CO at $75\,°C$ through the RWGS

3. Effect of water-product of RWGS.

4. Permanent change in catalyst surface by some side reaction.

Competitive adsorption behaviour may be rejected as irreversible shift is observed. While formation of CO at $75\,°C$ is not evident yet thermodynamically possible, therefore an in situ Diffuse Reflectance Infra-red Fourier Transformation (DRIFTS) analysis was conducted at this temperature to probe the possible formation of carbonyl surface species on the metal in collaboration with Mr. Fredric MEUNIER (LCS,Ensicaen). DRIFTS analysis were conducted in a modified cell provided by Spectra-Tech, cell details and operation is provided in annex D.

In Figure 3.15 a comparison between fresh, (partially) reduced and oxidised catalysts is presented. Catalyst tendency to absorb water from atmosphere is clearly depicted by the band at 1645 cm^{-1} for fresh sample catalyst under pure argon. Similarly presence of
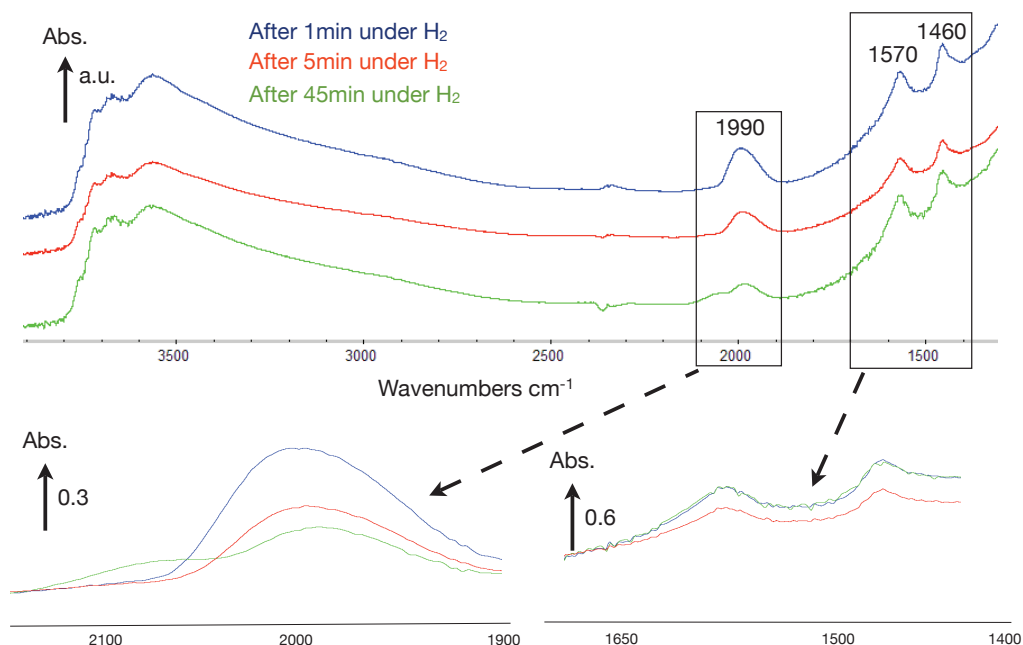
Figure 3.16: In situ DRIFTS transient reduction spectra of Pt/Al_2O_3 catalyst, during reduction by 40 % H_2 (blue-after 1 min, red-after 5 min, green-after 45 min)

carbonates, formates and carboxylate species is provided by the bands between 1700-1200 cm^{-1} (ill defined). These species may either be because of atmospheric carbon dioxide interaction or may have been there since catalyst preparation. The band at 2070 cm^{-1} is because of so-called ABC contour associated with combination bands of hydroxyl groups (and cannot be attributed to carbonyl species). After 1 min during reduction by 40 % hydrogen Pt-carbonyl specie is observed at band 2020 cm^{-1}. Such carbonyl may be because of carbonates, formates and carboxylates elimination from the catalyst surface as shown by the reduced intensity bands between 1700-1200 cm^{-1} compared to fresh catalyst, and their subsequent adsorption over platinum defective sites (linked sites between support and metal). Catalyst oxidation on the other hand by oxygen results in elimination of both hydroxyles and Pt-carbonyl groups observed over fresh and reduced catalyst. However bands between 1700-1200 cm^{-1} are same as that of reduced sample.

In kinetics section we observed that catalyst reduction depends upon hydrogen flow rate and time so transient reduction experiments are performed for the catalyst to get an insight for the catalyst surface changes during activation. As demonstrated by the magnifications of Pt-carbonyl bands at 1990 cm^{-1} in Figure 3.16, this band change with time as reduction proceeds indicating interaction of hydrogen with the removal of these carbonyl. The cause of shouldering of the Pt-CO band for 45 min is not known. On the other hand formate/carbonates bands at (1570/1460 cm^{-1}) does not change with time therefore it may be concluded that Pt-carbonyl group does have role in catalyst reactivation
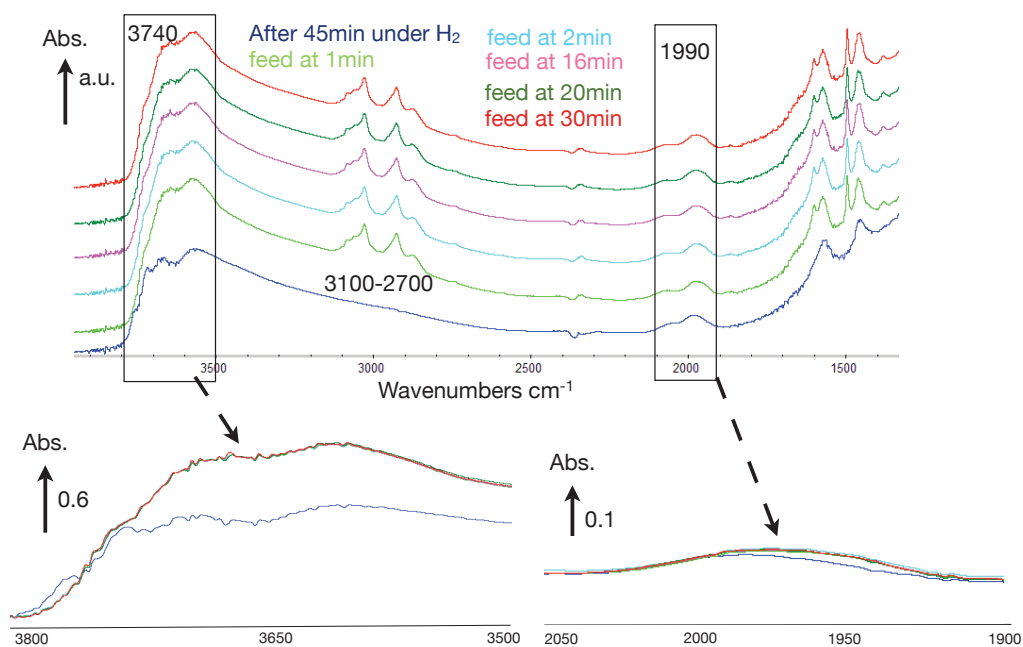
Figure 3.17: In situ DRIFTS toluene hydrogenation with no CO_2 spectra of Pt/Al_2O_3 catalyst, red - 45 min after reduction by 40 % H_2, T = 75 °C, Spectra after 1.6 % toluene and 40 % H_2 injection (from bottom to top after - 1 min, 2 min, 16 min, 20 min and 30 min)

and their removal is coupled with the residual catalytic activity.

In some other experiments (not shown), a reduced sample (never exposed to CO) was left under Ar only after reduction at 75 °C. The carbonyl bands showed a minor but significant shift upon removing H_2, showing that hydrogen adatoms (adsorbed atoms) were present on the Pt particles and interacted with the adsorbed CO. The fact that the carbonyl IR bands shift, when H_2 is present can be due to increased local concentration of carbonyl (e.g. island formation) due to repulsive interaction between CO and H adatoms, as shown for the case of Pt(111) surfaces by Hoge et al. [136].

With the available information at hand, now cell catalyst is subjected to toluene hydrogenation without CO_2. New bands between 3100 - 2700 cm^{-1} (Figure 3.17) corresponding to hydrocarbons appears. Interestingly the hydroxyl bands over alumina at 3740 cm^{-1} are largely modified by the toluene injection indicating that some of the alumina surface hydroxyl groups were in interaction with toluene molecules. Toluene is therefore absorbed in significant quantities on support surface. Similarly slight displacement of Pt-CO band at 1990 cm^{-1} indicates some adsorption of toluene over metallic sites also. The shifts are reversible when toluene is removed. This shows that toluene competes with CO for adsorption on the metal, particularly for the sites associated with the carbonyl band. By comparison, on Pt(111) the adsorption enthalpy of benzene is 71 $kJ \cdot mol^{-1}$, while that of
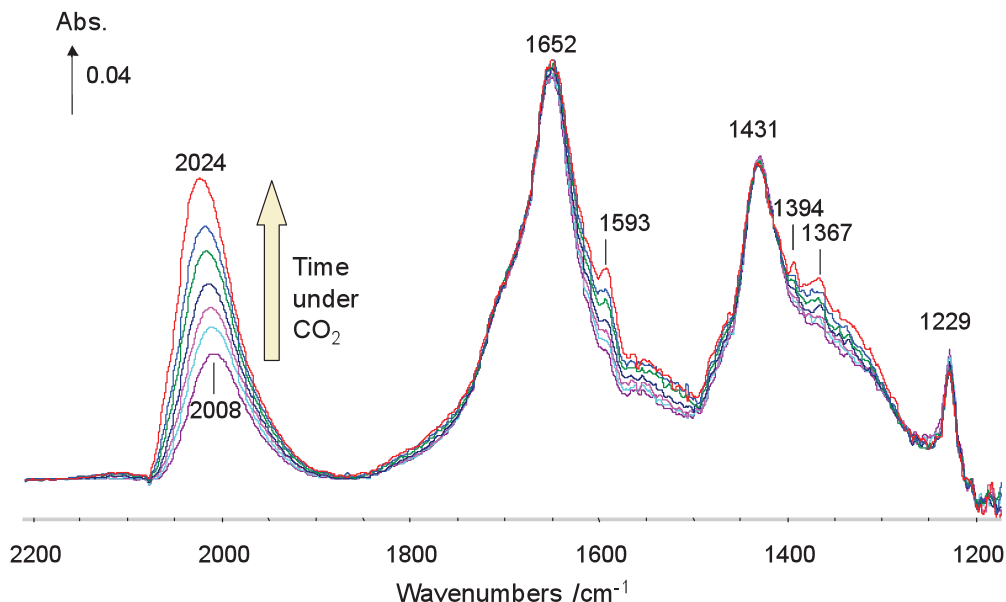
Figure 3.18: In situ DRIFTS spectra of the Pt/Al_2O_3 under a toluene/H_2 feed for various times on stream with additional 40 % CO_2: 81, 176, 273, 470, 847, 1244 and 3645 s. T = 75 °C , the spectrum of the sample recorded at the same temperature under toluene/H_2 was used as background.

cyclohexane is only 27 kJ·mol^{-1} [96]. It is therefore expected that methylcyclohexane desorption is extremely fast once formed and its steady-state coverage on the catalyst is likely negligible. Moreover the difference in toluene adsorption either on metal or support does not change with time. Also remarkable change in formates and carbonates bands 1700-1200 cm^{-1} further proves toluene adsorption over alumina.

As CO_2 is injected in the reactor toluene conversion drops dramatically. The carbonyl signal increases with time as shown in Figure 3.18, however toluene concentration (not shown) does not change. Since most of the toluene DRIFTS signal comes from species adsorbed on the alumina, this stresses that there is essentially no competitive adsorption between toluene and CO_2-derived species formed on the support under our experimental conditions. Additional bands with a positive growth are observed at 1593, 1394 and 1367 cm^{-1}, which corresponds to formate species, probably formed by the reaction of CO with surface alumina hydroxyl groups. It is likely that there are also other carbonate-type species and water present, the signal of which would overlap with the major bands already discussed.

Transition behaviour in toluene loss which was not observable in kinetic study is very eminent in DRIFTS analysis as shown in Figure 3.19. A clear loss in toluene activity with CO_2 injection over the time is presented. Carbonyl and formates increase with the
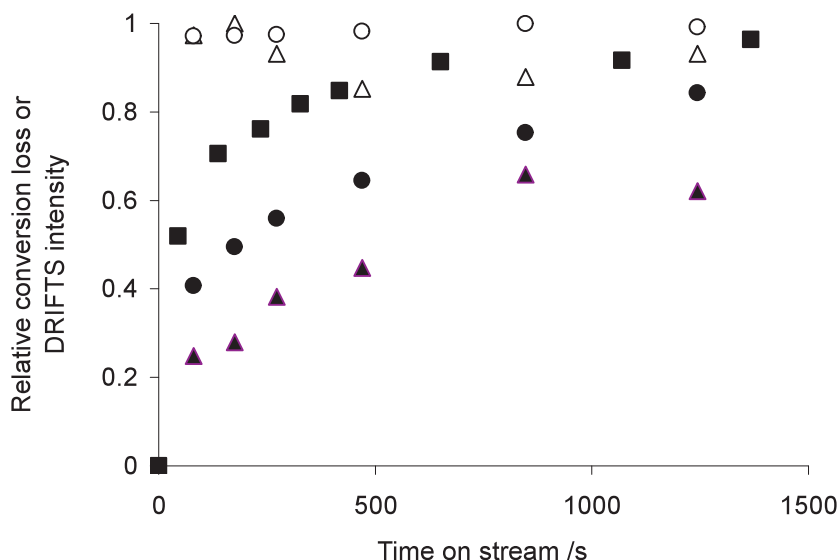
Figure 3.19: Relative conversion loss and DRIFTS intensity vs. time on stream during DRIFTS analysis over Pt/Al_2O_3 with 40 % CO_2 in the toluene/H_2 feed, ■-Relative loss in toluene conversion,•-carbonyl, ▲-formate, △-carbonates, ○-all the bands in the region 1800-1550 cm^{-1}.

same rate as that of toluene conversion drop rate. Not much is seen by analysing other species formation rate. These rates are calculated by integrating the respective peaks. It is interesting to note that full deactivation appears to be reached before the saturation of the Pt sites with carbonyl where as formates reach the saturation point along toluene conversion loss. This suggests some threshold limit of carbonyl species to total toluene conversion loss. Another experiment with 2 % CO_2 is conducted to observe the affect of its concentration (Figure not shown). All other peaks trend as that of Figure 3.19 are same except the formate signal, which was negligible in the case of the deactivation occurring under the feed containing the 2 % CO_2. Therefore it may be suggested that formates are not the origin of the loss of hydrogenation activity and they are only reservoirs of CO_2 over the catalyst surface, making catalyst reactivation by hydrogen slower and flow dependent.

Drop in toluene hydrogenation activity is equally observed for 2 % and 40 % CO_2 concentration in the reactor as shown in Figure 3.20a. The conversion due to the DRIFTS cell reactor filled only with SiC is indicated by the dotted line. However it is very interesting to note that toluene conversion drop corresponds to carbonyl band area irrespective of CO_2 partial pressure (Figure 3.20b). In other words, rate of formation of Pt-CO over catalyst surface is proportional to the CO_2 concentration, but the rate of activity loss is only dictated by number of available Pt-CO sites. This indicates that if formation of such sites is inhibited
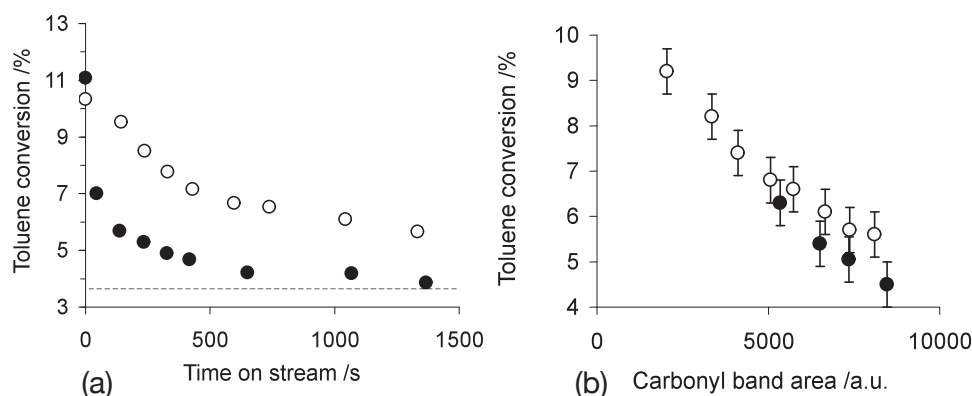
Figure 3.20: Toluene conversion vs. (a) time on stream and (b) carbonyl band area over the Pt/Al_2O_3 for 2 % and 40 % CO_2 concentration, P = 1 bar, $\tau = 1.04\,\text{kgcat}\cdot\text{s}\cdot\text{mol}^{-1}$, Feed: ○- 1.6 % toluene + 40 % H_2 + 2 % CO_2 in Ar, ●-1.6 % toluene + 40 % H_2 + 40 % CO_2 in Ar.

by some mean, CO_2 inert response may be evoked irrespective of its concentration. Such type of behaviour may suggest the preferential type of selective CO poisoning indicating some kind of layer formation between the two reactants i.e. hydrogen and toluene. While all other compounds behave as CO_2 reservoirs.

It is worthy to note that introduction of oxygen even at low temperature of 75 °C removes all kinds of species (bands) from the catalyst surface.

Similarly DRIFTS analysis are conducted for Pt/SiO_2 to compare it with Pt/Al_2O_3 and some interesting observations are made:

1. Apart from OH-groups not much is seen especially Pt-CO before and after catalyst reduction.

2. No carbonate growth is observed after CO_2 injection.

3. Pt-CO band is much smaller compared to that present on Pt/Al_2O_3.

All these points clearly indicate no support surface modification after CO_2 injection and the reaction by the interaction of support and metal prevails, yet much lower than expected mainly because of hydrogen consumption in hydrogenating CO_2 and subsequent metallic
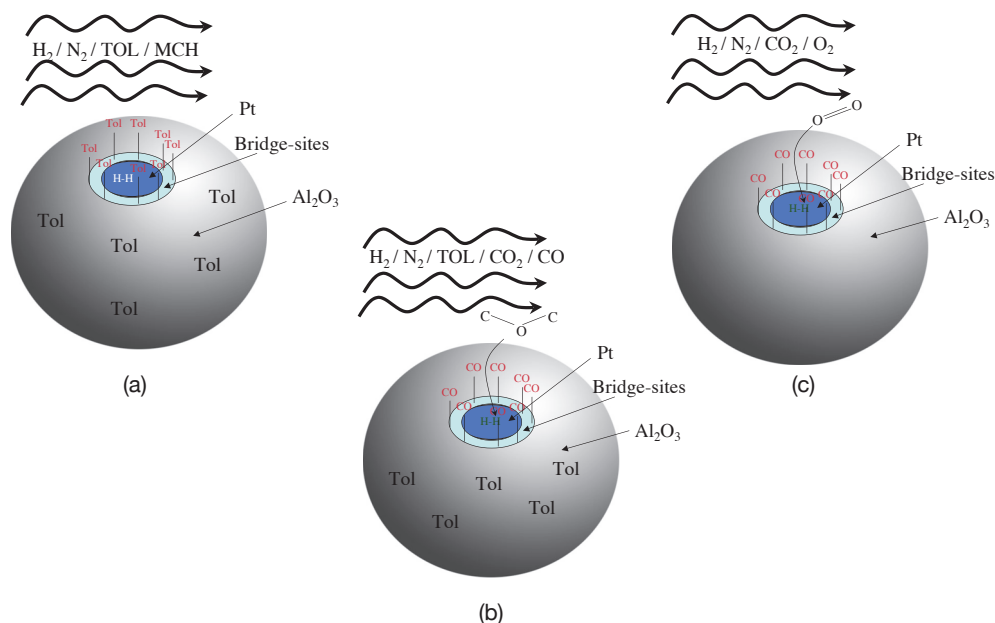
Figure 3.21: (a) - Toluene hydrogenations without CO_2 (b) - RWGS (c) - Effect of air on RWGS

site occupation by CO. CO_2 hydrogenation over Pt/SiO_2 is far less than alumina supported platinum mainly due to low metal dispersion.

Previously two different types of sites for such catalytic system were reported. However hydrogen transfer from one site type to other site is still under discussion. Hydrogen spillover is supported by one group [104] while other reported adjacency of the two different sites [108, 135].

It should be noted that adsorbed toluene is always found on the catalyst surface with or with no CO_2 but the inhibition may not be because of decrease in hydrogen adsorption or preferential consumption of dissociating hydrogen by CO_2 hydrogenation. Hydrogen reduces the catalyst at 350°C and results in partial removal of existing Pt-CO groups present over the surface. On the other hand formates or carbonates are not essentially removed by hydrogen at this temperature. The reverse water gas shift reaction resulting in CO production and hence the Pt-CO surface specie is in fact the basic cause of deactivation when CO_2 is injected. Atomic hydrogen produced over platinum main site is consumed for platinum reduction, formerly oxidised by CO_2 to produce CO, and no surface contact of such hydrogen with toluene is possible in presence of CO on linked sites between metal and support. As desorption of CO is not facile therefore, catalyst activity reversal is not observed upon curtailing CO_2. On the other hand reported reactivation at high temperature (Fuel Cell) is simply the desorption of CO from the bridge sites at such conditions.

In case of alumina based catalyst Pt-CO is not the only surface specie preventing the hydrogenation of toluene and presence of formates/carbonates on support further hinders toluene adsorption over linked sites thus requiring their removal by air. Hydrogen alone, although capable of removing Pt-CO specie, cannot reactivate the catalyst and air is required to remove other types of bands. Also CO_2 increases the carbonates reserve of the support thus may requiring prolong reactivation (for days depending upon the kinetics) under hydrogen to eliminate Pt-CO group formed when large amount of carbonates are removed. Whereas for rest of the Pt catalyst with support other than alumina, hydrogen alone can reactivate the catalyst as no carbonates or formates are observed. Therefore in their case Pt-CO may be the sole specie responsible of such activity loss for toluene hydrogenation under CO_2.

Low Pt dispersion resulting in some toluene conversion in the presence of CO_2 for silica based catalyst may also be explained. Pt-CO group is formed over interaction sites between metal and support. Such sites are less in number for Pt/SiO_2 because of low dispersion. Ratio of toluene adsorbed over Pt metal is thus higher to that of linked sites, so some conversion because of this toluene is observed. On the other hand when metal is well dispersed (Pt/SiO_2-TiO_2), its metallic ability to adsorb toluene decreases (considering toluene planner adsorption). As the only toluene converting to methylcyclohexane is that which is adsorbed on linked sites in contact to dissociating hydrogen, which are vulnerable to CO poisoning via preferential adsorption. Therefore it may be concluded that more the catalyst is equipped with linked sites, more it is hydrogenation efficient but less resistant to CO poisoning. Bimetallic catalyst may become immune to such type of CO poisoning because their toluene adsorption ability over metallic surface may be higher. Furthermore they may also decrease the energy of adsorbed CO by altering surface configuration of metal, resulting in weakening of CO cover during hydrogenation.

A proposed mechanism combining above observations is presented by Figure 3.21.

3.5 REACTION KINETICS

At the same time along the study of CO_2 effect understanding, additional kinetics studies have been performed for toluene hydrogenation with no CO_2 and RWGS based on our experimental results.

These studies are not directly linked to biogas valorization but have allowed a comparison between our and literature results.

3.5.1 KINETICS OF TOLUENE HYDROGENATION WITH NO CO_2

For toluene hydrogenation both approaches have been studied i.e. empirical one and a more mechanistic one.

3.5.1.1 EMPIRICAL LAW

According to Levenspiel [137] all the deactivating catalysts can be modelled empirically by the following set of equations:

$$r_A = -kC_A^x \varphi \tag{3.7}$$

$$\frac{\mathrm{d}\varphi}{\mathrm{d}t} = -k_d C_A^y \varphi^d \tag{3.8}$$

First equation (3.7) predicts the reaction rate while equation (3.8) estimates the available activity of the catalyst. These equations are modified for gaseous system by replacing concentration to partial pressure for individual components, and curve fitted. Parameters are estimated in two stages for these equations, first regression of the deactivation curve is done to get a general trend. The best fit shows that deactivation is an exponential function thus implying 'd = 1'. With this value of 'd' the general solution of equation (3.8) is given as follow:

$$\varphi = C_I \cdot exp(-k_d C_A^y t) \tag{3.9}$$

Value of exponential in equation (3.9) is provided by the exponential regression curve. This value is same for any given temperature. However value of C_A varies with time but k_d remain the same. Therefore value of y is adjusted to achieve constant k_d for conversion at different times. After estimating the values of k_d and y, φ in equation (3.7) is replaced by the equation (3.9). Resulting equation is then solved with all the values known except k and x which are estimated with a hit and trial optimization routine. Similarly the same procedure was repeated to estimate parameters at higher temperatures. This model does not achieve equilibrium state and activity fall to zero.

The resulted equations for empirical model are shown as follow (3.10) & (3.11):

$$r_A = -7.8 \cdot 10^{-3} \exp\left(\frac{-21.48}{T}\right) P_{H2}{}^{0.5} P_{Tol}{}^{0.1} \varphi \qquad [\frac{moles}{s \cdot kg \cdot cat}] \tag{3.10}$$

$$\frac{d\varphi}{dt} = -2.47 \cdot 10^5 \frac{P_{Tol}}{P_{H2}} \varphi \qquad [s^{-1}] \tag{3.11}$$

Many researchers have reported the order of the reaction as a function of temperature [89, 99, 100, 105, 106]. This postulate is controversial, as it is the rate constant that turns out to be temperature dependent and not the reaction orders. This empirical model is developed in wake of same i.e. to verify the independence of reaction orders on temperature. So, as depicted by the equations (3.10) & (3.11) does not show any dependence of reaction orders on temperature. However if deactivation is not considered then it will only converge if these are supposed to depend on temperature. So, the previous studies do not mention the catalytic deactivation but it was not detected because of small experiment durations. However with augmentation in temperature deactivation increases, therefore the data collected by other researchers may inculcate inherent catalytic deactivation. This shows that a simple empirical model without deactivation term cannot cope with the situation until or unless, order of reaction is defined as temperature dependent.

3.5.1.2 MECHANISTIC MODEL

In order to develop a mechanism for toluene hydrogenation number of assumptions are presumed.

The assumptions are described in Table 3.7 along with their basis. According to them

No.	Assumption	Basis
1	Activity loss is caused by adsorption of possible oligomers formation.	$\Rightarrow$ Reactivation dependence on purge rate (& Figure3.8).
2	There are two types of sites available for reagents adsorption, one offered by metal (S1), other dependent on support-metal interaction (S2).	$\Rightarrow$ Rate of reaction differs with different supports. [105]
3	All metal-support interaction sites (S2) are occupied by toluene	$\Rightarrow$ No activity if only alumina is used as catalyst [108]. $\Rightarrow$ Empirical model shows the order of reaction is close to zero implying abundant amount of toluene available for conversion
4	No metallic site is vacant. All metallic sites at start of reaction are occupied by hydrogen gradually replaced by toluene (or oligomers) until saturation. This gradual procurement of sites by toluene (or oligomers) is presumed as basis of poison base catalyst deactivation. So competitive type adsorption over metallic sites prevails.	$\Rightarrow$ Vacant sites presence needs estimation via LHHW [a] model, requiring quasi state equilibrium assumption for individual component thus inhibiting poison base catalyst deactivation $\Rightarrow$ Catalyst is reactivated by nitrogen (Figure 3.8) and activity is inhibited by toluene or oligomers produced by toluene (Figure 3.11).
5	Reaction takes place between toluene adsorbed on S2 sites and the hydrogen present on S1 sites. Transfer of hydrogen to S2 sites may be because of hydrogen spillover, hydrogen jump or just because, two sites (S1 and S2) are adjacent to each other. This is rate determining step i.e. transfer of H_2 to S2.	$\Rightarrow$ The strong bonded hydrogen results in SMSI effect and slightly tied hydrogen molecules are indeed involved in toluene hydrogenation [110]
6	Rate of hydrogenation for toluene present on metallic sites is negligible or in-existent compared to the reaction occurring on S2 sites.	$\Rightarrow$ Two sites mechanism is assumed
7	Conversion of toluene to methylcyclohexane is irreversible under the chosen conditions and no inhibition of sites is considered by the product.	$\Rightarrow$ Figure 3.11 $\Rightarrow$ Section 3.4
8	Dissociative type adsorption of hydrogen	$\Rightarrow$ Site balance for model is not achieved other wise.

Table 3.7: Various postulates assumed to establish toluene hydrogenation reaction mechanism

[a]LANGMUIR-HINSHELWOOD-HOUGEN-WATSON

a reaction mechanism for the 'transition stage' is developed for the following equations:

$$\text{(3.12a)}$$

$$H_2 + S1 \quad \underset{r_{d,H_2}}{\overset{r_{ad,H_2}}{\rightleftharpoons}} \quad 2H^{S1} \tag{3.12b}$$

$$\text{(3.12c)}$$
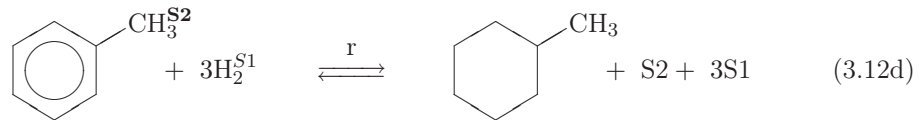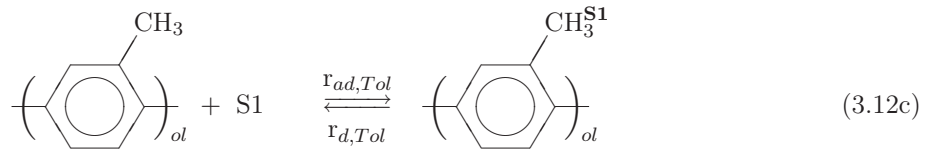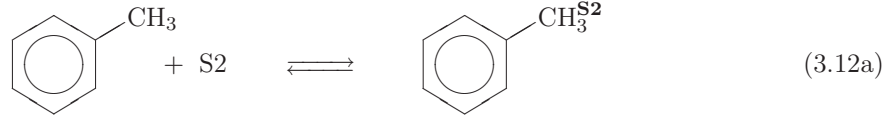
$$\text{(3.12d)}$$

At time $= 0$, all the metallic sites (S1) are occupied by hydrogen(3.12b) while, those of the metallic-support interaction (S2) are occupied by toluene (3.12a) (Assumption 2 & 3). The equation (3.12d) represents the reaction between hydrogen adsorbed on the metallic sites with toluene adsorbed on the metallic-support interaction sites (Assumption 5). Furthermore the equation (3.12c) represents that at any real time there are no vacant metallic sites available i.e. any metallic site liberated either by reaction or desorption of reactants is instantaneously occupied by the reactants or by any light oligomer of toluene. This corresponds to the competitive adsorption behaviour of hydrogen and toluene or "oligomers" over metallic site vacancies (Assumption 4). The distinction between toluene and/or oligomer (from toluene) has not been possible from the experimental work. However in our case, toluene adsorption or desorption rate could be taken as oligomer adsorption or desorption rate, where oligomer adsorption rate includes oligomer formation rate from toluene and its adsorption.

According to Assumption 5, the hydrogen transfer to alumina is therefore proportional to the number of sites occupied by the hydrogen and to the hydrogen partial pressure. This can be written as in the following equation:

$$r = kP_{H_2}^{\alpha}\mathbb{C}_{H_2} = kP_{H_2}^{\alpha}(\mathbb{C}_t - \mathbb{C}_{Tol}) \tag{3.13}$$

Also as deduced from assumption 4 (no vacant metallic site) the overall site balance become 0 thus:

$$3r + r_{d,Tol} + r_{d,H_2} = r_{ad,Tol} + r_{ad,H_2} \tag{3.14}$$

$$\Rightarrow \frac{3r}{r_{ad,Tol} + r_{ad,H_2} - r_{d,Tol} - r_{d,H_2}} = 1 \qquad (3.15)$$

As toluene or oligomer adsorbed on metallic sites does not take part in the reaction, (assumption 6), so any change in the number of toluene metallic sites is simply the difference between its rate of adsorption and desorption as:

$$\frac{d\mathbb{C}_{Tol}}{dt} = r_{ad,Tol} - r_{d,Tol} \qquad (3.16)$$

Multiplying equation (3.15) with (3.16)

$$\frac{d\mathbb{C}_{Tol}}{dt} = \frac{3r \cdot (r_{ad,Tol} - r_{d,Tol})}{r_{ad,Tol} + r_{ad,H_2} - r_{d,Tol} - r_{d,H_2}} \qquad (3.17)$$

The adsorption rate for hydrogen and toluene or oligomer is simply proportional to the partial pressures of hydrogen and toluene and the rate of metallic site liberation. While desorption rate is simply proportional to the platinum sites occupied by individual species so, in the above equation (3.17)

$$r_{ad,Tol} = k_{ad,Tol} P_{Tol} R_{site\ liberation} \qquad (3.18a)$$

$$r_{d,Tol} = k_{d,Tol} \mathbb{C}_{Tol} \qquad (3.18b)$$

$$r_{ad,H_2} = k_{ad,H_2} P_{H_2}^{\frac{1}{2}} R_{site\ liberation} \qquad (3.18c)$$

$$r_{d,H_2} = k_{d,H_2} (\mathbb{C}_t - \mathbb{C}_{Tol}) \qquad (3.18d)$$

$$where: R_{site\ liberation} = 3r + r_{d,Tol} + r_{d,H_2} \qquad (3.18e)$$

In equation (3.17), the fraction $\frac{r_{ad,Tol} - r_{d,Tol}}{r_{ad,Tol} + r_{ad,H_2} - r_{d,Tol} - r_{d,H_2}}$ (Γ) calculates the probability of toluene or oligomer to compete for the metallic sites and can be termed as the 'deactivation' factor. As the reaction is limited by hydrogen transfer dependent upon hydrogen adsorption, which is in turn dependent upon toluene adsorption, then according to this model toluene or oligomer adsorption on metallic sites is the root cause of 'deactivation' (assumption 1). Thus, equation (3.19) is written so as to show the 'deactivation' term in the model.

$$\frac{d\mathbb{C}_{Tol}}{dt} = \Gamma \cdot 3r \qquad (3.19)$$

where

$$\Gamma = \frac{r_{ad,Tol} - r_{d,Tol}}{r_{ad,Tol} + r_{ad,H_2} - r_{d,Tol} - r_{d,H_2}} \qquad (3.20)$$

These equations (3.13) & (3.19) are combined with the mass balance equation for a plug flow reactor and the simulation results are shown in Figures 3.22 & 3.23. Unlike for the empirical model, this model includes the equilibrium limit and the catalyst does not deactivate further beyond a certain limit, dictated by temperature and reactant mixture composition. By applying boundary conditions on equation (3.17) i.e. at t $= \infty$, $\frac{d\mathbb{C}_{Tol}}{dt} = 0$(equilibrium state)

$$\Rightarrow (r_{ad,Tol} - r_{de,Tol}) = 0 \qquad as \qquad 3r \neq 0 \qquad (3.21)$$

Solving above equation for $k_{ad,Tol}$ gives

$$k_{ad,Tol} = \frac{k_{d,Tol}}{P_{Tol}[3kP_{H_2}^{\alpha}(\frac{\mathbb{C}_t}{\mathbb{C}_{Tol}} - 1) + k_{d,Tol} + k_{d,H_2}(\frac{\mathbb{C}_t}{\mathbb{C}_{Tol}} - 1)]} \tag{3.22}$$

Also from the metallic site mass balance it is concluded that

$$k_{ad,Tol}P_{Tol} + k_{ad,H_2}P_{H_2}^{\frac{1}{2}} = 1 \tag{3.23}$$

Hydrogen dissociative type adsorption is mathematically confirmed for metallic sites as the above model does not converge otherwise.

From standard experimental observations, the deactivation seems to stop when $\sim 81\%$ of catalyst surface is occupied by toluene. The total number of sites from catalyst surface calculations comes out to be $\mathbb{C}_t = 0.0244$ mol·kgcata^{-1}, this implies that at $t = \infty$, $\mathbb{C}_{Tol,\infty} = 0.0198 mol \cdot kgcata^{-1}$. Knowing that the average partial pressures throughout the reactor are $P_{Tol} = 5705$ Pa and $P_{H2} = 35154$ Pa, the above equation can be solved to estimate the value of K_{Tol} and hence K_{H_2} (the ratios between k_{ad} and k_d), thus decreasing the number of parameters to be estimated. An in-house program was written to achieve this and the resulting parameters obtained are found to follow Arrhenius trend (Figure 3.24) Pre-exponential factors, activation energy and enthalpy for adsorption to desorption ratio $(\frac{k_{ad,x}}{k_{d,x}})$ in comparison to previous findings are reported in Table 3.8.

The transition behaviour discussed is caused by toluene adsorption over the metallic sites. The activity variation calculated by model is shown in Figure 3.25. Catalyst activity decreases rapidly for initial reactor zones compared to latter ones. It readily explains the effect of reaction rate on activity loss; the higher the rate of hydrogenation the greater the toluene or oligomer adsorption induced activity loss will be. This is also confirmed by the temperature rise activity augmentation (Figure 3.26).
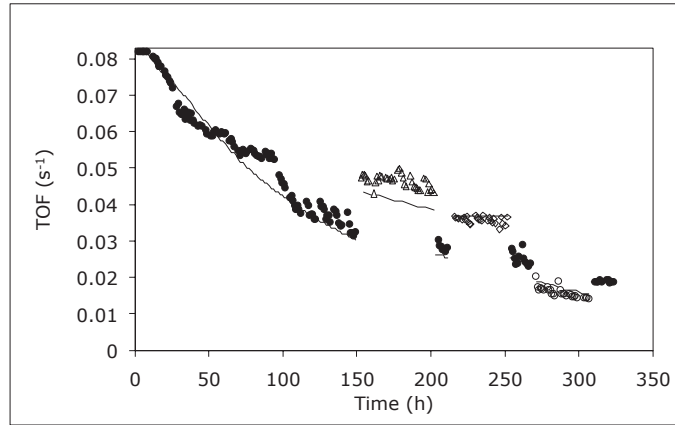
Figure 3.22: Mechanistic model , $\tau = 50$ kgcat $\cdot$ s $\cdot$ mol^{-1}, T= 75°C, P=1 bar, $——$model, $\bullet -$ standard conditions, $\triangle - P_{H2} = 0.9$ bar, P$_{Tol} = 0.1$ bar, $\diamond - P_{H2} = 0.95$ bar, P$_{Tol} = 0.05$ bar, $\circ - P_{H2} = 0.3$ bar, P$_{Tol} = 0.1$ bar
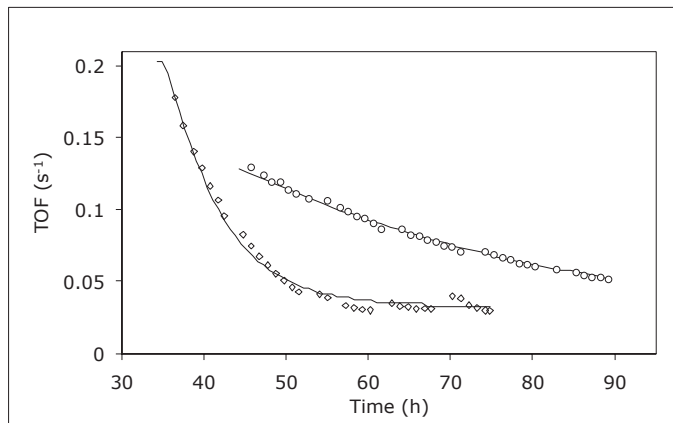
Figure 3.23: Mechanistic model at high temperature, $P_{H2} = 0.45\,\mathrm{bar}$, $P_{Tol} = 0.1\,\mathrm{bar}$, —–model, $\circ - T = 100\,°C$, $\tau = 30\,\mathrm{kgcat \cdot s \cdot mol^{-1}}$, $\diamond - T = 125\,°C$, $\tau = 20\,\mathrm{kgcat \cdot s \cdot mol^{-1}}$

Parameter	Pre-exponential factor	$\triangle H_{ad}$ - $\triangle H_d$ kJ/mol	ref
$\dfrac{k_{ad,TOL}}{k_{d,TOL}}$	8×10^3	-4.7	This study
$\dfrac{k_{ad,H_2}}{k_{d,H_2}}$	1.88×10^2	-2.1×10^{-3}	This study
		Activation energy	
k	1.06	24	This study
k	-	42.2	[89]
k	-	25	[87]

Table 3.8: Activation energy and pre-exponential factors for toluene hydrogenation over Pt/Al_2O_3

69
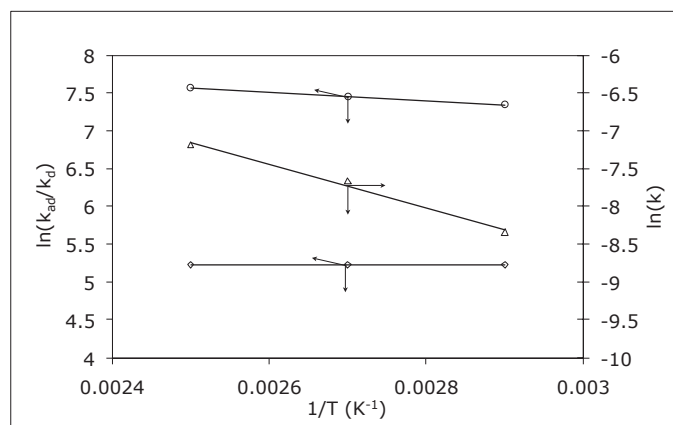
Figure 3.24: Arrhenius graph for coefficients (Mechanistic Model), $\circ$ − Toluene, $\diamond$ − Hydrogen, $(K = k_{ad}/k_d)$, $\triangle$-Rate constant
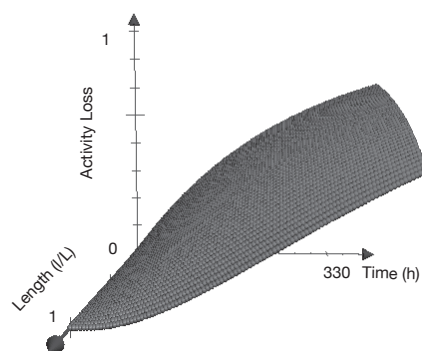
Figure 3.25: Activity variation trend in reactor, standard reaction conditions.
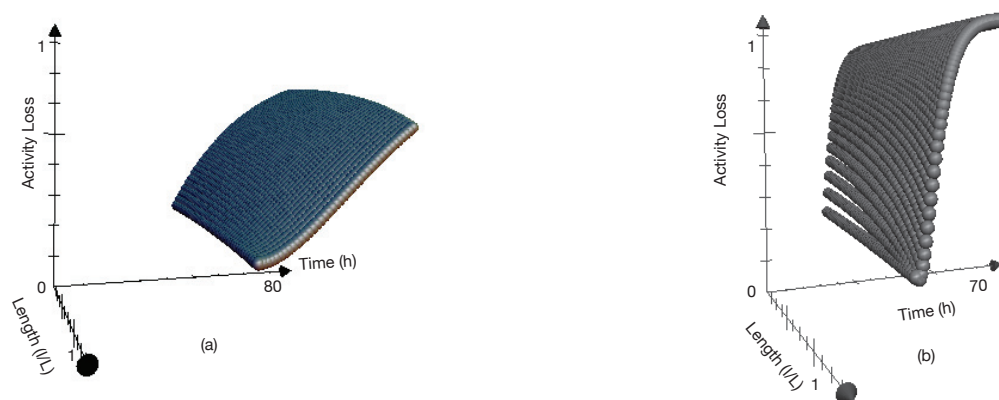
Figure 3.26: Activity variation trend in reactor, (a) $-\mathrm{T} = 100\,^{\circ}\mathrm{C}$, $\tau = 30\,\mathrm{kgcat} \cdot \mathrm{s} \cdot \mathrm{mol}^{-1}$ (b) $-\mathrm{T} = 125\,^{\circ}\mathrm{C}$, $\tau = 20\,\mathrm{kgcat} \cdot \mathrm{s} \cdot \mathrm{mol}^{-1}$

3.5.2 KINETICS OF REVERSE WATER GAS SHIFT (RWGS)

Reaction kinetics for RWGS reaction at low temperature is useful in explaining the permanent activity shift of the catalyst. A number of assumptions inferred from the experiments are shown in Table 3.8 along their possible basis.

No.	Assumption	Basis
1	H_2 adsorbs on metallic sites	No hydrogenation reaction if Pt is not present.
2	CO_2 directly forms CO and adsorbed oxygen	Pt is well known for its oxygen affinity.
3	Nascent hydrogen produced by Pt scavenges adsorbed oxygen and is rate determining step	As oxygen eliminates all types of bands (DRIFTS analysis) and hydrogen rehabilitates the active sites
4	CO adsorption may hinder the reaction by adsorbing on metallic sites	DRIFTS analysis Model do not converge properly otherwise
5	Water poisoning is negligible	DRIFTS analysis Its effect makes the fitting curve convex

Table 3.9: Assumptions to derive CO_2 hydrogenation mechanism

So logical conclusion to the mechanism of the reaction is shown in equations (3.24a)-(3.24d)

$$H_2 + 2\theta \underset{r_{d,H_2}}{\overset{r_{ad,H_2}}{\rightleftharpoons}} H^* \tag{3.24a}$$

$$CO_2 + \theta \underset{r_{d,CO_2}}{\overset{r_{ad,CO_2}}{\rightleftharpoons}} CO + O^* \tag{3.24b}$$

$$CO + \theta \underset{r_{d,CO}}{\overset{r_{ad,CO}}{\rightleftharpoons}} CO^* \tag{3.24c}$$

$$2H^* + O^* \overset{r}{\longrightarrow} H_2O + 3\theta \tag{3.24d}$$
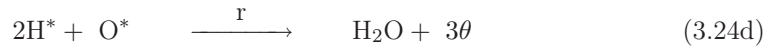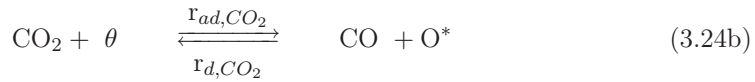
The adsorption and desorption steps presented by equations (3.24a), (3.24b) and (3.24c)

are assumed to be in quasi state equilibrium.

$$r_{ad,H_2} = r_{d,H_2} \tag{3.25a}$$

$$k_{ad,H_2} P H_2 \theta^2 = k_{d,H_2} H^{*2} \tag{3.25b}$$

$$H^* = (K_{H_2} P_{H_2} \theta^2)^{\frac{1}{2}} \tag{3.25c}$$

$$r_{ad,CO_2} = r_{d,CO_2} \tag{3.25d}$$

$$k_{ad,CO_2} P CO2 \theta = k_{d,CO_2} P_{CO} O^* \tag{3.25e}$$

$$O^* = \frac{K_{CO_2} P_{CO_2} \theta}{P_{CO}} \tag{3.25f}$$

$$r_{ad,CO} = r_{d,CO} \tag{3.25g}$$

$$k_{ad,CO} P CO \theta = k_{d,CO} CO^* \tag{3.25h}$$

$$CO^* = K_{CO} P_{CO} \theta \tag{3.25i}$$

According to assumption No.3, the rate of reaction is thus determined by following equation

$$r = k H^{*2} O^* \tag{3.26}$$

Also the site balance becomes equal to

$$\theta + H^* + O^* + CO^* = C_t \tag{3.27}$$

Solving the above equations a mechanistic model is derived and is shown by equation (3.28)

$$r = \frac{C_t{}^3 k K_{H_2} K_{CO_2} P_{H_2} P_{CO_2}}{P_{CO}(1 + (K_{H_2} P_{H_2})^{\frac{1}{2}} + \frac{K_{CO_2} P_{CO_2}}{P_{CO}})^3} \tag{3.28}$$

The model is in good agreement with experimental data is shown in Figure 3.27a. As discussed in DRIFTS analysis, if water bonding is considered in deriving above equation it results in more convex curve and fitting becomes poor. Parameters estimation is also done for temperature profile and resulted parity diagram is shown in Figure 3.27b. The corresponding pre-exponential factor, activations energy and ratio of adsorption to desorption enthalpies can be seen in Table 3.10

3.6 CONCLUSION

Overall platinum is an efficient catalyst for hydrogenation but the selectivity shift from toluene to CO_2 hydrogenation is the basic cause of its inactivity towards toluene in presence of CO_2 even at low pressure and temperature. Mechanistic details provided for CO base inhibition may be very useful in exploring other catalysts e.g. bimetallic to realise aromatic hydrogenation in its presence. Such catalyst if developed, may also be used in fuel cells as possible CO production via CO_2 containing hydrogen diminishes their electric potential.
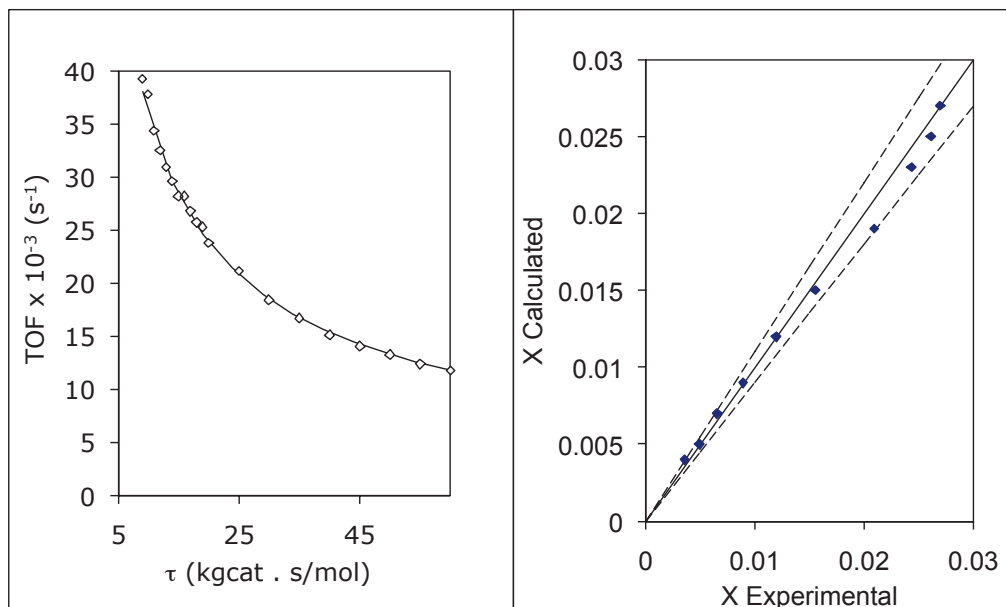
Figure 3.27: RWGS reaction kinetics (a) ◇ - experimental data, - model, (b) Parity diagram for parameters estimation

Alumina for its ability to interact with CO_2 to form carbonates or formates is not further be used as support for toluene hydrogenation under CO_2. Behaviour of other metals like cobalt or nickel is not sure as both of them are equally good for RWGS also. On the other hand it is worthy to note that because of strong adsorption of CO over platinum, some other unsaturated compound hydrogenation having comparable adsorption energy to that of CO (toluene adsorption energy is much lower) may be realised. This may result in breach of the inhibitory layer produced by CO and the availability of dissociative hydrogen to other reactant may be possible. Acetic acid adsorption energy is about 134 - 146 kJ/mol [138] which is comparable to that of CO adsorption enthalpy of 144 - 173 kJ/mol (for toluene it is 50 - 60 kJ/mol) thus some selectivity shift from RWGS to acid hydrogenation may be possible in presence of CO_2. Furthermore these acids are also present in the fermentor as co-product of hydrogen containing biogas. In next chapter we will deal with their hydrogenation in detail.

Parameter	Pre-exponential factor	Activation energy kJ/mol
k	1.44×10^{19}	73.21
		$\triangle H_{ad} - \triangle H_d$
K_{CO_2}	7533	-40.37
K_{H_2}	1.1×10^6	-47.46
K_{CO}	304	-27.88

Table 3.10: Activation energy and pre-exponential factors for CO_2 hydrogenation over Pt/Al_2O_3

4

CARBOXYLIC ACIDS CONVERSION

4.1 INTRODUCTION

In the section 2.2.3, we have seen that process of hydrogen formation through fermentation is coupled with the production of aliphatic carboxylic acids (Volatile Fatty Acids-VFAs). These acids are the main cause of change in pH in bioreactor. They are abundant, low value products and are usually fermented to methane in subsequent process as shown in Figure 4.1. The ethanol is produced in the second step, however it is diluted with water thus require high energy for their purification. On the other hand, if we use these acids produced in first step via catalytic hydrogenation reaction to produce valuable products, a green process may be envisaged.

These acids should be removed continuously from the reactor as pH control is crucial for microbial life in dark fermentative environment. Hybrid processes (section: 2.2.4) on the other hand consume these acids and hence are avoided for VFAs production. These acids are usually mixture of acetic, butyric and occasionally propionic, lactic, succinic and pentanoic acids. The mixture composition and the yields depend on the waste treated, bacterial strain and process used for fermentation. Some examples of recent published results are given in Table 4.1.

Dinamarca and Bakke [140] conducted a useful study on acids and hydrogen yield balance. According to them, acids production can be increased at the expense of hydrogen reduction. Mixed microbe culture (non treated inocculum) will result in significant decrease in hydrogen production as described in section 2.3.1, however on the other hand, this may be useful in enhancing VFAs. These VFAs thus produced are mainly composed of acetic and butyric acids. Han and Shin [141] gave a comparative study on the effect of retention time and initial dilution rate over VFAs production. They concluded that food wastes are easily fermented to hydrogen and acids while optimum dilution exists for hydrogen production. However after certain retention time, hydrogen ceases to produce but acids production in fermenter continue. Similarly, the effect of soaring may also be exploited to enhance VFAs production [27, 67]. Wang et al. [23] studied the effect of temperature, pH and substrate concentration on the yield of respective acids. High temperature (i.e. $\sim 41\,^{\circ}\mathrm{C}$) favours the VFAs and higher acids (butyrate) are dominant. A pH of 6 is reported optimal for

Reactor type	Substrate type	Substrate concentration (g/l)	VFAs concentration (g/l)	Reference
CSTR[a]	Glucose	4270	2551	[73]
Batch	Glycerol	5	1.43	[139]
UASB[b]	Glucose	2	1.42	[77]
Batch	Starch	9.23	4.39	[37]
Batch	Waste Water	3.4 $\frac{COD}{m^3 \cdot day}$	2.68	[76]
Batch	Rice		14.405	[33]

[a]Continuous stirred tank reactor
[b]Upflow anaerobic sludge blanket reactor

Table 4.1: VFAs produced with hydrogen production

butyric acid production with 91 % purity and 45 % yield from glucose through an extractive fermentation technique [142].

In fermenter, depending on pH level VFAs are dissolved in water as salts (e.g. acetates). To remove the maximum amount of VFAs, the pH have to be dropped. In the following work we are only interested in VFAs conversion, considering these salts can be transformed in VFAs.

As previously seen in chapter 3 raw biogas to hydrogenate hydrocarbons could be valorized with low efficiency only over poorly dispersed catalyst having little activity for RWGS. On the other hand RWGS catalysts may be efficient to reduce oxygenated molecules like carboxylic acids because of their high acidity compared to CO_2, making the former to adsorb preferentially over the catalyst surface. Consequently this chapter is the synthesis of published work and our findings on the valorization of VFAs and biogas at the same time, using catalytic process.

The main overall reactions for acetic acid reduction reported in literature are summarised below:

$$CH_3 - \overset{\overset{\displaystyle O}{\|}}{C} - OH \ + \ H_2 \quad \longrightarrow \quad CH_3 - \overset{\overset{\displaystyle O}{\|}}{C} - H \ + \ H_2O \qquad (4.1)$$

$$CH_3 - \overset{\overset{\displaystyle O}{\|}}{C} - OH \ + \ 2H_2 \quad \longrightarrow \quad CH_3 - CH_2 - OH \ + \ H_2O \qquad (4.2)$$

$$CH_3 - \overset{\overset{\displaystyle O}{\|}}{C} - OH \ + \ 3H_2 \quad \longrightarrow \quad C_2H_6 + \ 2H_2O \qquad (4.3)$$

78

Biogas from Dark Fermentation
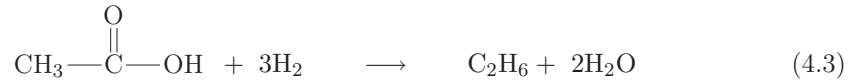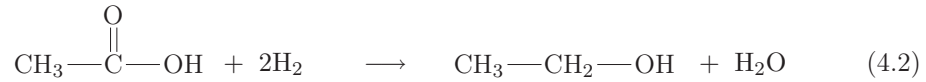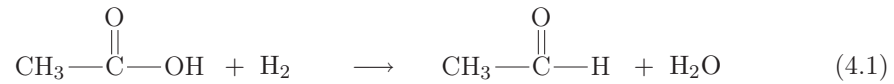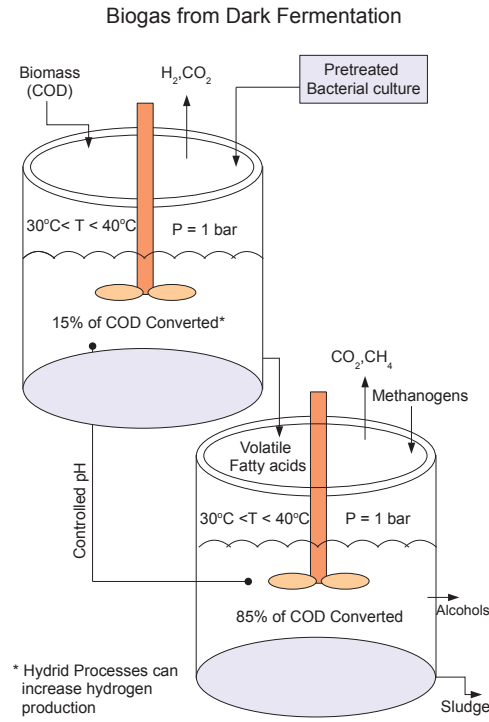
Figure 4.1: Overall two step fermentation process

$$2CH_3 \overset{\overset{\displaystyle O}{\|}}{-C} -OH \ + \ 3H_2 \qquad \longrightarrow \qquad 3CH_4 + \ 2H_2O + \ CO_2 \qquad (4.4)$$

$$CH_3 \overset{\overset{\displaystyle O}{\|}}{-C} -OH \ + \ H_2 \qquad \longrightarrow \qquad CH_4 + \ H_2O + \ CO \qquad (4.5)$$

$$2CH_3 \overset{\overset{\displaystyle O}{\|}}{-C} -OH \qquad \longrightarrow \qquad CH_3 \overset{\overset{\displaystyle O}{\|}}{-C} -CH_3 \ + \ H_2O + \ CO_2 \qquad (4.6)$$

$$2CH_3 \overset{\overset{\displaystyle O}{\|}}{-C} -OH \ + \ H_2 \qquad \longrightarrow \qquad CH_3 \overset{\overset{\displaystyle O}{\|}}{-C} -OC_2H_5 \ + \ H_2O \qquad (4.7)$$
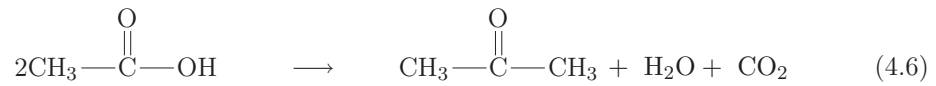
According to above there are three main categories for hydrogenation of acids:

1. simple reduction to aldehydes (4.1), alcohols (4.2) and alkanes (4.3)

2. reduction and cracking of oxyl-group to alkanes as in (4.4) & (4.5)

3. formation of esters (4.7) and to ketones (4.6).

In a process of coupling fermentation and catalytic reaction, alkane production such as CH_4 through acetic acid has no real interest as it is a direct product of fermentation. However production of aldehydes, alcohols (without large quantity of water) and ketones via this green (relatively inexpensive) process may become attractive.

Aldehydes are widely used as synthesis blocks for organic fine chemicals including medicines, agrochemicals and perfumes. Several methods have been employed for their production, which are not usually environment friendly [143]. Also most of these processes require high energy as to create extreme conditions, along with expensive catalysts.

As shown in Figure 4.2, equilibrium conversion of acetic acid to acetaldehyde, production increases with temperature and it is only 17 % at 75 °C. Thus production of aldehydes will be realised at 200 - 300 °C. At much higher temperature the acids easily decomposes to alkanes decreasing the production of aldehydes.
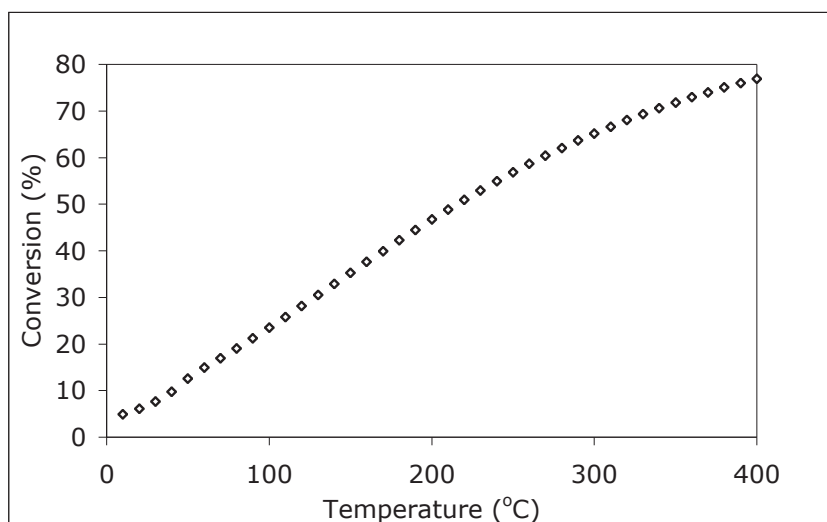
Figure 4.2: Equilibrium conversion of acetic acid to aldehyde, P = 1 bar, $\frac{H_2}{CO_2} = 1$, $\frac{Acid}{Gas} = 0.1$ (*Data calculated through HYSYS*)

Pestman et al. [144, 145] have compared various metal oxides including Pt/Oxides catalyst for aldehyde production. According to them Pt/Fe_2O_3 is the best known catalyst for aldehyde selection. They also reported relation between metal-oxygen bond and aldehyde selectivity (as shown in Figure 4.3) showing Cu and Fe with most of selectivity. Furthermore addition of Pt to metal oxides results in the inhibition of the side reactions accompanying aldehyde production. However more than certain limit has an inverse effect [145]. Generally following factors increase aldehyde selectivity:

1. increase in reduction temperature for oxides [145].

2. augmentation in metal content of the catalyst [146, 147].

3. decrease in acid conversion [148, 149].

4. increase in hydrogen partial pressure [146, 148].

All the above factors increase the dissociated hydrogen available for the reaction. So it can safely be concluded that aldehyde production is promoted by available hydrogen quantity. This fact is clearly shown in the study conducted by Grootendorst et al. [146] as a comparison between acetic acid conversion behaviour with and without hydrogen over Fe_2O_3 catalyst.
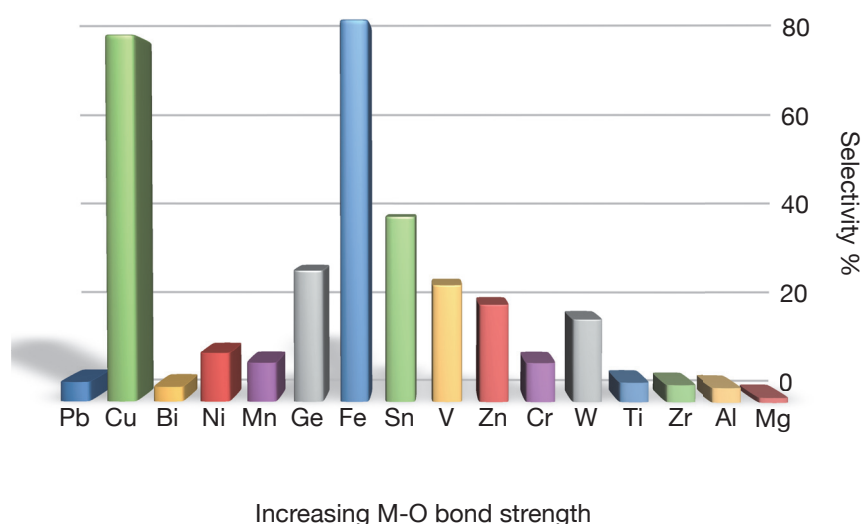
Figure 4.3: Plot of maximum selectivity to aldehyde as a function of increasing metal-oxygen bond strength [145]

Acid to alcohol hydrogenation is relatively easy compared to aldehydes as latter needs mild reducing environment thus requiring more control of the conditions. Alcohols may simply be obtained by increasing pressure i.e. ensuring strong acid adsorption or increasing the amount of free dissociated hydrogen through high metal on catalysts.

As shown in Figure 4.4, low temperature is thermodynamically favourable in ethanol production through acetic acid.

This alcohol produced through carboxylic acid hydrogenation can be further converted to corresponding esters as per equation (4.7). Long chain esters (methyl/ethyl) are used as biodiesel [150]. However waste fermentation does not produce long chain fatty acids, thus to get biodiesel external sources of such acids should have to be exploited.

Same catalyst, as for aldehyde production, are efficient for the production of alcohol through acids, while the ratio between the two is dictated by thermodynamics. Some
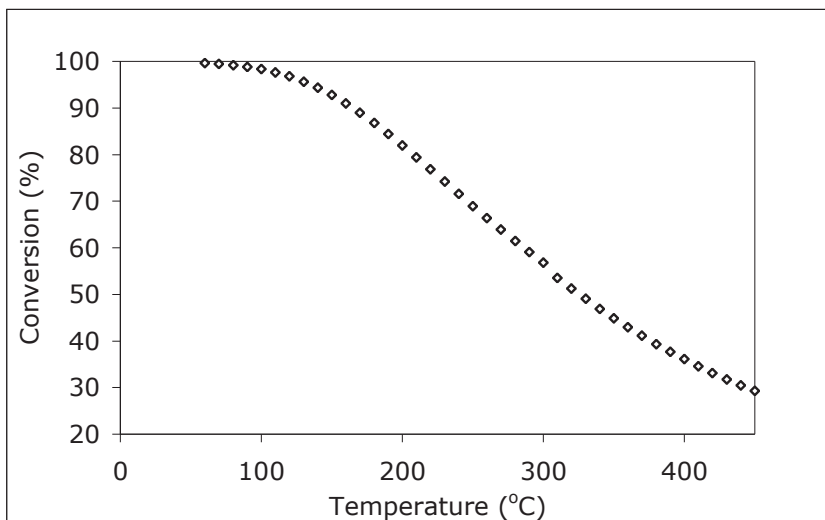
Figure 4.4: Equilibrium conversion of acetic acid to alcohol, P = 1bar, $\frac{H_2}{CO_2} = 1$, $\frac{Acid}{Gas} = 0.1$

authors [144,146,151] mentioned the presence of ketone in outlet flows. But the production of ketone does not require hydrogen (as per equation (4.6)). Thus hydrogen deficiency may lead to its production [146], such deficiency may be realised either by no hydrogen injection or excluding metal component of the catalyst leading to no dissociated hydrogen production. CO_2 is in fact the product of such a reaction and its adverse effect over catalytic activity is not foreseen as catalyst in oxidised form is efficient/required for its production. Mechanistic detail of ketonisation is provided by in equation (4.8) [151]. Such type of reaction includes an unsaturated intermediate thus explaining hydrogen negative effect. Ketone production is 100% thermodynamically possible in the temperature range considered (i.e. above 50 °C).

$$CH_3 - \overset{\overset{\displaystyle O}{\|}}{C} - OH \quad \xrightarrow{[Cat.]/\triangle} \quad H_2C{=}C{=}O \quad + \quad H_2O \tag{4.8a}$$

$$H_2C{=}C{=}O \quad + \quad CH_3 - \overset{\overset{\displaystyle O}{\|}}{C} - OH \quad \xrightarrow{[Cat.]/\triangle} \quad CH_3 - \overset{\overset{\displaystyle O}{\|}}{C} - CH_3 \quad + \quad CO_2 \tag{4.8b}$$
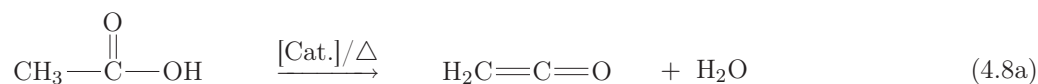
An extensive survey of the literature to various products through hydrogenation of carboxylic acids is provided in Table 4.2. The overall conversion for acetic acid is usually kept low to establish differential conditions in the reactor.

T °C	Acid	Conv. %	Prod. & selec. %	Catalyst	T_{Red} °C	Ref.
343	Acetic	4	Acetone-50 Decomp. Prod.-50	1.5%Fe/SiO$_2$	400	[147]
260	Acetic	4	Ethanal-100	3.0%Fe/SiO$_2$	450	[147]
270	Acetic	8	Ethanal-90 Ethanol-7 Ethyl Ester-4	3.0%Fe/SiO$_2$	450	[147]
245	Acetic	3	Ethanal-90 Ethanol-6 Acetone-2 Decomp. Prod.-2	4.1%Fe/SiO$_2$	500	[147]
277	Acetic	8	Ethanal-90 Ethanol-2 Acetone-4 Decomp. Prod.-4	4.1%Fe/SiO$_2$	500	[147]
180	Acetic	2	Ethanal-100	30%Fe/SiO$_2$	400	[147]
230	Acetic	11	Ethanal-95 Ethanol - 5	30%Fe/SiO$_2$	400	[147]
280	Acetic	5	Ethanal-64 Ethanol-11 Ethyl Ester-3 Acetone-11 Decomp. Prod.-11	5.7%Fe/Carbon	400	[147]
230	Acetic	4	Ethanal-100	Fe$_2$O$_3$	400	[147]
260	Acetic	12	Ethanal-95 Ethanol-5	Fe$_2$O$_3$	400	[147]
220	Acetic	5	Ethanal-100	Fe powder	400	[147]
240	Acetic	10	Ethanal-94 Ethanol-6	Fe powder	400	[147]
174	Acetic	5.9	Ethanol-59 Ethane-14 Ethyl Ester-27	0.69%Pt/TiO$_2$	500	[138]

T °C	Acid	Conv. %	Prod. & selec. %	Catalyst	T_{Red} °C	Ref.
170	Acetic	5.6	Ethanol-51 Ethane-20 Ethyl Ester-29	$0.69\%Pt/TiO_2$	200	[138]
147	Acetic	5	Ethanol-70 Ethane-16 Ethyl Ester-14	$2.01\%Pt/TiO_2$	200	[138]
250	Acetic	4.7	Ethanol-8 Ethane-10 Ethyl Ester-4 Decomp. prod.-78	$0.78\%Pt/\eta - Al_2O_3$	450	[138]
238	Acetic	2	Decomp. prod.-100	$0.49\%Pt/SiO_2$	450	[138]
250	Acetic	4	Ethanal-80 Ethanol-20	$1.91\%Pt/Fe_2O_3$	450	[138]
315	Acetic	4.7	Decomp. prod.-100	Pt powder	450	[138]
227	Acetic	4	Ethanal-79 Ethanol-21	Fe_2O_3	450	[138]
370	10-undecylenic	74	UDEH-98 Ketone-1	Cr_2O_3		[148]
330	10-undecylenic	87	UDEH-83 Ketone-16	Cr/Zr_2O_3		[148]
330	10-undecylenic	97	UDEH-10 Ketone-79	Zr_2O_3		[148]
350	Octanoic	91	Octanal-97	Cr_2O_3		[148]
350	Dodecanoic	97	Dodecanal-97	Cr_2O_3		[148]
350	Octadecanoic	98	Octadecanal-93	Cr_2O_3		[148]

Table 4.2: Comparison of various catalysts used for carboxylic acid hydrogenation

It can be seen in Table 4.2 that both conversion and selectivity can be greatly affected by operating conditions like catalyst type, its reduction and reaction temperature.

A comprehensive mechanistic model has been proposed by Rachmady and Vannice [149] for the production of aldehyde, alcohol and alkane from acetic acid as shown in equation

(4.9). This mechanism shows that reaction is sensible to hydrogen partial pressure and both metal and support of the catalyst take part in reaction.

$$H_{2(g)} + 2^* \quad \underset{}{\overset{K_{H_2}}{\rightleftharpoons}} \quad 2H^* \tag{4.9a}$$

$$CH_3COOH_{(g)} + 2^* \quad \underset{}{\overset{K_{Ac}}{\rightleftharpoons}} \quad CH_3COO^* + H^* \tag{4.9b}$$

$$CH_3COOH_{(g)} + S \quad \underset{}{\overset{K_A}{\rightleftharpoons}} \quad CH_3COOH\text{-}S \tag{4.9c}$$

$$CH_3COOH\text{-}S \quad \underset{}{\overset{K_{Acy}}{\rightleftharpoons}} \quad CH_3CO\text{-}S\text{-}OH \tag{4.9d}$$

$$CH_3CO\text{-}S\text{-}OH + H^* \quad \underset{}{\overset{k_1}{\rightleftharpoons}} \quad CH_3CHO\text{-}S\text{-}OH + {}^* \tag{4.9e}$$

$$CH_3CHO\text{-}S\text{-}OH + H^* \quad \underset{}{\overset{k_2}{\rightleftharpoons}} \quad CH_3CHO\text{-}S + {}^* + H_2O_{(g)} \tag{4.9f}$$

$$CH_3CHO\text{-}S \quad \underset{k_{-3}}{\overset{k_3}{\rightleftharpoons}} \quad CH_3CHO_{(g)} + S \tag{4.9g}$$

$$CH_3CHO\text{-}S + H^* \quad \overset{k_4}{\longrightarrow} \quad CH_3CH_2O\text{-}S + {}^* \tag{4.9h}$$

$$CH_3CH_2O\text{-}S + H^* \quad \overset{k_5}{\longrightarrow} \quad CH_3CH_2OH\text{-}S + {}^* \tag{4.9i}$$

$$CH_3CH_2OH\text{-}S \quad \underset{k_{-6}}{\overset{k_6}{\rightleftharpoons}} \quad CH_3CH_2OH_{(g)} + S \tag{4.9j}$$

$$CH_3CH_2OH\text{-}S + H^* \quad \overset{k_7}{\longrightarrow} \quad CH_3CH_2OH_2\text{-}S + {}^* \tag{4.9k}$$

$$CH_3CH_2OH_2\text{-}S + H^* \quad \overset{k_8}{\longrightarrow} \quad CH_3CH_3\text{-}S + {}^* + H_2O_{(g)} \tag{4.9l}$$

$$CH_3CH_3\text{-}S \quad \underset{k_{-9}}{\overset{k_9}{\rightleftharpoons}} \quad CH_3CH_{3(g)} + S \tag{4.9m}$$
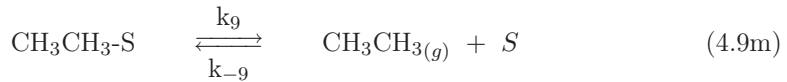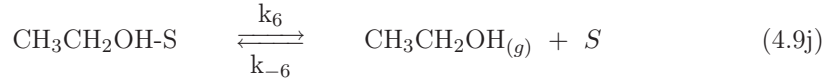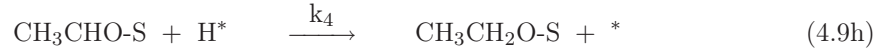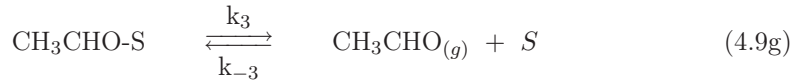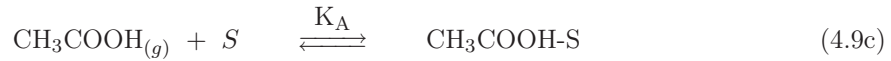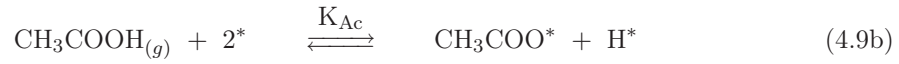
These equations (first four in quasi state equilibrium) lead to the following (4.10) Langmuir-Hinshelwood-Hougen-Watson (LHHW) type rate law via first principal reaction kinetics. The reaction rate law does not take into account all the reaction products effect and can thus be criticised.

$$r_{HOAc} = \frac{k_1 K_{Acy} K_A K_{H_2}^{\frac{1}{2}} P_A P_{H_2}^{\frac{1}{2}}}{(K_{H_2}^{\frac{1}{2}} P_{H_2}^{\frac{1}{2}} + K_{Ac} P_A / K_{H_2}^{\frac{1}{2}} P_{H_2}^{\frac{1}{2}})(1 + K_A(1 + K_{Acy})P_A)} \tag{4.10}$$

In this study, the authors have tested several catalysts showing very different selectivities (Table 4.2). Catalyst such as Pt/SiO_2 and Pt/Al_2O_3 are active in the presence of CO_2 and CO (co-product of ketones and alkanes) for carboxylic acids hydrogenation. The conversion of acids is low for the said catalysts thus concentration of carbon oxides are on lower side. However according to the results from DRIFTS study, even a few ppm of CO are enough

for catalyst inactivity for hydrogenation. This clearly indicates that acids can be treated with CO_2 containing biogas.

4.2 HYDROGENATION OF CARBOXYLIC ACIDS ON Pt/SiO$_2$-TiO$_2$

In this part, at the same time other than the evaluation of CO_2 effect, the effect of carboxylic acids chain length has also been studied. For this purpose two representative acids are chosen, acetic acid one for the lower chain and octanoic acid for the higher chain.

Octanoic acid or caprylic acid is chosen because of its ease in handling. Furthermore, its liquid products generated through hydrogenation are easy to collect in a cold bath and carbon balance calculations do not require much data compared to liquid and gas mixtures. Lower acids than octanoic acid (but higher than acetic acid) are rejected as they will produce products with conflicting melting and boiling points thus requiring more than one condenser, operating at different temperatures. Higher acids are solid at ambient temperature thus requiring the modification of hot trace linings, hence avoided. The experimental set up and procedures are same as used for toluene hydrogenation (section: 3.3.1) except the chromatograph column and procedure which are detailed in Annexe C.

A representative of fermentation broth acids is worth to evaluate. Acetic acid is chosen because the results of its hydrogenation in pure hydrogen are already published for comparison with CO_2 containing hydrogen. Furthermore possibility of products isomerism is small because of short chain length with relatively small number of products. Acetic acid is comparatively easy to handle compared to butyric acid as products are easily available in gaseous form to be evaluated by an online chromatograph. Hydrogenation products of acetic acids are also of high value especially acetaldehyde. Moreover detailed physical data is available (acetic acid and its products) for simulation to evaluate the feasibility of overall process.

To evaluate acetic acid hydrogenation the set-up and procedures are slightly changed as an on-line chromatograph can now provide the conversion with the products in gaseous form.

Catalysts	Temp	Conv.	Selectivity (mol%)						
	(K)	(%)	Ethanal	Ethanol	Ethane	Ester	CO_2	CO	CH_4
0.69% Pt/TiO$_2$ (HTR)^a	447	5.9	0	59	14	27	0	0	0
0.69% Pt/TiO$_2$ (LTR)^b	443	5.6	0	51	20	29	0	0	0
2.01% Pt/TiO$_2$ (LTR)^b	420	5	0	70	16	14	0	0	0
0.78% Pt/η-Al$_2$O$_3$	523	4.7	0	8	10	4	5	33	40
0.49% Pt/SiO$_2$	511	2	0	0	0	0	0	50	50
1.91% Pt/Fe$_2$O$_3$	523	4	80	20	0	0	0	0	0
Pt Powder	588	43.7	0	0	0	0	32	21	47
Fe$_2$O$_3$	500	4	79	21	0	0	0	0	0

^{a}Catalyst reduced at 773 K

^{b}Catalyst reduced at 473 K

Table 4.3: Product selectivity during acetic acid hydrogenation over various catalysts [149]

As dictated by mechanistic details in literature and observation, support does play an important role in hydrogenation. The modification of alumina in Pt/Al$_2$O$_3$ by CO_2 (DRIFTS study) may prevent its use as catalyst even for carboxylic acid hydrogenation.

Even if used without CO_2 it results in appreciable acid decomposition (Table 4.3). Also Pt/SiO_2 is a good decomposition catalyst as mentioned by Rachmady et al [149], hence its utilization for the very purpose is ruled out. As Pt/TiO_2 catalyst is an effective hydrogenation catalyst, so we used Pt/SiO_2-TiO_2 catalyst because of the limitation of our experimental set-up as explained in section 3.3.4. Even though some decomposition is expected because of silica.

4.2.1 OCTANOIC ACID HYDROGENATION
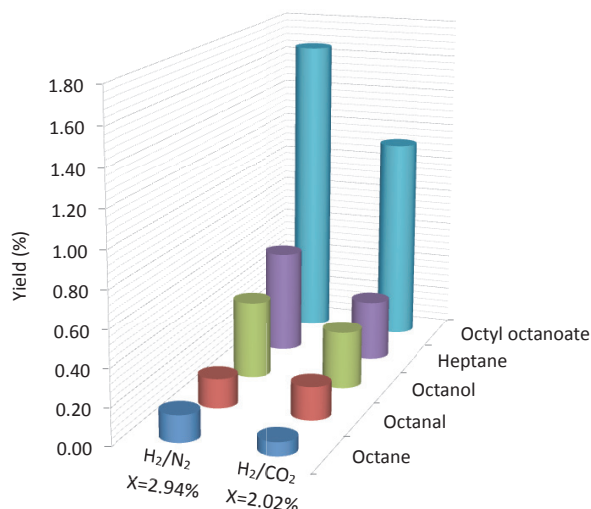
Figure 4.5: Effect of CO_2 on octanoic acid hydrogenation over Pt/TiO_2 - SiO_2, T = 200 °C, $\tau = 52$ kgcat $\cdot$ s $\cdot$ mol^{-1}, $H_2 = 46.7$ %, N_2 or $CO_2 = 46.7$ %, Acid = 6.6 %

To evaluate the effect of CO_2 in large quantity (as of biogas) comparison with and with no CO_2 is done. It should be noted that CO_2 may still be present in the reactor although not injected, as it can be indigenously produced via acid decomposition. Two experiments one with CO_2 whereas other with no CO_2 are done as shown in Figure 4.5. In case of no CO_2, N_2 is used to adjust partial pressures of H_2 and the acid. All other conditions remain same during the test run. The results clearly depict decrease in overall catalyst activity when CO_2 is introduced in the reactor. Same is true for individual product yield except that of octanal. As octanal is an intermediate to alcohol and later require more drastic hydrogenation conditions which are undermined by CO_2 oxidative effect thus increasing aldehyde production. This positive feature of CO_2 may then be exploited to produce aldehyde instead of complete acid hydrogenation.
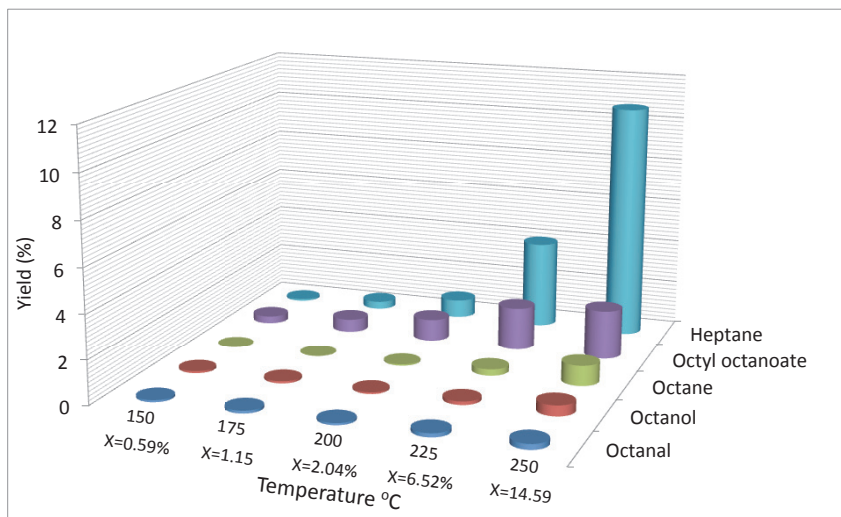
Figure 4.6: Octanoic acid reduction at different temperatures, P = 1 bar, $\frac{H_2}{CO_2} = 1$, $\frac{Acid}{Gas} = 0.05$, $\tau = 100$ kgcat $\cdot$ s $\cdot$ mol^{-1}
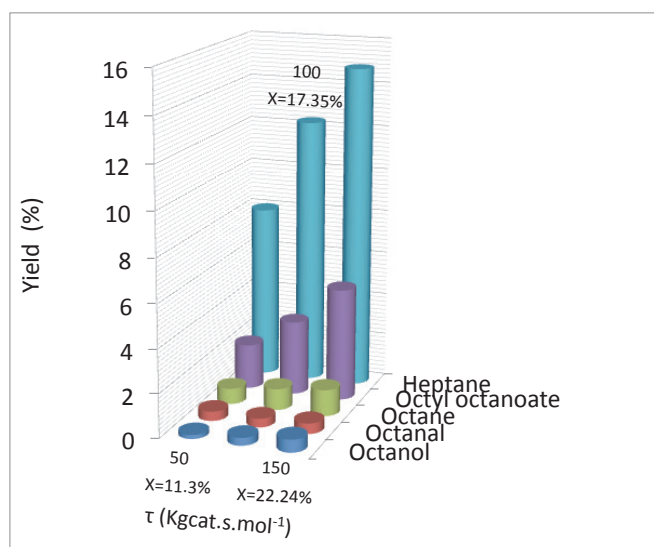
Figure 4.7: Octanoic acid reduction at different τ, P = 1 bar, $\frac{H_2}{CO_2} = 1$, $\frac{Acid}{Gas} = 0.05$, T = 250 °C

Hydrogenation of octanoic acid with CO_2 at different temperatures is shown in Figure 4.6. Overall conversion of the octanoic acid increases with temperature. However this increase is mainly because of decomposed products i.e. heptane and octane. At low temperature i.e. below 175 °C conversion to octanal is negligible. Kinetics for alcohol is also retarded at this temperature. Gradual increase in the reduced product is observed with temperature. Ester at low temperature is not present in appreciable amounts but its concentration increases with temperature augmentation. At high temperature its production is lowered mainly because of alcohol thermodynamics (main reactant for esterification) and as depicted in Figure 4.6, i.e. at 225 °C and 250 °C, ester production is essentially the same.

Similarly effect of residence time over acid conversion is shown in Figure 4.7. Overall conversion of acid as well as individual yield increase with increase in τ. However effect on octanal production is not very prominent. This is mainly because more contact time will increase the probability of complete reduction to alcohols which on the other hand gives esters over the catalyst.

4.2.2 ACETIC ACID HYDROGENATION
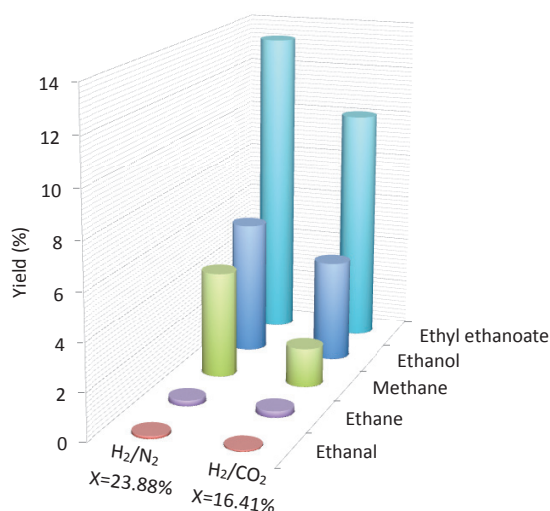
Figure 4.8: Effect of CO_2 on acetic acid hydrogenation over Pt/TiO₂ - SiO₂, T = 200 °C, $\tau = 50$ kgcat $\cdot$ s $\cdot$ mol^{-1}, H₂ = 47.5 %, N₂ or CO₂ = 47.5 %, Acid = 5 %
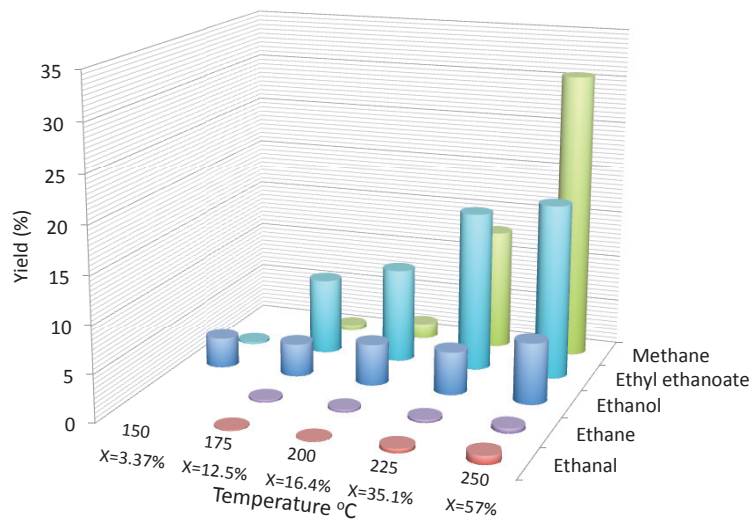
Figure 4.9: Acetic acid reduction at different temperatures, P = 1 bar, $\frac{H_2}{CO_2}$ = 1, $\frac{Acid}{Gas}$ = 0.05, τ = 50 kgcat $\cdot$ s $\cdot$ mol^{-1}
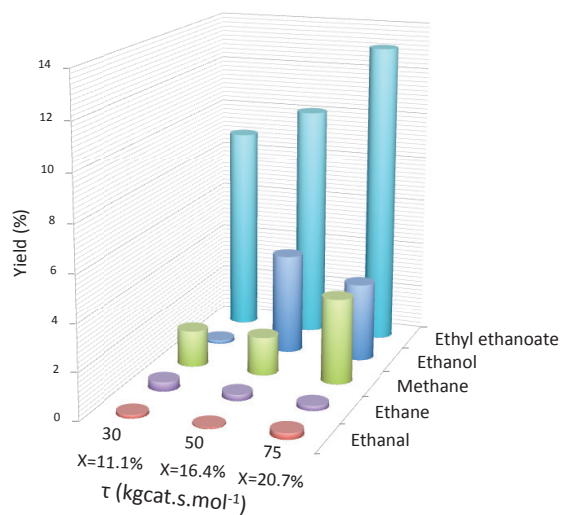
Figure 4.10: Acetic acid reduction at different τ, P = bar, $\frac{H_2}{CO_2}$ = 1, $\frac{Acid}{Gas}$ = 0.05, T = 200 °C

Short chain acids are also tested on the same catalyst to determine chain length effect. Effect of CO_2 and that of acid chain length can be seen in Figure 4.8. Same as in case of octanoic acid, conditions are adjusted by nitrogen to keep partial pressures for the two same. It is worthy to note that chain length has a negative effect on acid conversion as it is higher for acetic acid. Similarly acid conversion to methane is also compromised because of CO_2 as it is the co-product. Effect of CO_2 on ethanol and ester dictates low conversion as a result of decreased hydrogenation. Ethane and ethanal almost remains the same largely because of small selectivity. So it may be concluded that irrespective of acid chain length, effect of CO_2 on acid conversion over Pt/SiO$_2$-TiO$_2$ is negative but less negative in comparison with its effect on toluene hydrogenation. Furthermore negative effect of CO_2 over methane and heptane production can be exploited.

Temperature profile for this acid conversion is shown in Figure 4.9. Although conversion is high compared to long chain counter part but trend in product distribution is almost the same. Decomposition of acetic acid to methane dominates at high temperature i.e. above $200\,^\circ$C as heptane formation dominates for octanoic acid. Ester production, as observed for octanoic acid, also increases with temperature but then seems to stabilize above $225\,^\circ$C. Ethanol production although increases with temperature augmentation but this effect is neutralized mainly by ester production.

Trend of residence time for acetic acid is shown in Figure 4.10. Not much can be inferred from ethane and ethanal production as they are small.

Effect of hydrogen partial pressure is shown in Figure 4.11. The production of decomposed product i.e methane clearly drops compared to ethanol and ester, which on the other hand increase. Overall acid conversion is decreased with hydrogen partial pressure mainly because of negative hydrogen effect on alkane production.

Effect of acid partial pressure is also evaluated and is represented by Figure 4.12. Conversion increases with increase in acid injection. This is in accordance with published reaction rate (equation 4.10). Increase in ethanol presence at 5 % acid concentration is because of low ethyl ethanoate production. Catalyst deactivation is not detected as after each four experiments standard reaction mixture is injected to check for the deactivation (Figure 4.13). This standard reaction is done at $250\,^\circ$C and 1 bar pressure while percentage of acid is maintained at 5 % rest being the equi-molar mixture of H_2 and CO_2. Residence time is adjusted to 50 kgcat $\cdot$ s $\cdot$ mol^{-1}.
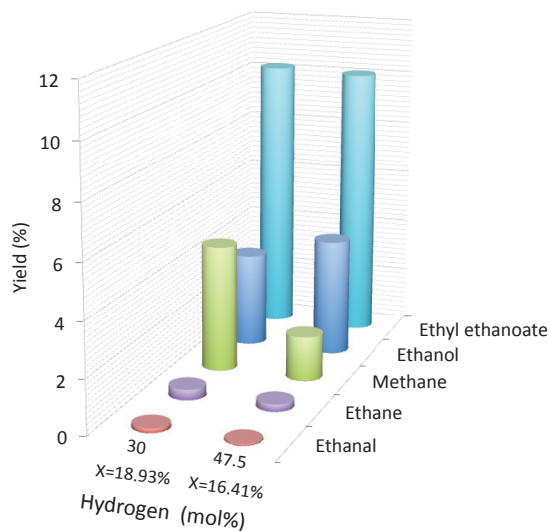
Figure 4.11: Effect of hydrogen on acetic acid conversion, P = 1 bar, T = 200 °C, Acid = 5 %, CO$_2$ = 47.5 %, N$_2$ = 100-Acid-H$_2$-CO$_2$, τ = 50 kgcat $\cdot$ s $\cdot$ mol^{-1}.
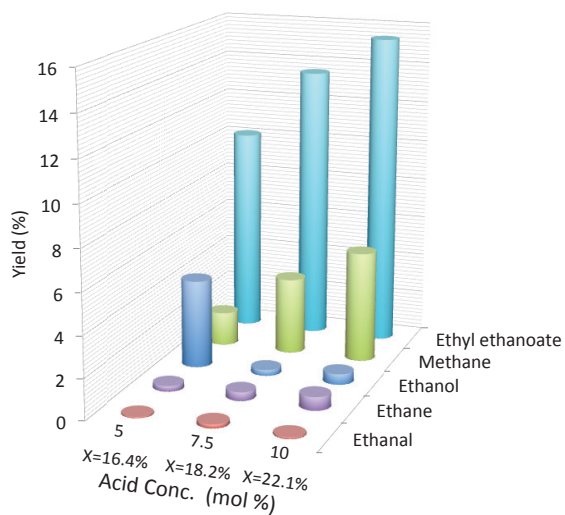
Figure 4.12: Effect of acid concentration, P = 1 bar, T = 200 °C, $\frac{H_2}{CO_2}$ = 1, τ = 50 kgcat $\cdot$ s $\cdot$ mol^{-1}.
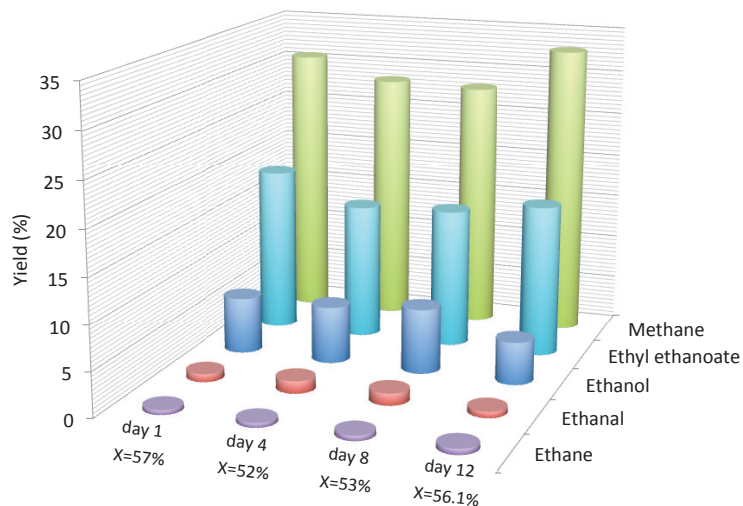
Figure 4.13: Pt/SiO$_2$ - TiO$_2$ deactivation under acid, P = 1 bar, T = 250 °C, $\frac{H_2}{CO_2}$ = 1, τ = 50 kgcat $\cdot$ s $\cdot$ mol^{-1}, Acid = 5 %.
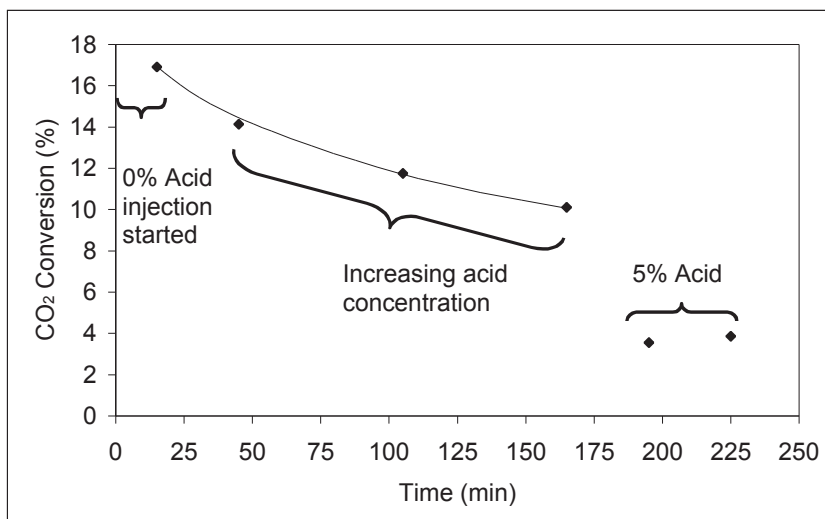
Figure 4.14: Selectivity shift from CO$_2$ to acid reduction. T = 250 °C, P = 1 bar, H$_2$ = 51 ml/min, CO$_2$ = 51 ml/min. At t = 0 min acid injection started. At t = 195 min equilibrium is approached in the evaporator (acid concentration is stabilised) with final τ = 50 kgcat $\cdot$ s $\cdot$ mol^{-1}. 195 min>t>0 min gradual increase of acid concentration in the reactor.

4.2.3 CARBOXYLIC ACID EFFECT ON CO FORMATION

To confirm the selectivity shift which was observed in toluene hydrogenation with CO_2, an experiment has been done following CO_2 conversion evolution during the start of acetic acid injection (Figure 4.14). After the stabilisation of H_2 and CO_2 flow of 51 ml/min each at $250\,°C$, acid injection is started at t = 0 min to achieve 5 % molar content of acetic acid with an overall $\tau = 50 \ \mathrm{kgcat \cdot s \cdot mol^{-1}}$. CO production via CO_2 hydrogenation is evident but it drops with increase in acid concentration entering into the reactor. This depreciation stabilises with increase in acid and eventually an agreement between the selectivity ratio is achieved for CO_2 and acid hydrogenation. This is important to evaluate the optimum level of acid injection into the reactor and to avoid excessive CO production. It is worthy to note that appreciable amount of methane is also present in the effluent gases which is also conjugated with CO_2 production thus increasing the amount of CO_2 in the reactor. This validates our hypothesis regarding CO preferential adsorption over bridge sites compared to toluene while, competition does exists in case of acid hydrogenation.

4.2.4 CONCLUSION

For acid reduction over Pt/SiO_2-TiO_2 it may be concluded that platinum metal is an excellent metallic catalyst for acid hydrogenation and creates drastic conditions for the reaction but it also produces CO via CO_2 reduction (RWGS). Although compromised by selectivity shift with acid concentration in the reactor but still appreciable amount of CO is produced. As confirmed from literature review that SiO_2 support promotes decomposed products while TiO_2 promotes hydrogenated products, our experiments with SiO_2-TiO_2 have shown the effect of both along with acid esterification utilising alcohols-product of the same reaction. Furthermore it has been seen that long chain acids are not as readily reduced as short chains and ketones are also not observed over Pt/SiO_2-TiO_2 rather complete carbonyl group decomposition occurs than its shift, thus resulting in alkanes. In order to further suppress CO production a less active hydrogenation catalyst like Fe_2O_3 is needed to produce aldehydes. Next section of this report deals with the same.

4.3 IRON OXIDES

4.3.1 INTRODUCTION

As seen in Table 4.3 iron oxide is reported as an active catalyst for aldehydes, alcohols and ketones production by pure hydrogen [144] with its several other advantages like i) it is cheap and abundantly available, ii) has low toxicity, iii) shows high resistance to thermal shocks. iv) availability at various levels of activation, v) easiness to caste in shapes and deposit and vi) with no reported RWGS activity.

Iron oxide is a non-stoichiometric compound. Iron to oxygen ratio varies with the reduction temperature as shown in Figure 4.15 [146]. Generally there are three types of oxides present in market i) hematite Fe_2O_3 (rust) ii) magnetite Fe_3O_4 and iii) wüstite FeO. In fact all of these forms are Iron oxides i.e. Fe_2O_3, but with varying amount of free Fe^0.

Product selectivity greatly depends on catalyst reduction temperature. Pestman et al. [146, 152] have conducted a very useful study over the product distribution at different catalyst reduction temperatures or catalyst states. As shown in Figure 4.16, more the catalyst is capable of reducing hydrogen, more it will produce hydrogenated product i.e.
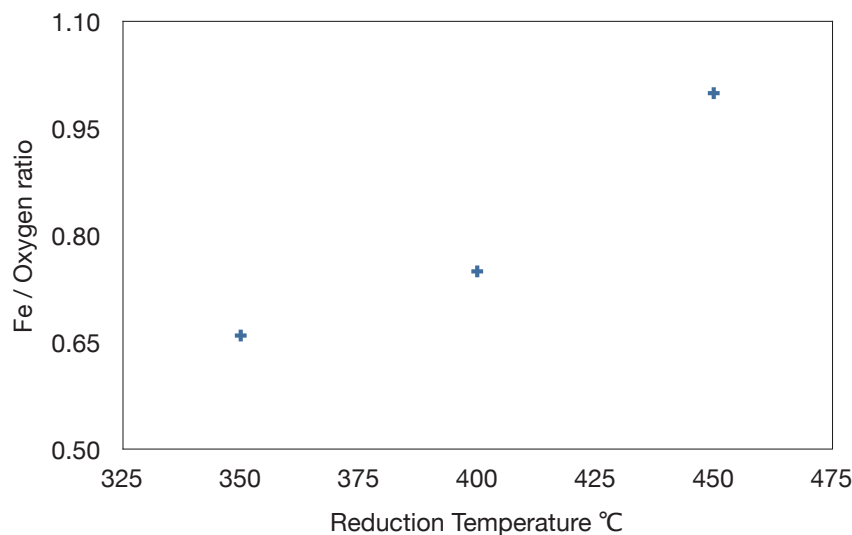
Figure 4.15: Ratio of Fe to Oxygen at different reduction temperatures [146]

aldehyde. However, reduced and unreduced both sites seem important for aldehyde production as its selectivity drops rapidly with the total reduction of iron. On the other hand oxygenated sites are also efficient to produce acetone from acetic acid (Figure 4.16).

Acetone is an important solvent and is also used as raw material to methyl methacrylate, methyl isobutyl ketone and bisphenol production. It is rated among the top 50 volume chemicals. The cumene-phenol process is a major contributor to acetone production. Propylene oxidation is another way of current acetone production along hydrogen peroxide [153]. However, theses processes are not essentially environmental friendly. Acetic acid conversion to acetone via biogas is an attractive option both economically and environmentally.

Iron (along some promoters) is industrially used as catalyst in Haber's process for ammonia production under high pressure from synthesis gas. Synthesis gas is usually obtained by catalytic methane reforming in steam at high temperature. Such reforming produces CO_2, CO and hydrogen. With nitrogen taken from air, this gas is thoroughly stripped off from CO_2 by using amine solutions. Furthermore such set-ups are usually equipped by methanators (reactor to convert CO_2 traces back to methane) indicating its adverse effect over reduced iron. According to Haldor Topsøe (ammonia catalyst provider) oxygen and its compounds including water are termed as temporary poison to the reduced catalyst and their operating limits are shown in Table 4.4.

According to XANES-XRD study conducted by Nordhei et al. [154], almost no FeO and free iron exist below 200 °C and 450°C respectively, under hydrogen. However after this threshold temperature, both start to increase gradually and at 500 °C no magnetite is found. On the other hand CO_2 in absence of hydrogen rapidly oxidises the free iron and magnetite dominates the catalyst structure.

The goal of this part is to evaluate the use of biogas in a acetone production unit from acetic acid on iron oxides catalysts.
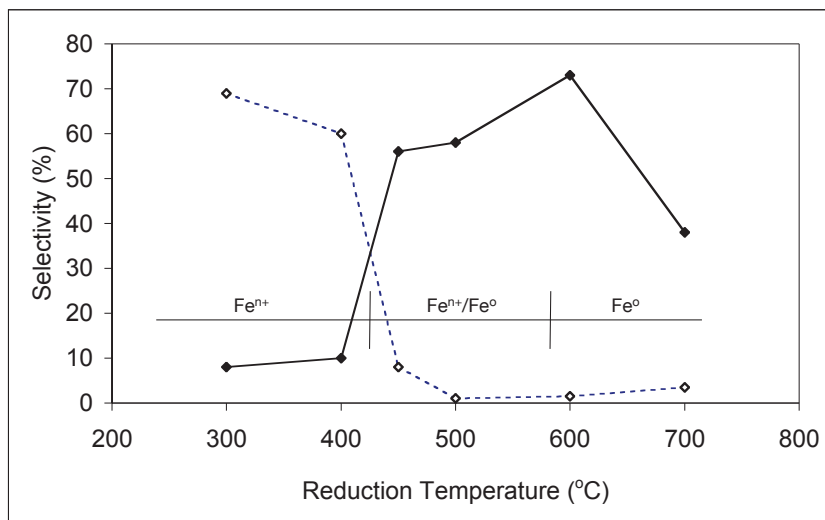
Figure 4.16: Selectivity of iron catalysts plotted as a function of pre-reduction temperature, presented together with an indication of the phase composition as determined by XRD [152]. $\diamond$ - Acetone $\blacklozenge$ - Aldehyde

0-2 ppm O EQV	Ideal
2-4 ppm O EQV	Continued operation for a few months
4-6 ppm O EQV	Continued operation for a few weeks
6-10 ppm O EQV	Continued operation for a few days

Table 4.4: Oxygen equivalent in converter feed gas-Recommended maximum period of operation. *Courtesy of Haldor Topsøe.*

4.3.2 EXPERIMENTAL SETUP AND PROCEDURE

Same set-up as for toluene and octanoic acid hydrogenation is used for acetic acid hydrogenation. However as the product range from acetic acid contain volatiles so all the products are kept in gaseous form via hot tracing of the setup. On-line chromatograph thus can be used to analyse the products in every 5 min (Annexes C.2 and C.3). This feature is not available previously with toluene and octanoic acid and is used to get an insight of selectivity shift as shown in Figure 4.14 other than an increased rate of sampling.

Iron oxide in FeO form is directly used as catalyst. It is purchased from Sigma Aldrich with 99.98% purity level (Ref No. 203513) and is in oxidised form. It is provided in powder or small chunks. Size of particles varies but particles are smaller than 10 mesh.
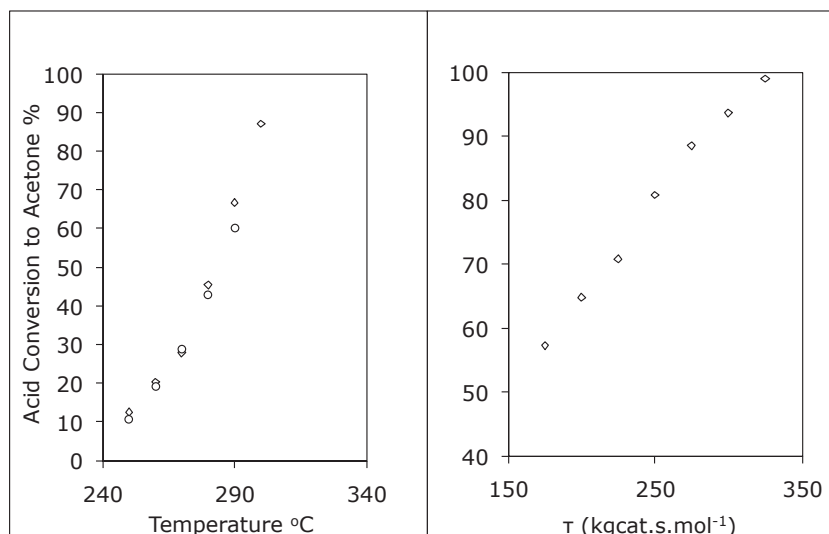
Figure 4.17: Temperature and residence time effect on acetone production, P = 1 bar, τ = 250 kgcat·s·mol^{-1}, $\frac{H_2}{CO_2}$ = 1, $\frac{Acetic\ acid}{H_2+CO_2}$ = 0.05 a) Temperature profile $\diamond$ = ascending, $\circ$ = descending b) Residence time profile T = 300 °C

4.3.3 EXPERIMENTAL RESULTS FOR ACETONE PRODUCTION

In these experiments, FeO catalyst is used showing good selectivity for aldehyde and ketones also. Ferrous oxide in its oxidative form (oxidised at 450 °C under air) is an effective catalyst for acetone production. Its conversion increases with temperature (Figure 4.17a). Good agreement between the ascending and descending curves rules out the possibility of any appreciable deactivation rate during the development of temperature profile. However above 300 °C some deactivation is observed and catalyst is needed to be oxidized with air to become active again for acetone production.

Reaction rate at different residence times gives a straight line (Figure 4.17b), clearly indicating the order of reaction equal to zero perhaps due to an abundant amount of acid on the catalyst surface. This is probably because of large surface area provided by the catalyst for acid adsorption and high activation energy for the reaction. Also further investigations are required to actually determine the cause of such large amount of reactant on catalyst surface. The simplified zero order reaction kinetics is well proven by the parameter following Arrhenius law with an activation energy of 101 kJ·mol^{-1} (± 0.5 kJ·mol^{-1}).

However such a model does not take into account the changing surface of the catalyst in oxidative or reductive environment. Two site behaviour is observed for acetone production. This may be inferred from the Figures 4.18 & 4.19. Figure 4.18a shows the effect of CO$_2$ over acetone production. Although the catalyst is oxidised at 450 °C under air, still there are some reduced sites available to bring about acetic acid conversion to acetone. Such sites are indeed oxidised by CO$_2$ while H$_2$ increases them. This is shown by the increase in acetic acid conversion when hydrogen is injected over the catalyst (Figure 4.18b). The gas mix

was obtained through nitrogen mixing and no effect of nitrogen over acetone production is observed as inferred from Figure 4.18c. For biogas, the effect of CO_2 in biogas is well compensated by H_2 as elucidated by the Figure 4.18d. The initial catalyst activity is not constant in these figures as surface configuration at t=0 is likely to be not same for each set. This is confirmed by the tail to tail experiments done in a day as shown in Figure 4.19.
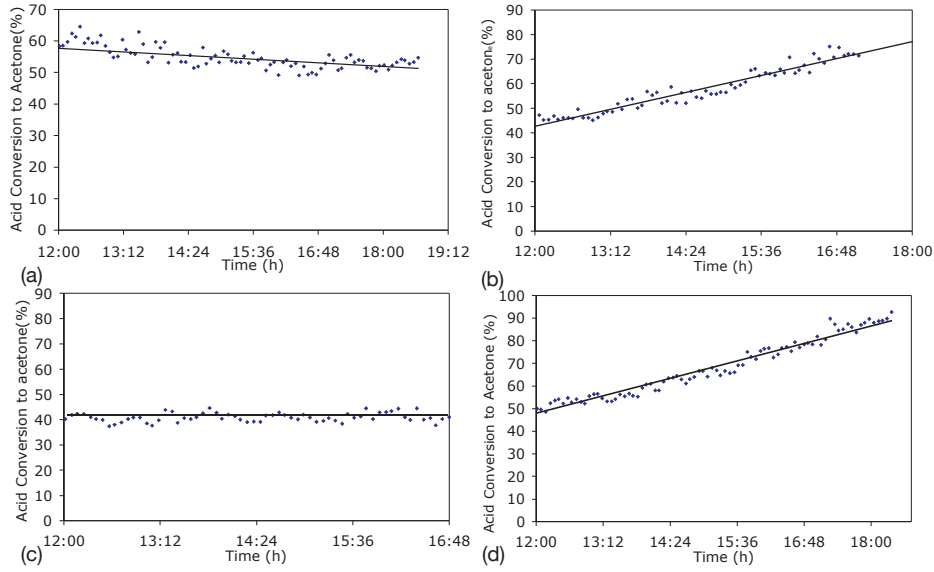
Figure 4.18: Effect of (a) CO_2, (b) H_2, (c) N_2 and (d) biogas on acetone production over Fe_2O_3, T = 300 °C, $\frac{X}{N_2}$ = 1 (Biogas $\frac{H_2}{CO_2}$ = 1), Acid = 5 %, τ = 200 kgcat·s·mol^{-1}
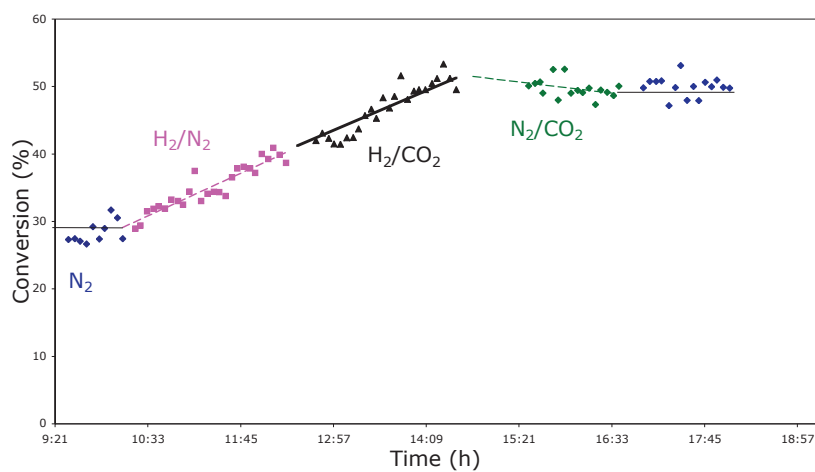
Figure 4.19: Effect of various mixtures on acetone production over Fe_2O_3, T = 300 °C, $\frac{X}{N_2}$ = 1, Acid = 5 %, τ = 200 kgcat·s·mol^{-1}

4.3.4 POSSIBLE MECHANISM TO ACETONE PRODUCTION

From the above results two site type mechanism is confirmed and both oxidised and reduced sites are indeed required for the acetone production. One of the product of this reaction is CO_2 and if acid concentration entering the reactor is high, it will result in high conversion and thus huge proportion of CO_2 in the reaction mixture, resulting in catalyst activity loss. Such loss however can be compensated by hydrogen endorsing reduced sites protection. However a threshold limit for hydrogen concentration under certain condition have to be determined as more than enough will result in highly reduced catalyst, abating acetone production. An optimum of the two gases and acid injection is indeed necessary to keep catalyst surface active and stable for such a reaction. The proposed mechanism may be defined by equations (4.11).

$$—Fe^{+3}\diagup O \diagdown Fe^{+3}— \quad \underset{}{\overset{H_2}{\rightleftharpoons}} \quad —Fe^{+3}\diagup O \diagdown Fe^{+2}— \qquad (4.11a)$$

$$—Fe^{+3}\diagup O \diagdown Fe^{+2}— \quad \underset{}{\overset{CO_2}{\rightleftharpoons}} \quad —Fe^{+3}\diagup O \diagdown Fe^{+3}— \qquad (4.11b)$$

$$—Fe^{+3}\diagup O \diagdown Fe^{+2}— \quad \underset{}{\overset{CH_3COOH}{\rightleftharpoons}} \quad —Fe^{+3}\diagup \overset{\overset{H}{|}}{O} \diagdown Fe^{+2}—OOCCH_3 \qquad (4.11c)$$

$$—Fe^{+3}\diagup \overset{\overset{H}{|}}{O} \diagdown Fe^{+2}—OOCCH_3 \quad \underset{}{\overset{CH_3COOH}{\rightleftharpoons}} \quad —Fe^{+3}\diagup \overset{\overset{H\cdots(OH)—OCCH_3}{|}}{O} \diagdown Fe^{+2}—OOCCH_3 \qquad (4.11d)$$

$$—Fe^{+3}\diagup \overset{\overset{H\cdots(OH)—OCCH_3}{|}}{O} \diagdown Fe^{+2}—OOCCH_3 \quad \underset{-H_2O/-CO_2}{\overset{-CH_3COCH_3}{\rightleftharpoons}} \quad —Fe^{+3}\diagup O \diagdown Fe^{+2}— \qquad (4.11e)$$
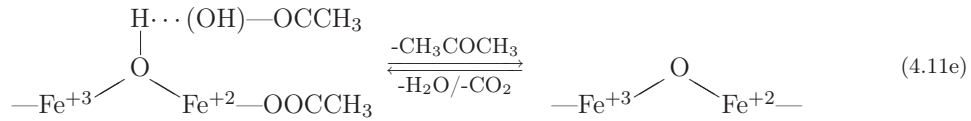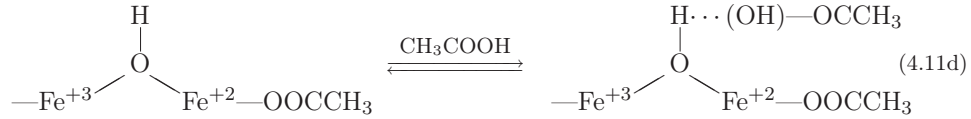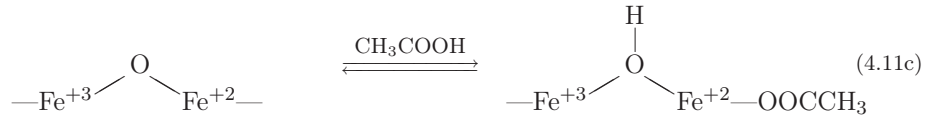
$$(4.11f)$$

Conversion of acetic acid to acetone does not require hydrogen (biogas) as shown in equation (4.6). However hydrogen is essential to keep some catalyst sites in reduced form (4.11a), which are otherwise vulnerable to CO_2 temporary poisoning via oxidation (4.11b). Although iron is not very active for RWGS reaction and CO is below detection limit but prolong catalyst run under high loading considerably alter catalyst activity. In fact reduced sites are known for their oxygen affinity so they are probably attacked by oxygen and get hydrogen ion dissipated (4.11c). The other type of sites (oxidised) may physically adsorb acid (4.11d) subsequently scavenging water from the molecule by the help of H^+ ion (4.11e). The adjacency of the two types of sites result in acetone production along CO_2 and water. Hydrogen other than keeping reduced sites may also reduce acetic acid decomposition to

coke at high temperature. Water, as per experience, may also oxidise the catalyst surface (*Haldor Topsøe*) but its activity for such reaction is less aggravated compared to CO_2 as former also produces hydrogen and does have low oxygen ratio in the molecule.

Finally warm acetic acid in contact with iron is drastically corrosive especially in our case where iron is used as catalyst having high surface area (conventionally metals are protected through protective layering). Iron corrodes to yellowish compound of ferric acetate in the presence of acetic acid, but our experiments confirm the decrease in catalyst corrosion in the presence of biogas. In Figure 4.20 two samples of acid in contact with the catalyst (FeO) are prepared and remain in contact to iron under air (left) or biogas (right). The solution under biogas does not show the presence of ferric acetate while yellowish colour confirms its presence in solution under air. This is an indirect test and further investigations are needed to deal with this problem in detail.

Figure 4.20: Effect of acetic acid on iron under biogas *(right)* and air *(left)*

4.3.5   EXPERIMENTAL RESULTS FOR ALDEHYDE PRODUCTION

As in the study of Pestman et al. [152] (Figure 4.16) catalyst selectivity shift to acetaldehyde is dictated by the degree of reduction. However similarly as acetone production, two sites are required to realise aldehyde from acetic acid. The catalyst after reduction at 450 °C for 1h is selective for ethanal production (Figure 4.21). Catalyst when charged was in the form of FeO which if oxidised cannot be recovered by reduction at 450 °C as shown by the decreased ethanal selectivity. Totally reduced iron is not capable of producing acetaldehyde. Iron in its reduced form is highly pyrophoric and is tested for ethanal production giving almost no acetaldehyde. Therefore some degree of oxidation, although not enough to produce acetone, is still required. Catalyst in an intermediate state produces both the acetaldehyde and acetone depending upon the ratio of the two sites.

On the other hand, alcohol and aldehyde ratio depends on the thermodynamics as all of the acetic acid can be fully hydrogenated to alcohol at low temperature like in fermentation broth. But at high temperature alcohol is thermodynamically hindered. Furthermore catalyst inability to total reduction further decrease ethanol selectivity. Equilibrium selectivity at 300 °C is 47% but the catalyst selectivity is only between 10-20 % as inferred from Figure 4.21. Same mechanism as that of acetone can fully explain this type of behaviour. Fortunately CO_2 kinetics to oxidise the catalyst is not high compared to reduction kinetics
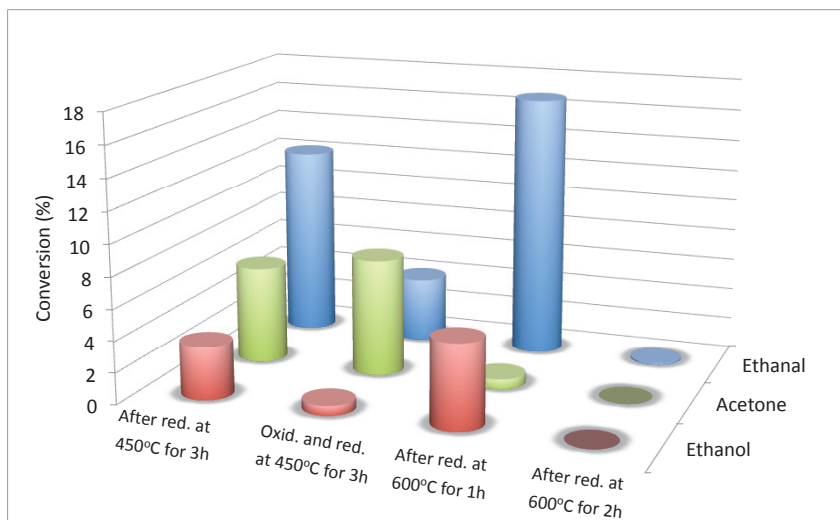
Figure 4.21: Product distribution vs state of iron reduction, T = 300 °C, $\frac{X}{N_2}$ = 1, Acid = 5 %, τ = 200 kgcat·s·mol^{-1}

induced by hydrogen. Further experiments will not give an insight because on-line determination of catalyst surface change during the experimental run is essential to derive very exact results, regarding conversion and selectivity versus reduction state.

Platinum is also used to increase the amount of dissociated hydrogen quantity deposited over Fe_2O_3 [147]. However this cannot be used with biogas as it will enhance CO production while, no CO is detected at temperature below 300 °C with iron oxide. On the contrary results shown by Grootendorst et al. [146] (in contradiction to Rachmaday et al. [138, 147, 149]) give high methane and CO_2 in effluent at high temperature (above 300 °C) and may be attributed to product decomposition at that temperature.

4.4 CONCLUSION

It has been seen in this chapter that although carboxylic acid reduction results in decrease in RWGS selectivity but still a less active catalyst like iron oxide is needed to suppress CO production completely. However such catalyst is very sensitive to its degree of reduction and oxidation towards product selection. It has been seen that totally reduced or oxidised catalyst is not active to either of the product i.e. acetone or aldehyde, thus confirming two sites behaviour. Stable production of acetone is possible in presence of biogas keeping catalyst surface stabilised which otherwise is oxidised by in-situ CO_2 production.

Given character and healthy imagination, it is possible to reconstruct this world of sin and misery into a veritable paradise.

Iqbal

5

ACETONE PRODUCTION PROCESS DESIGN VIA ACETIC ACID AND BIOGAS

5.1 INTRODUCTION

The goal of this part is to evaluate the feasibility of a hydrogenation process using biogas. In previous chapter 4, we have seen that Pt deposited on oxidised supports are affected by CO_2 as they are re-oxidised by CO_2 to form CO and thus results in catalyst deactivation. Such deactivation may be limited (as in case of Pt/SiO_2) and seems to depend on Pt dispersion. But catalyst with low Pt dispersion is not very active to hydrogenate toluene. Thus hydrogenation of toluene via biogas is ruled out for process design. It would be reconsidered for the catalyst, if such catalyst exists and found, not effected by RWGS thus promoting hydrogenation.

Regarding carboxylic acids hydrogenation on supported Pt, the measured conversion and selectivities for added value molecules are too low to be considered for process development. However acetone production on iron oxides can easily achieve 100% conversion and selectivity and industrial potential of biogas to keep the conversion stable can be studied. Process of ethanal production needs some other surface findings and thus is left for future studies.

Industrial production of acetone starts as early as in 1900. At that time acetone was mainly produced by the decomposition of calcium acetate obtained through the reaction of calcium with vinegar. With acetone usage as solvent, its demand increased and in early 1920s it was started to be produced via iso-propanol dehydrogenation. This is a two step process of absorbing propylene in concentrated sulphuric acid, thus producing iso-propyl sulphate which is then hydrolysed to iso-propanol with subsequent dehydrogenation to acetone. World War II has seen an increase in chemical market demand, thus leading to fermentation processes development towards acetone production. These processes were however out dated because of low production rates and inferior purity levels. Such process includes special conditions and bacterial culture to produce acetone in fermentation broth which is subsequently separated. High cost of energy in present scenario makes such separation economically infeasible.

A remarkable industrial revolution (1960s) in making of acetone was actually a process of phenol production, producing acetone as by product. It is known as cumene-phenol process. About 0.62 tonne of acetone is produced per tonne of phenol via this process. As in 1960s and 70s, phenol usage was moderate compared to acetone usage, thus if acetone is produced via this process, it would have resulted in high surplus volumes of phenols. So other propylene based processes were used to meet market demands for acetone.

Era of 1980s comes with an increased demand of phenol because of various phenolic resins development. This has an inverse effect on acetone market supply with surplus acetone production. In wake of same, major chemical companies had gone out of business for acetone production via processes other than cumene-phenol process.

Overall cumene-phenol process is shown in equation (5.1). This process has some disadvantages regarding environmental issues. Furthermore steady increase in propylene cost results in high cost phenol. In order to address these issues, a new plant incorporating proprietary one-step phenol manufacturing technology, first discovered by scientists in Russia's Boreskov Institute of Catalysis and perfected and commercialized in conjunction with *Solutia* engineers, is used as shown in equation (5.2). This process uses nitrous oxide and zeolites based catalysts for converting benzene to phenol with 95 % selectivity.

$$\text{C}_6\text{H}_6 + \text{CH}_2{=}\text{CH}{-}\text{CH}_3 \xrightarrow{+O_2} \text{C}_6\text{H}_5\text{OH} + \text{CH}_3{-}\overset{\text{O}}{\underset{\|}{\text{C}}}{-}\text{CH}_3 \quad (5.1)$$

$$\text{C}_6\text{H}_6 + \text{N}_2\text{O} \longrightarrow \text{C}_6\text{H}_5\text{OH} + \text{N}_2 \quad (5.2)$$
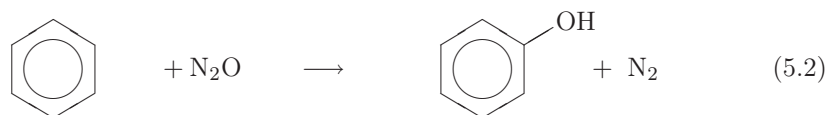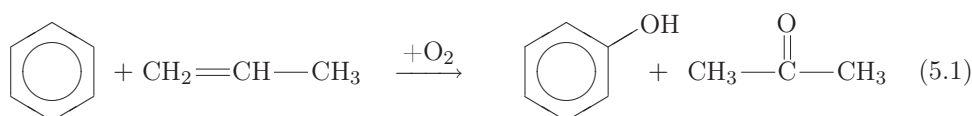
This novel process not only eliminates the high value feed stocks but also does not produce acetone thus requiring alternate routes for its production. Apart from other commercial uses acetone on the other hand is required for bisphenol A production (main ingredient for epoxy and poly-carbonate resins), consuming about 28 % of the total phenol production. Propylene however cannot be eliminated from acetone production via conventional processes [153]. Thus a new process for high purity acetone production through fermentation product is essential, in order to reap the environmental and cost benefits of eliminating the cumene-phenol process.

5.2   PROCESS DESCRIPTION

Usually bio-reactor is a concoction of dozens of chemical substrates and microbial life. Extraction of acids to acceptable purity level, for further valorization is indispensable and is of economical significance. A literature survey for available methods for acetic acid
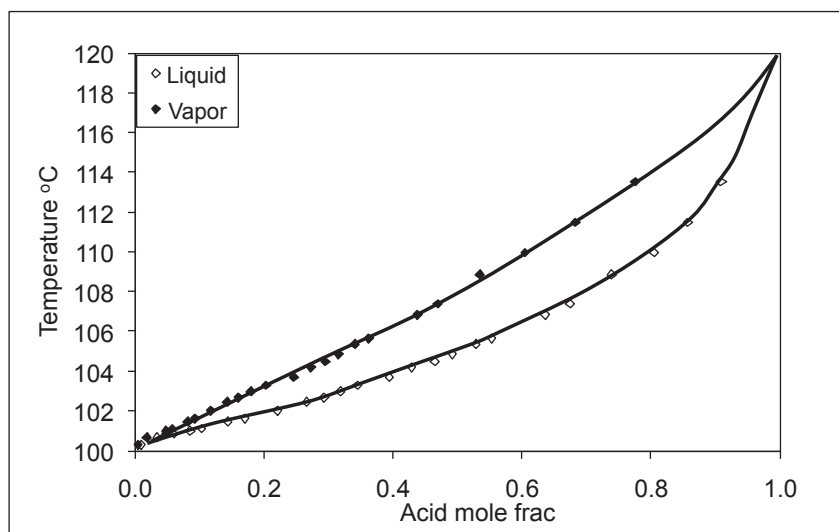
Figure 5.1: Vapour Liquid equilibria acetic acid and water (P = 1 bar) [155]

separation is done. Acetic acid is chosen because of its abundance in the fermenter. Mainly three types of techniques are reported in literature as:

1. distillation

2. solvent extraction

3. separation by neutralisation.

Acetic acid does not form an azotrope with water, however separation of the acetic acid and water mixture by simple rectification or adjustment is ruled out in this respect, since this mixture has a very small separating factor (Figure 5.1), thus requiring high towers with huge number of stages, which would have to be operated with high reflux ratio. This would necessarily involve high energy and operating cost mounts immensely.

Apart from energy considerations, recovery method using liquid liquid extraction must be taken into consideration, irrespective of the concentration, as supplementary impurities in the initial mixture, like salts, would cause problems during direct recovery by distillation.

Conventional extraction plant for the recovery of acetic acid consists of the extraction tower, the rectification tower for the recovery of the extraction agent, and the water-stripping tower. As a rule, the feed mixture has a greater density than the solvent, and is fed in at the top end of the extraction tower. Inside the tower it streams towards the bottom and in the process gives off acetic acid to the extraction agent. Depending on the effort, residual concentrations of 0.1-0.5 wt% can be achieved. Since the aqueous phase is simultaneously saturated with the extraction agent in the extraction tower, it is recovered in a downstream stripping tower. It can in this respect be performed with live steam. Various solvents used for this purpose are tabulated in Table 5.1 along with their properties significant to liquid liquid extraction.

Name	Av. distribution coefficient kg/kg	Density kg/m^3	Enthalpy of vaporisation kJ/kg	Boiling point °C	Azeotrope	
					Water Wt %	Temp °C
Ethyl acetate	0.84	900	395	76.7	8.47	70.4
iso-propyl acetate	0.55	877	361	88.6	10.50	76.5
n-Propyl acetate	0.50	891	336	101.6	13.20	82.2
2-Pentanone	0.97	810	384	102.3	19.50	83.3
4-Methyl-2-Pentanone	0.50	810	488	115.9	24.30	87.9
Methyl-tert.-butyl ether	0.75	740	322	55	4	52.6

Table 5.1: Common solvents used to extract acetic acid

Exploitation of acidic feature, by alkaline amines to separate acidic gases is well known industrially. Acids from fermentation broth may also be removed in same way. BP Amoco Chemicals, Integrated Genomics, Sulzer Chemtech GmbH and Argonne National Laboratory are main partners towards developing an industrial process, using ammonia to separate acids from dark fermentation products (Figure 5.2) [156]. They are also focusing on controlling broth pH a very important feature (section 2.3.2). Tertiary amines can also be used to achieve this [157,158]. A novel method of using ion exchange resins to remove acids is also reported by Lin et al. [159]. In this process evaluation acetate separation is not considered as this step is beyond the scope of current work and is studied in future. We have only considered the down stream process of acetic acid hydrogenation to acetone.
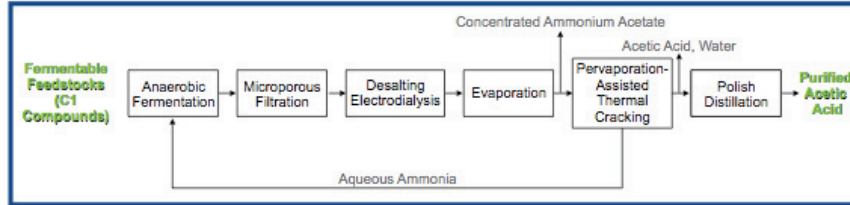
Figure 5.2: Acid separation by ammonia [156]

5.2.1 RAW FEED

As acetone production is based upon fermentation raw products so, a case study conducted by Gavala et al. [65] for glucose is taken as basis for fermentation product. The process described by these researchers is continuous with CSTR type fermenter. Moderate hydraulic retention time and mesophilic conditions of 4h and 35°C are selected respectively. The bacterial anaerobic sludge is taken from waste water treatment plant with heat treatment (100°C) to remove any hydrogen consumers.

The fermentation products contain VFAs and Ethanol. Among the VFAs acetic, butyric and lactic acids are reported. Ethanol and lactic acids are ignored because of their

negligible production in CSTR with retention time of 4h. Moreover Ethanol is a direct result of hydrogen usage by bacterial life, therefore use of selected strains may eliminate its production completely. Butyric acid on the other hand may be present in considerable quantity. Acetic acid is the first product in metabolic path of fermentation. If acetic acid is removed as it is produced in fermenter then its production may significantly be enhanced along with hydrogen. So the respective production of the two is adjusted with a supposition of no butyric acid production. An earlier work [160] also established the reaction of ethanol and acetic acid to produce butyric acid. Ethanol formation reduces hydrogen production as it requires complete hydrogenation of the acids. So any genetically modified bacterial strains may further enhance hydrogen production by inhibiting ethanol and thus butyric acid.

In order to evaluate the process I have chosen 1 tonne glucose conversion to acetic acid as in Table 5.2:

Component	Liquid phase [65]	Gas phase [65]	Production rate	Production rate with no Butyric acid
	mmol/l	ml/h	tonne/tonne	tonne/tonne
			Basis: 1 tonne glucose consumed per hour	
Acetic acid	8.4	-	0.16	0.34
Butyric acid	9.6	-	0.27	-
Hydrogen	-	108.2	0.024	0.04
CO_2	-	133.8	0.67	0.67

Table 5.2: Raw feed to catalytic reactor

5.2.2 SIMULATION PACKAGE

In order to simulate acetone production process we have used HYSYS (simulation software) to carry out the mass and energy balance calculations. Finding good values for inadequate or missing physical property parameters is the key to a successful simulation and this depends upon choosing the right method. As our components to be simulated are polar in nature and although, acid do dissociate in water but constant of dissociation is not very high for acetic acid, so mixture is assumed to be non-electrolytic. This assumption is often taken in choosing simulation package, a comprehensive package choice algorithm is shown in Figure 5.3. This assumption is also confirmed through the examples provided by the software vendor. As almost all of the binary coefficients are known, so Non Random Two Liquids (NRTL) method is used with others unknowns are estimated through UNIFAC method. All other properties are estimated via extended NRTL prediction equations.
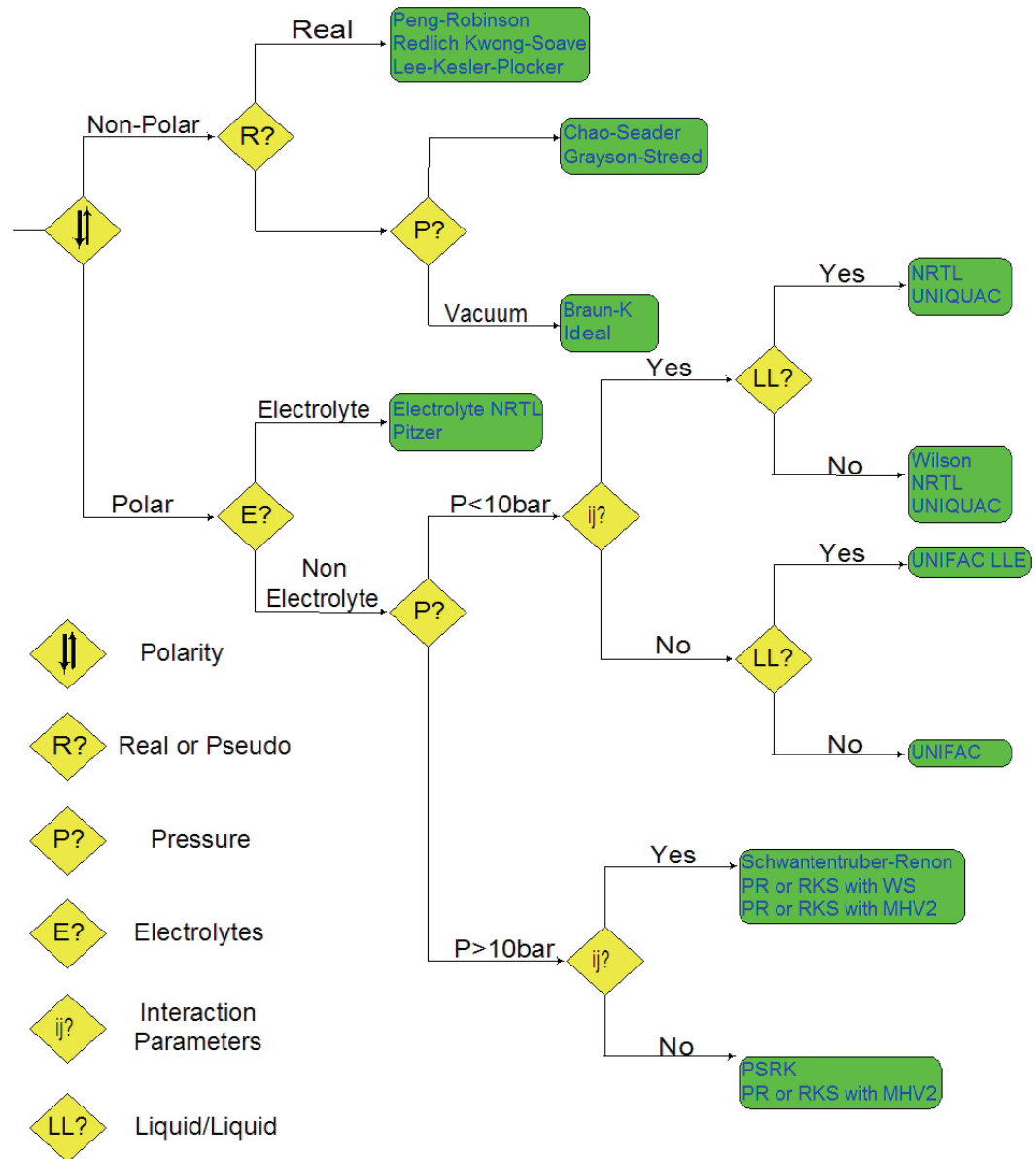
Figure 5.3: Physical property package selection

5.2.3 PROCESS FLOW DIAGRAM

Process Flow Diagram (PFD) is shown in Figure 5.4. As discussed earlier, ratio of acid to biogas is essential to maintain the catalyst surface active for acetone production, so acid percentage is changed from 1 to 50%. Exact percentage of acid in biogas depends upon the optimisation of the two sites mechanism.
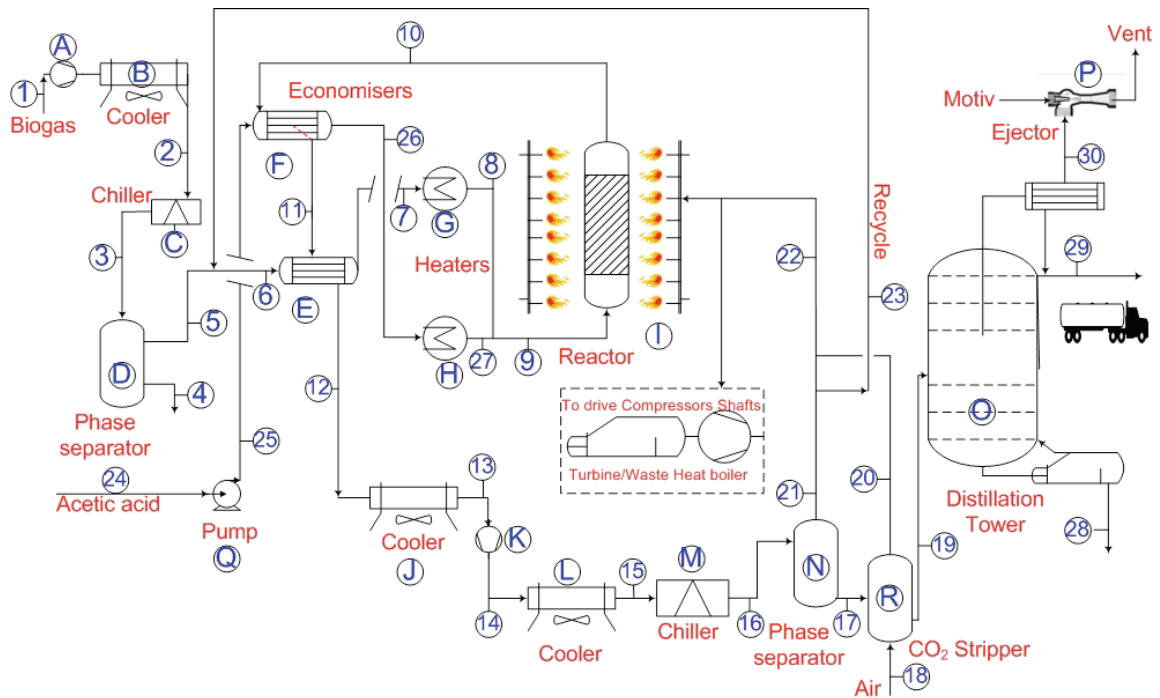
Figure 5.4: Process Flow Diagram for acetone production (HYSYS)

Detailed mass and energy balance is provided in annex F.

5.2.3.1 BIOGAS DE-WATERING

As fermenter contains huge amount of water, so the biogas produced is assumed to be at its dew point at moderate temperature of 25 °C and atmospheric pressure. This water should be removed prior the further usage of biogas as if not it decreases the purity level of the product (acetone) produced in reactor and hence augments the duty of fractionating column at downstream of the process. So a chiller is provided at downstream of the biogas compressor (P = 446 kPa) to decrease its temperature to 5 °C, thus decreasing the dew point for water at high pressure resulting in its elimination in downstream separator. Duty of this chiller is calculating by considering saturated biogas. Under these conditions about 94 % of the water present in the biogas can be removed.

5.2.3.2 CATALYTIC REACTOR

The catalyst mass and reactor volume have been calculated for different temperatures, for 100 % acetic acid conversion to acetone with catalyst oxidised at 450 °C (figure 5.5).

Exponential increase in catalyst mass with temperature dictates a limit to the minimum temperature that can be selected. As the activation energy is about 100 kJ/mol so about 8 tonnes of iron oxide is needed at $300\,°C$ to treat 340 kg/h of acetic acid. On the other hand pure acetic acid if used deactivates the catalyst rapidly as described previously so, it is to be diluted with biogas in the reactor containing active iron oxide catalyst to produce acetone. Biogas is used as a carrier gas to increase catalyst activity via provision of hydrogen to regenerate not only the reduced sites but also the coked surface. Sharp increase in conversion with increase in reduced sites for oxidised catalyst can considerably decrease the volume of the catalytic bed. However too much of such sites are avoided. A recycle stream of biogas is provided to achieve optimum acid concentration in the reactor. Furthermore high temperature should be restricted as excessive heat can decompose such kind of hydrocarbons.
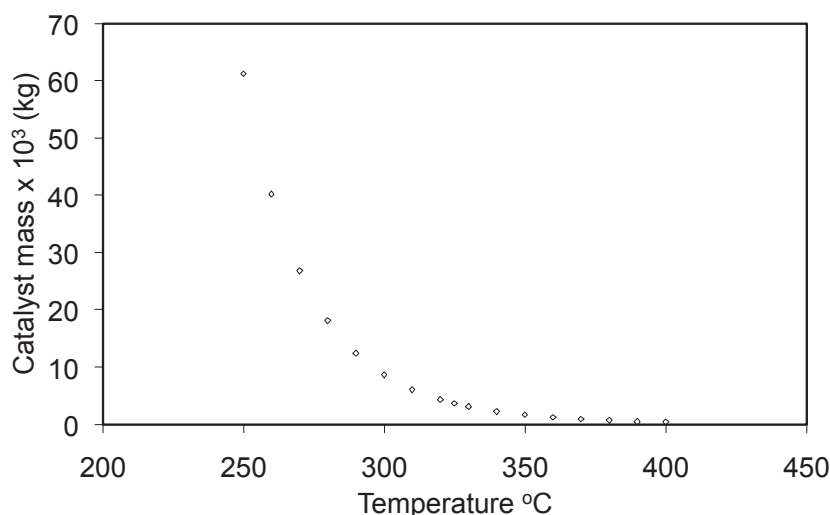
Figure 5.5: Calculated catalyst mass needed in the reactor for different temperatures

5.2.3.3 ACETONE SEPARATION

First step in acetone recovery is phase separation. Such phase separation is done at high pressure to compromise the chiller duty. Selection of pressure is done by optimizing the energy consumption by compression against amount of acetone recovered as shown in figure 5.6. It may be concluded from the figure that after certain compression, recovery is not economical. But still initial compression before cooling aids a lot in acetone recovery, for an instance about 22 % (wt %) more acetone may be recovered at 450 kPa compared to atmospheric pressure.

CO_2 is moderately soluble in water, although conditions are acidic (i.e. not favourable) still carbonic acid may be present in the recovered acetone water mixture. This CO_2 if not removed will result in low temperature condensation in the condenser of distillation tower.
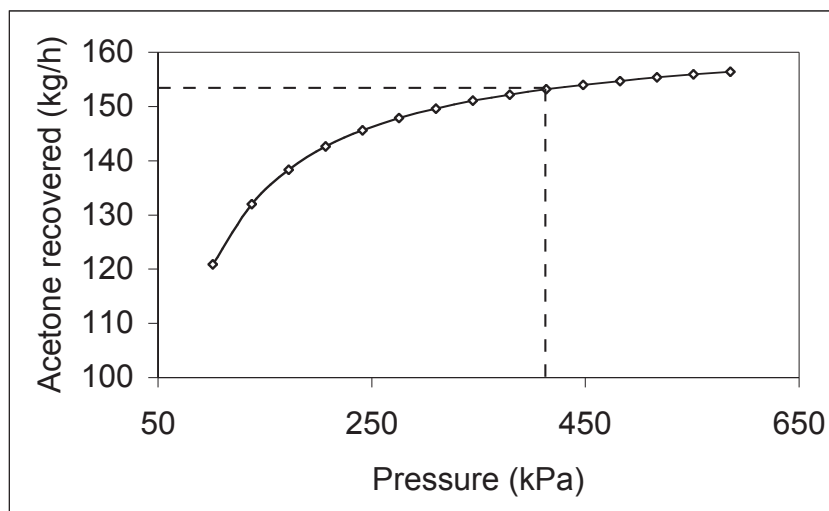
Figure 5.6: Acetone recovery via phase separation at different pressures

If temperature is not set to low value then considerable quantity of acetone will be inhaled
by the downstream ejector to keep distillation tower below atmospheric pressure. So in
second step, this pre-distillation CO_2 strippage will ensure the optimum acetone recovery.
Air is blown through such mixture to evacuate acetone. However amount of air should be
optimised as more than certain level will result in acetone loss as shown in Figure 5.7.

Finally main impurity that rests with acetone is then water. Separation is not very
difficult, acetone and water do not form azeotrope and may easily be separated by vacuum
distillation. Under our condition only four stages are required for distilling acetone to the
purity level of 96 %. Reboiler duty is considerably reduced by operating column under low
pressure.

5.2.4   OVERALL ENERGY FEASIBILITY

The process parameters used in simulation with raw feed input presented in table 5.2, are
shown in table 5.3 . These parameters are typically used in preliminary estimates and are
deliberately taken on the lower side (Ft factor ensures the logical and rational heat transfer
surface area for heat exchangers).
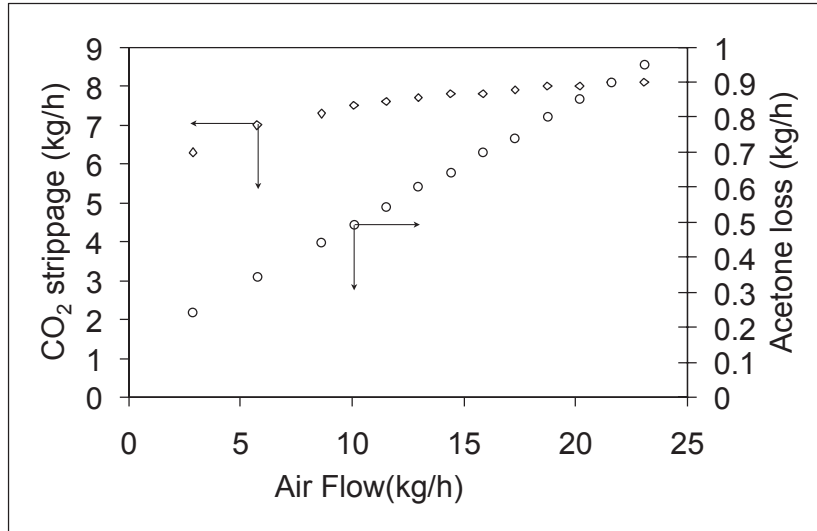
Figure 5.7: Effect of air flow on CO_2 strippage and acetone loss

Parameter	Value	Units
Reactor temperature	300	°C
Acetic acid conversion to acetone	99.3	%
Ft factor for economisers	> 0.8	
Heat loss	20	%
ΔP for each side	< 10	psi
Chiller temperature	-20	°C
Chiller COP	2	
Chiller drive efficiency	40	%
Minimum acetone purity	96	%
Acetone accompanying impurities		
H_2O	3	%
Acetaldehyde	0.8	%
Acetone recovery	92	%
Pure acetone production per tonne glucose	151	kg/h
Flue gas temperature after biogas combustion	180	°C
Efficiency of steam generation and turbine for compression	40	%

Table 5.3: Parameters adjusted for energy balance

The energy balance thus conducted is presented in Figure 5.8. The break even point for acetone process is with 9 % (mol frac) acetic acid entering into the reactor. This gives the minimum limit for acetic acid concentration entering the reactor, in order to keep process remote from any external energy source. Moreover the factors are taken at their minimum values i.e. after pilot plant tests conduction they may be further adjusted to more accurate value. Chillers and compressors duty can be decreased by introducing the cooling water, further shifting the energy balance in the favour of the process. The sharp decrease in energy required after 15% acetic acid is due to the curtail of recycle stream thus eliminating the recycle compressor. A part of the gas thus bypassed the reactor and is not chilled to remove water thus further decreasing the compression work.
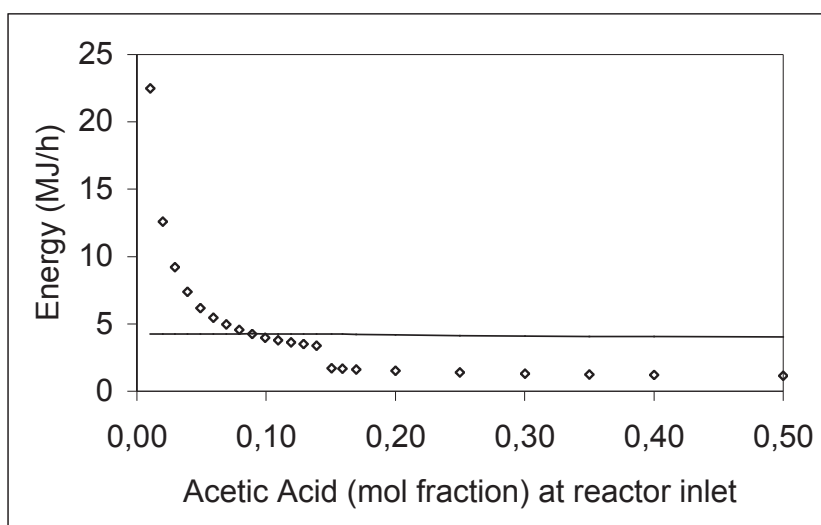
Figure 5.8: Energy feasibility of coupled bio-acetone process ◇ - energy required by the process, Continuous line - energy available

5.3 CONCLUSION

The extracted carboxylic acids from fermenter can thus further be used to generate ketones. The process simulated uses biogas to minimize iron corrosion by acetic acid as well as to keep catalyst active. Considerable energy can be saved by removing water from biogas and CO_2 strippage before distillation. About 151 kg of acetone is recovered from one tonne glucose consumed plus 13 % loss in purge and waste water. Process is energetically feasible as far as acid concentration entering the reactor is above 9 %. However depending on catalyst surface response, considerable energy can be saved by minimizing or even by complete stoppage of the recycle. So optimum acid concentration entering the reactor is to be evaluated considering catalyst surface response, acid conversion, available energy and last but not the least iron corrosion. Waste water contaminated with acetone can be recycled

to fermenter as it does not contain any poison for the bacterial colonies, thus making this process 100 % pollutant free. Efficient acid separation from the fermenter is however a concern for future studies.

Two reeds drink from one stream. One is hollow, the other is sugar-cane.

<div align="right">Rumi</div>

6
CONCLUSION AND PERSPECTIVE

Production of hydrogen through renewables is the need of hour. Biomass fermentation is extensively studied for this purpose and it is only matter of time that this process will be commercially available. Some Hybrid techniques are found effective in high hydrogen yield and rate but economical feasibility of the overall process is a key factor to choose between them. Use of this biogas for simple burning may not be justified for combined cycles as biogas containing methane gives better efficiency when burned in such a system. Furthermore pretreatment is generally required to augment its calorific value and to get rid of pollutants. Such pretreatment processes may require high energy and investment. Fuel cells, although may use this biogas to generate electricity but they are operated at high temperature to avoid CO_2 poisoning (Fuel cell efficiency operating below 150°C is inhibited by CO_2) and usually employ corrosive medium for electron transfer. Furthermore their life span is too short to be economical as they are very expensive to replace.

Storage and transfer of this raw biogas as such may not be possible without the expense of huge energy. So toluene was tried as hydrogen storage molecule with its conversion to methylcyclohexane along some other benefits. Conversion of toluene to methylcyclohexane is thermodynamically 100% possible as far as temperature is below 150°C. All elements of group 8 to 10 of periodic table can be used as catalyst for aromatics hydrogenation while internal and external transfer resistances are not important as far as catalyst of reasonable size with appreciable space velocity. Intermediate products are thermodynamically suppressed and inhibition by reaction product i.e. methylcyclohexane is not reckoned. No general consensus over rate law and reaction mechanism between various researchers exist.

Transition activity loss is observed for the catalytic system with a stable equilibrium point after which no further deactivation is observed under pure H_2 (with no CO_2) over Pt/Al_2O_3. High temperature results in rapid activity loss with lower stabilization/equilibrium point. Arguable phenomenon of hydrogen spillover or transfer may dictate such two sites kinetics. Pt/Al_2O_3 regeneration depends upon purge rate while catalyst total regain of activity by nitrogen rules out the deactivation by sulphur or coke. Nitrogen is an inert and can be used to adjust experimental conditions over platinum catalyst. Contrary to toluene, no adverse effect of methycyclohexane is observed on reaction kinetics. High activity of Pt with other supports i.e. silica and titanium oxide is observed.

Exact behaviour of CO_2 over the catalyst was not known in literature. It was found that alumina based platinum is an excellent catalyst for toluene hydrogenation until CO_2 interaction is avoided. CO_2 exposure deactivates the catalysts irreversibly through formation of surface complexes. Drastic effect of CO_2 is observed over metal surface with Pt-CO bonds and Pt/Al_2O_3 cannot be regenerated until treated by air contrary to other Pt catalysts having different supports. CO_2 inhibitory effect may still be observed for Pt/SiO_2 and Pt/SiO_2-TiO_2 as far as toluene hydrogenation is considered. Only Pt/SiO_2 shows small hydrogenation activity in CO_2 environment mainly because of some surface phenomena. Reverse water gas shift reaction resulting in CO formation and hence the preferential adsorption of CO over metal catalyst linked sites may hinder aromatic hydrogenation and results in catalyst deactivation. This may generally conclude that more the catalyst is active in aromatic hydrogenation, more it shifts to CO_2 hydrogenation selectivity producing CO. Methane which might be present in traces in biogas may safely be taken as an inert.

According to the mechanism of CO poisoning, catalyst must be sought out with its linked sites immune to poisoning to bring aromatic hydrogenation. Such catalyst is also essential for use in fuel cells at low temperature. Bi-metallic catalysts like Pt-Re may be further tested in this regard. Open chain aliphatic hydrocarbons (alkenes/alkynes) may also be considered for hydrogenation under biogas to evaluate any negative ring effect of aromatics. CO poisoning may be compromised by hydrogenating such a compound having comparable adsorption enthalpy to CO. Further brain storming and literature review is recommended to dig out such entities (like nitro, oxy or halo rings). These compounds if found may also serve as storage molecules.

Dark fermentation, hydrogen producing, processes also result in carboxylic acids production that can further be valorized by conversion to high value products. Removal of these acids from fermentation broth enhances the efficiency of fermentation process via pH control. Extensive work is going on for removal of such acids and established patents are already been submitted. The comparable adsorption energy of carboxylic acids to that of CO can shift the selectivity from CO_2 to acids hydrogenation. A thermodynamic balance exists between alcohol and aldehyde production with high pressure favouring the former and high temperature favouring the latter. Conversion of acids to ketones is 100% thermodynamically possible above 50 °C. Pt/Al_2O_3 and Pt/SiO_2 are not used for acids hydrogenation mainly because of alumina-CO_2 complexes formation and acid decomposition respectively. Long chain acids (octanoic) kinetics is lower compared to short chain acids (Acetic) with high temperature favouring decomposition over Pt/SiO_2-TiO_2. Ketones are not observed over this catalyst. Such conversion of acids is because of selectivity shift between RWGS and acids hydrogenation.

Iron oxide may produce both ketones and aldehyde-alcohol pair depending upon its oxidation or reduction state. If catalyst is more oxidised it produces ketones although some reduced sites are also required for acid condensation to ketones. However more than certain degree of reduction shifts the balance in favour of aldehydes. Hydrogen, although having no part in reaction, is needed during ketone formation to keep balance between two types of sites required to produce such compounds, as CO_2 the product of acetone formation may oxidise the catalyst surface resulting in decrease in ketone production. No appreciable amount of CO via reverse water gas shift reaction is observed over iron oxide.

Acetone production process is required to replace the current phenol-cumene process by green nitrous oxide process and overall process devised is energetically feasible with no external source of energy requirement. Prior drying of the biogas is required to decrease the duty of reboiler for distilling acetone out of water. Similarly in order to keep distillation

under vacuum CO_2 stripping by air from the condensed stream is necessary. Much of the acetone produced in the reactor can be purified and recovered.

Direct measure of active sites (reductive or oxidative) for iron oxide by catalyst surface chemistry evaluation is to be used to optimize the process of acetone or ethanal production from acetone. Such an on-line system is essential for the development of reaction mechanism and kinetics along catalyst surface change. Furthermore DRIFT study or any other surface study technique should be applied to assess direct surface effect of CO_2. Some other acids like butyric may further be tested over iron oxide with an added value to the product. Furthermore a combination of two acids may result in non symmetrical and industrially useful ketones as further process development in this area is bound to industrial interest. In this regard production of specific carboxylic acid via bacterial genetic modification may further optimize the process.

Effect of acetic acid corrosion over iron should be evaluated in the presence of biogas and ways to minimize the catalyst loss via corrosion must be determined and quantified.

NOMENCLATURE

Nomenclature	
Alphabatical symbols	
C	concentration of specie (mol·m^{-3})
$\mathbb{C}$	sites on platinum (mol·kgcat^{-1})
f$_e x$	external diffusion resistance factor
H	enthalpy (kJ·mol^{-1})
k	rate constant for reaction/adsorption constant
K	equilibrium rat or adsorption constant
n	number of moles (mol)
P	partial or total pressures (Pa)
r	rate (mol·s^{-1}· kgcat^{-1})
$S1$	sites offered by metal
$S2$	sites offered by support
T	temperature (K)
t	time (s)
τ	space velocity (kgcat · s · mol^{-1})
TOF	Turn over frequency (s^{-1})
X	Conversion (%)
Greek Symbols	
Δ	gradient
Γ	deactivation factor
φ	deactivation rate
θ	Vacant sites
τ	space velocity
superscripts	
'	support constants
$*$	Adsorbed species
α	hydrogen reaction order
β	toluene reaction order
d	order of deactivation
m	order of reaction for toluene
n	order of reaction for hydrogen
$S1$	specie adsorbed on platinum
$S2$	specie adsorbed on support
x	order of reaction
y	order of reaction causing deactivation
	Continued on next page...

Nomenclature	
Subscripts	
A	reactant
ad, CO_2	Carbon dioxide adsorption
ad, CO	Carbon monoxide adsorption
ad, H_2	hydrogen adsorption
ad, Tol	toluene adsorption
b	benzene
d	deactivation
d, CO_2	Carbon dioxide desorption
d, CO	Carbon monoxide desorption
d, H_2	hydrogen desorption
d, Tol	toluene desorption
H_2	hydrogen
Pt	Platinum
s	specie adsorbed on support
Tol	toluene
t	total
x	stoichiometric ratio

Bibliography

[1] L. Barreto, A. Makihira, K. Riahi, The hydrogen economy in the 21st century: a sustainable development scenario, International Journal of Hydrogen Energy 28 (2003) 267–284.

[2] P. Westermann, B. Jorgensen, L. Lange, B. K. Ahring, C. H. Christensen, Maximizing renewable hydrogen production from biomass in a bio/catalytic refinery, International Journal of Hydrogen Energy 32 (2007) 4135–4141.

[3] Energy information administration.
URL http://www.eia.doe.gov/

[4] D. klass, Biomass for Renewabel Energy, Fuels and Chemicals, Acedamic Press.

[5] L. Luo, E. van der Voet, G. Huppes, Biorefining of lignocellulosic feedstock-technical, economic and environmental considerations, Bioresource Technology 101 (2010) 5023–5032.

[6] [link].
URL http://www.inforse.dk/europe/dieret/Biomass/biomass.html

[7] D. Das, T. N. Veziroglu, Hydrogen production by biological processes: a survey of literature, International Journal of Chemical Reactor Engineering 26 (2001) 13–28.

[8] J. Woodward, M. Orr, K. Cordray, E. Greenbaum, Enzymatic production of biohydrogen, Nature 405 (2000) 1014–1015.

[9] J. R. Benemann, Feasibilty analysis of photobiological hydrogen production, International Journal of Hydrogen Energy 22 (1997) 979–987.

[10] D. B. Levin, L. Pitt, M. Love, Biohydrogen production: prospects and limitations to practical application, Interational Journal of Hydrogen Energy 29 (2004) 173–185.

[11] T. Katsuda, M. Azuma, J. Kato, S. Takakuwa, H. Ooshima, Effects of ethanolamine as a nitrogen source on hydrogen production by rhodobacter capsulatus, Biosci. Biotechnol. Biochem. 64(2) (2000) 248–253.

[12] C.-M. Lee, P.-C. Chen, C.-C. Wang, Y.-C. Tung, Photohydrogen production using purple nonsulfur bacteria with hydrogen fermentation reactor effluent, International Journal of Hydrogen Energy 27 (2002) 1309–1313.

[13] H. Koku, I. Eroglua, U. Gunduz, M. Yucel, L. Turkerc, Aspects of the metabolism of hydrogen production by rhodobacter sphaeroides, International Journal of Hydrogen Energy 27 (2002) 1315–1329.

[14] J. Obeid, J.-P. Magnin, J.-M. Flaus, O. Adrot, J. C. Willison, R. Zlatev, Modelling of hydrogen production in batch cultures of the photosynthetic bacterium rhodobacter capsulatus, International Journal of Hydrogen Energy 34 (2009) 180–185.

[15] T. Katsuda, T. Arimoto, K. Igarashi, M. Azuma, J. Kato, S. Takakuwa, H. Ooshima, Light intensity distribution in the externally illuminated cylindrical photo-bioreactor and its application to hydrogen production by rhodobacter capsulatus., Biochemical Engineering Journal 5 (2000) 157–164.

[16] E. Nakada, Y. Asada, T. Arai, J. Miyake, Light penetration into cell suspensions of photosynthetic bacteria and relation to hydrogen production, Journal of Fermentation and Bioengineering 80(1) (1995) 53–57.

[17] X.-Y. Shi, H.-Q. Yu, Optimization of volatile fatty acid compositions for hydrogen production by rhodopseudomonas capsulata, Journal of Chemical Technology and Biotechnology 80 (2005) 1198–1203.

[18] M. J. Barbosa, J. M. Rocha, J. Tramper, R. H. Wijffels, Acetate as a carbon source for hydrogen production by photosynthetic bacteria, Journal of Biotechnology 85 (2001) 25–33.

[19] H. Su, J. Cheng, J. Zhou, W. Song, K. Cen, Improving hydrogen production from cassava starch by combination of dark and photo fermentation, International Journal of Hydrogen Energy 34 (2009) 1780–1786.

[20] H. H. Fang, H. Zhu, T. Zhang, Phototrophic hydrogen production from glucose by pure and co-cultures of clostridium butyricum and rhodobacter sphaeroides, Interational Journal of Hydrogen Energy 31 (2006) 2223–2230.

[21] H.-L. Chin, Z.-S. Chen, C. P. Chou, Fedbatch operation using clostridium acetobutylicum suspension culture as biocatalyst for enhancing hydrogen production, Biotechnol. Prog. 19 (2003) 383–388.

[22] C. C. Chen, C.-Y. Lin, M.-C. Lin, Acid-base enrichment enhances anaerobic hydrogen production process, Applied Microbiol Biotechnology 58 (2002) 224–228.

[23] G. Wang, Y. Mu, H.-Q. Yu, Response surface analysis to evaluate the influence of pH, temperature and substrate concentration on the acidogenesis of sucrose-rich wastewater, Biochemical Engineering Journal 23 (2005) 175–184.

[24] X. Wang, P. Monis, C. Saint, B. Jin, Biochemical kinetics of fermentative hydrogen production by clostridium butyricum w5, International Journal of Hydrogen Energy 34 (2009) 791–798.

[25] H. Zhang, M. A. Bruns, B. E. Logan, Biological hydrogen production by clostridium acetobutylicum in an unsaturated flow reactor, Water Research 40 (2006) 728–734.

[26] C. Collet, N. Adler, J.-P. Schwitzguebel, P. P. eringer, Hydrogen production by clostridium thermolacticum during continuous fermentation of lactose, Interational Journal of Hydrogen Energy 29 (2004) 1479–1485.

[27] L. Magnusson, N. Cicek, R. Sparling, D. Levin, Continuous hydrogen production during fermentation of α-cellulose by the thermophillic bacterium clostridium thermocellum, Biotechnol. Bioeng. 102 (2009) 759–766.

[28] H. H. Fang, H. Liu, Effect of pH on hydrogen production from glucose by a mixed culture, Biosource Technology 82 (2002) 87–93.

[29] T. Zhang, H. Liu, H. H. Fang, Biohydrogen production from starch in wastewater under thermophilic condition, Journal of Environmental Management 69 (2003) 149–156.

[30] S. Tanisho, Y. Ishiwata, Continuous hydrogen production from molasses by fermentation using urethane foam as a supporf of flocks, Interational Journal of Hydrogen Energy 20 (1995) 541–545.

[31] H. Yokoyama, H. Ohmori, M. Waki, A. Ogino, Y. Tanaka, Continuous hydrogen production from glucose by using extreme thermophilic anaerobic microflora, Journal of Bioscience and Bioengineering 107(1) (2009) 64–66.

[32] X.-J. Zheng, H.-Q. Yu, Roles of pH in biologic production of hydrogen and volatile fatty acids from glucose by enriched anaerobic cultures, Applied Biochem. Biotechnol. 112(2) (2004) 79–90.

[33] L. Dong, Y. Zhenhong, S. Yongming, K. Xiaoying, Z. Yu, Hydrogen production characteristics of the organic fraction of municipal solid wastes by anaerobic mixed culture fermentation, International Journal of Hydrogen Energy 34 (2009) 812–820.

[34] J.-J. Lay, K.-S. Fan, James-Chang, C.-H. Ku, Influence of chemical nature of organic wastes on their conversion to hydrogen by heat-shock digested sludge, International Journal of Hydrogen Energy 28 (2003) 1361–1367.

[35] B. F. Belokopytov, K. S. Laurinavichius, T. V. Laurinavichene, M. L. Ghirardi, M. Seibert, A. A. Tsygankov, Towards the integration of dark- and photo-fermentative waste treatment. 2. optimization of starch-dependent fermentative hydrogen production, International Journal of Hydrogen Energy 34 (2009) 3324–3332.

[36] B. Uyar, I. Eroglu, M. Yucel, U. Gunduz, Photofermentative hydrogen production from volatile fatty acids present in dark fermentation effluents, International Journal of Hydrogen Energy 34 (2009) 4517–4523.

[37] H. Argun, F. Kargi, I. K. Kapdan, Hydrogen production by combined dark and light fermentation of ground wheat solution, International Journal of Hydrogen Energy 34 (2009) 4305–4311.

[38] L. Lu, N. Ren, D. Xing, B. E. Logan, Hydrogen production with effluent from an ethanol-H_2-coproducing fermentation reactor using a single-chamber microbial electrolysis cell, Biosensors and Bioelectronics 24 (2009) 3055–3060.

[39] B.-F. Liu, N.-Q. Ren, J. Tang, J. Ding, W.-Z. Liu, J.-F. Xu, G.-L. Cao, W.-Q. Guo, G.-J. Xie, Bio-hydrogen production by mixed culture of photo- and dark-fermentation bacteria, iInternational Journal of Hydrogen Eneregy 35 (2010) 2858–2862.

[40] B. Xiao, J. Liu, Biological hydrogen production from sterilized sewage sludge by anaerobic self-fermentation, Journal of Hazardous Materials 168 (2009) 163–167.

[41] S.-Y. Wu, C.-N. Lin, J.-S. Chang, Hydrogen production with immobilized sewage sludge in three-phase fluidized-bed bioreactors, Biotechnol. Prog. 19 (2003) 828–832.

[42] H. Argun, F. Kargi, I. K. Kapdan, Microbial culture selection for bio-hydrogen production from waste ground wheat by dark fermentation, International Journal of Hydrogen Energy 34 (2009) 2195–2200.

[43] J. Wang, W. Wan, Comparison of different pretreatment methods for enriching hydrogen-producing bacteria from digested sludge, International Journal of Hydrogen Energy 33 (2008) 2934–2941.

[44] S.-E. Oh, S. V. Ginkel, B. E. Logan, The relative effectiveness of pH control and heat treatment for enhancing biohydrogen gas production, Environ. Sci. Technol. 37(22) (2003) 5186–5190.

[45] B. Hu, S. Chen, Pretreatment of methanogenic granules for immobilized hydrogen fermentation, Interational Journal of Hydrogen Energy 32(15) (2007) 3266–3273.

[46] B. E. Logan, S.-E. Oh, I. S. Kim, S. V. Ginkel, Biological hydrogen production measured in batch anaerobic respirometers, Environ. Sci. Technol. 36(11) (2002) 2530–2535.

[47] P. Iyer, M. A. Bruns, H. Zhang, S. V. Ginkel, B. E. Logan, H_2-producing bacterial communities from a heat-treated soil inoculum, Appl Microbiol Biotechnol 66(2) (2004) 166–173.

[48] Y. Fan, C. Li, J.-J. Lay, H. Hou, G. Zhang, Optimization of initial substrate and pH levels for germination of sporing hydrogen-producing anaerobes in cow dung compost., Bioresource Technology 91(6) (2004) 189–193.

[49] H. Zhu, M. Béland, Evaluation of alternative methods of preparing hydrogen producing seeds from digested wastewater sludge, Interational Journal of Hydrogen Energy 31(14) (2006) 1980–1988.

[50] Y. Mu, H.-Q. Yu, G. Wang, Evaluation of three methods for enriching H_2-producing cultures from anaerobic sludge, Enzyme and Microbial Technology 40(4) (2007) 947–953.

[51] Y. Zhang, G. Liu, J. Shen, Hydrogen production in batch culture of mixed bacteria with sucrose under different iron concentrations, Interational Journal of Hydrogen Energy 30(8) (2005) 855–860.

[52] C. Y. Lin, C. H. Lay, A nutrient formulation for fermentative hydrogen production using anaerobic sewage sludge microflora, Interational Journal of Hydrogen Energy 30(3) (2005) 285–292.

[53] F.-Y. Chang, C.-Y. Lin, Biohydrogen production using an up-flow anaerobic sludge blanket reactor, Interational Journal of Hydrogen Energy 29(1) (2004) 33–39.

[54] C. Y. Lin, C. H. Lay, Carbon/nitrogen-ratio effect on fermentative hydrogen production by mixed microflora, Interational Journal of Hydrogen Energy 29 (2004) 41–45.

[55] C. Y. Lin, C. H. Lay, Effects of carbonate and phosphate concentrations on hydrogen production using anaerobic sewage sludge microflora, Interational Journal of Hydrogen Energy 29(3) (2004) 275–281.

[56] C. Lin, C. Chou, Anaerobic hydrogen production from sucrose using an acid-enriched sewage sludge microflora, Engineering Life in Science 41(4) (2004) 66–70.

[57] C.-Y. Lin, C.-Y. Lee, I.-C. Tseng, I. Shiao, Biohydrogen production from sucrose using base-enriched anaerobic mixed microflora, Process Biochemistry 41(4) (2006) 915–919.

[58] T.-M. Liang, S.-S. Cheng, K.-L. Wu, Behavioral study on hydrogen fermentation reactor installed with silicone rubber membrane, Interational Journal of Hydrogen Energy 27(11-12) (2002) 1157–1165.

[59] M. Morimotoa, M. Atsuko, A. Atif, M. Ngan, A. Fakhrul-Razib, S. Iyuke, A. Bakir, Biological productionof hydrogen from glucose by natural anaerobic microflora, Interational Journal of Hydrogen Energy 29 (2004) 709–714.

[60] M. Ferchichi, E. Crabbe, G.-H. Gil, W. Hintz, A. Almadidy, Influence of initial pH on hydrogen production from cheese whey, Journal of Biotechnology 120 (2005) 402–409.

[61] W.-H. Chen, S. Sung, S.-Y. Chen, Biological hydrogen production in an anaerobic sequencing batch reactor: pH and cyclic duration effects, International Journal of Hydrogen Energy 34 (2009) 227–234.

[62] J. Wang, W. Wan, Kinetic models for fermentative hydrogen production: A review, International Journal of Hydrogen Energy 34 (2009) 3313–3323.

[63] J.-J. Lay, Modeling and optimization of anaerobic digested sludge converting starch to hydrogen, Biotechnology and Bioengineering 68 (2000) 269–278.

[64] Y. Mu, X.-J. Zheng, H.-Q. Yu, R.-F. Zhu, Biological hydrogen production by anaerobic sludge at various temperatures, International Journal of Hydrogen Energy 31 (2006) 780–785.

[65] H. N. Gavala, I. V. Skiadas, B. K. Ahring, Biological hydrogen production in suspended and attached growth anaerobic reactor systems, International Journal of Hydrogen Energy 31 (2006) 1164–1175.

[66] V. Gadhamshetty, D. C. Johnson, N. Nirmalakhandan, G. B. Smith, S. Deng, Feasibility of biohydrogen production at low temperatures in unbuffered reactors, International Journal of Hydrogen Energy 34 (2009) 1233–1243.

[67] S. V. Mohan, V. L. Babu, P. Sarma, Anaerobic biohydrogen production from dairy wastewater treatment in sequencing batch reactor (AnSBR): Effect of organic loading rate, Enzyme and Microbial Technology 41 (2007) 506–515.

[68] N. Venetsaneas, G. Antonopoulou, K. Stamatelatou, M. Kornaros, G. Lyberatos, Using cheese whey for hydrogen and methane generation in a two-stage continuous process with alternative ph controlling approaches, Bioresource Technology 100 (2009) 3713–3717.

[69] K.-S. Lee, J.-F. Wu, Y.-S. Lo, Y.-C. Lo, P.-J. Lin, J.-S. Chang, Anaerobic hydrogen production with an efficient carrier-induced granular sludge bed bioreactor, Biotechnol. Bioeng. 87 (2004) 648–657.

[70] C.-Y. Lin, C.-H. Cheng, Fermentative hydrogen production from xylose using anaerobic mixed microflora, International Journal of Hydrogen Energy 31 (2006) 832–840.

[71] H. Koku, I. Eroglua, U. Gunduzb, M. Yucel, L. Turkerc, Kinetics of biological hydrogen production by the photosynthetic bacterium rhodobacter sphaeroides O.U. 001, International Journal of Hydrogen Energy 28 (2003) 381–388.

[72] F. Kargi, M. Y. Pamukoglu, Dark fermentation of ground wheat starch for biohydrogen production by fed-batch operation, International Journal of Hydrogen Energy 34 (2009) 2940–2946.

[73] L. Shen, D. M. Bagley, S. N. Liss, Effect of organic loading rate on fermentative hydrogen production from continuous stirred tank and membrane bioreactors, International Journal of Hydrogen Energy 34 (2009) 3689–3696.

[74] Y. Lu, Q. Lai, C. Zhang, H. Zhao, K. Ma, X. Zhao, H. Chen, D. Liu, X.-H. Xing, Characteristics of hydrogen and methane production from cornstalks by an augmented two- or three-stage anaerobic fermentation process, Bioresource Technology 100 (2009) 2889–2895.

[75] J. Miyake, S. Kawamura, Efficiency of light energy conversion to hydrogen by the photosynthetic bacterium rhodobacter sphaeroides, International Journal of Chemical Reactor Engineering 12(3) (1987) 147–149.

[76] V. L. Babu, S. V. Mohan, P. Sarma, Influence of reactor configration on fermentative hydrogen production during wastewater treatment, International Journal of Hydrogen Energy 34 (2009) 3305–3312.

[77] E. L. C. de Amorim, A. R. Barros, M. H. R. Z. Damianovic, E. L. Silva, Anaerobic fludized bed reactor with expanded clay as support for hydrogen production through dark fermentation of glucose, International Journal of Hydrogen Energy 34 (2009) 783–790.

[78] S.-E. Oh, P. Iyer, M. A. Bruns, B. E. Logan, Biological hydrogen production using a membrane bioreactor, Biotechnol. Bioeng. 87 (2004) 119–127.

[79] [link].
URL www.ge.com

[80] F. Zaza, C. Paoletti, R. LoPresti, E. Simonetti, M. Pasquali, Studies on sulfur poisoning and development of advanced anodic materials for waste-to-energy fuel cells applications, Journal of Power Sources 195 (2010) 4043–4050.

[81] W.-M. Yan, H.-S. Chu, M.-X. Lu, F.-B. Weng, G.-B. Jung, C.-Y. Lee, Degradation of proton exchange membrane fuel cells due to CO and CO_2 poisoning, Journal of Power Sources 188 (2009) 141–147.

[82] F. de Bruijn, D. Papageorgopoulos, E. Sitters, G. Janssen, The influence of carbon dioxide on PEM fuel cell anodes, Journal of Power Sources 110 (2002) 117–124.

[83] [link].
URL `www1.eere.energy.gov`

[84] A. Kohl, R. Nielson, Gas Purification, Gulf Publishing Company, 1997.

[85] [link].
URL `www.uop.com/objects/99benfield.pdf`

[86] [link].
URL `http://www.catacarb.com`

[87] J. M. Orozco, G. Webb, The adsorption and hydrogenation of benzene and toluene on alumina and silica supported palladium and platinum catalyst, Applied Catalysis, 6 (1983) 67–84.

[88] R. Szymanski, H. Charcosset, P. Gallezot, J. Massardier, L. Tournayan, Characterization of platinum-zirconium alloys by competitive hydrogenation of toluene and benzene, Journal of Catalysis 97 (1986) 366–373.

[89] J. L. Rousset, L. Stievano, F. J. C. S. Aires, C. Geantet, A. J. Renouprez, M. Pellarin, Hydrogenation of toluene over γ-Al_2O_3-supported Pt, Pd, and Pd-Pt model catalysts obtained by laser vaporization of bulk metals, Journal of Catalysis 197 (2001) 335–343.

[90] J. Wang, L. Huang, Q. Li, Influence of different diluents in Pt/Al_2O_3 catalyst on the hydrogenation of benzene, toluene and o-xylene, Applied Catalysis A: General 175 (1998) 191–199.

[91] A.-G. A. Ali, L. I. Ali, S. Aboul-Fotouh, A. K. Aboul-Gheit, Hydrogenation of aromatics on modifed platinum-alumina catalysts, Applied Catalysis A: General 170 (1998) 285–296.

[92] D. Klvana, J. Chaouki, D. Kusohorsky, C. Chavarie, Catalytic storage of hydrogen: Hydrogenation of toluene over a nickel/silica aerogel catalyst in integral flow conditions, Applied Catalysis 42 (1988) 121–130.

[93] T. Kaufmann, A. Kaldor, G. Stuntz, M. Kerby, L. Ansell, Catalysis science and technology for cleaner transportation fuels, Catalysis Today 62 (2000) 77–90.

[94] C. N. Satterfield, Heterogenous catalysis in Practice, McGraw Hill Co., 1980.

[95] G. C. Bond, Metal-Catalysed Reactions of hydrocarbons, Springer Science + Business Media Inc., 2005.

[96] M. Saeys, M.-F. Reyniers, J. W. Thybaut, M. Neurock, G. B. Marin, First-principles based kinetic model for the hydrogenation of toluene, Journal of Catalysis 236 (2005) 129–138.

[97] S. D. Lin, M. A. Vannice, Hydrogenation of aromatic hydrocarbons over supported pt catalysts II. Toluene hydrogenation, Journal of Catalysis 143 (1993) 554–562.

[98] M. V. Rahaman, M. A. Vannice, The hydrogenation of toluene and o-, m-, and p-xylene over palladium II. Reaction model, Journal of Catalysis 127 (1991) 267–275.

[99] M. A. Keane, P. M. Patterson, The role of hydrogen partial pressure in the gas-phase hydrogenation of aromatics over supported nickel, Ind. Eng. Chem. Res. 38 (1999) 1295–1305.

[100] M. A. Keane, P. M. Patterson, Compensation behaviour in the hydrogenation of benzene, toluene and o-xylene over Ni/SiO_2 determination of true activation energies, J. Chern. Soc., Faraday Trans., 92 (1996) 1413–1421.

[101] J. Quartararo, S. Mignard, S. Kasztelan, Trends for mono-aromatic compounds hydrogenation over sulfided Ni, Mo and NiMo hydrotreating catalysts, Catalysis Letters 61 (1999) 167–172.

[102] F. Benseradj, F. Sadi, M. Chater, Etude de l effet des additifs Fe, Co, Ni, sur l interaction Rh-Toluéne sur Rh/Al_2O_3, C. R. Chimie 7 (2004) 669–677.

[103] J. W. Thybaut, M. Saeys, G. B. Marin, Hydrogenation kinetics of toluene on Pt/ZSM-22, Chemical Engineering Journal 90 (2002) 117–129.

[104] M. A. Keane, G. Tavoularis, The role of spillover hydrogen initial gas phase catalytic aromatic hydroechlorination and hydrogenation over nickel/silica, React.Kinet.Catal.Lett. 78 (2003) 11–18.

[105] L. P. Lindfors, T. Salmi, S. Smeds, Kinetics of toluene hydrogenation onto Ni/Al_2O_3 cayalyst, Chemical Engineering Science 48 (1993) 3813–3828.

[106] L. P. Lindfors, T. Salmi, Kinetics of toluene hydrogenation on a supported Ni catalyst, Ind. Eng. Chem. Res. 32 (1993) 34–42.

[107] J. Chupin, N. Gnep, S. Lacombe, M. Guisnet, Influence of the metal and of the support on the activity and stability of bifunctional catalysts for toluene hydrogenation, Applied Catalysis A: General 206 (2001) 43–56.

[108] R. Slioor, J. Kanervo, T. Keskitalo, A. Krause, Gas phase adsorption and desorption kinetics of toluene on Ni/γ-Al_2O_3, Applied Catalysis A: General 344 (2008) 183–190.

[109] P. Castano, J. M. Arandes, B. Pawelec, J. L. G. Fierro, A. Gutierrez, J. Bilbao, Kinetic model discrimination for toluene hydrogenation over noble-metal-supported catalysts, Ind. Eng. Chem. Res. 46 (2007) 7417–7425.

[110] N. Gaidai, R. Kazantsev, N. Nekrasov, Y. Shulga, I. Ivleva, Kinetics of toluene hydrogenation over platinum-titana catalysts in conditions of strong metal-support interaction, React.Kinet.Catal.Lett. 75 (2002) 55–61.

[111] R. V. Kazantsev, N. A. Gaidai, N. V. Nekrasov, K. Tenchev, L. Petrov, A. L. Lapidus, Kinetics of benzene and toluene hydrogenation on a Pt/TiO_2 catalyst, Kinetics and Catalysis, 44 (2003) 529–535.

[112] S. D. Lin, M. A. Vannice, Hydrogenation of aromatic hydrocarbons over supported Pt catalysts III. reaction models for metal surfaces and acidc sites on oxide supports, Journal of Catalysis 143 (1993) 563–572.

[113] M. V. Rahaman, M. A. Vannice, The hydrogenation of toluene and o-, m-, and p-xylene over palladium I. kinetic behavior and o-xylene isomerization, Journal of Catalysis 127 (1991) 251–266.

[114] C. H. Bartholomew, Mechanisms of catalyst deactivation, Applied Catalysis A: General 212 (2001) 17–60.

[115] M. Huang, S. Kaliaguine, S. Suppiah, Surface interaction between H_2, and CO_2, over silicalite-supported platinum, Applied Surface Science 90 (1995) 393–407.

[116] L. Chen, B. Chen, C. Zhou, J. Wu, R. C. Forrey, H. Cheng, Influence of CO poisoning on hydrogen chemisorption onto a Pt-cluster, J. Phys. Chem. C 112 (2008) 13937–13942.

[117] S. Tsang, J. Claridge, M. Green, Recent advances in the conversion of methane to synthesis gas, Catalysis Today 23 (1995) 3–15.

[118] A. Goguet, D. Tibiletti, F. Meunier, J. Breen, R. Burch, Spectrokinetic investigation of reverse water-gas-shift reaction intermediates over a Pt/CeO_2 catalyst, J. Phys. Chem. B 52 (2004) 20240–20246.

[119] R. Dagle, A. Platon, D. Palo, A. Datye, J. Vohs, Y. Wang, PdZnAl catalysts for the reactions of water-gas-shift, methanol steam reforming, and reverse-water-gas-shift, Applied Catalysis A: General 342 (2008) 63–68.

[120] G. Roberts, P. Chin, X. Sun, J. J. Spivey, Preferential oxidation of carbon monoxide with Pt/Fe monolithic catalysts: interactions between external transport and the reverse water-gas-shift reaction, Applied Catalysis B. 46 (2003) 601–611.

[121] G. Papoian, J. K. Noskov, R. J. Hoffmann, A comparative theoretical study of the hydrogen, methyl, and ethyl chemisorption on the Pt(111) surface, Am. Chem. Soc. 122 (2000) 4129–4144.

[122] D. Godbey, G. A. Somorjai, The adsorption and desorption of hydrogen and carbon monoxide on bimetallic Re-Pt (111) surfaces, Surface Science 301-318 (1988) 204.

[123] B. Pennemann, K. Oster, K. Wandelt, Hydrogen adsorption on Pt(100) at low temperatures: work function and thermal desorption data, Surface Science 249 (1991) 35–43.

[124] S. E. Mason, I. Grinberg, A. M. Rappe, AdsorbateâĹŠadsorbate interactions and chemisorption at different coverages studied by accurate ab initio calculations: Co on transition metal surfaces, J. Phys. Chem. B 112 (2006) 3816–3822.

[125] M. Burgener, D. Ferri, J.-D. Grunwaldt, T. Mallat, A. Baiker, Supercritical carbon dioxide: An inert solvent for catalytic hydrogenation?, J. Phys. Chem. B 2005, 109, 16794-16800 109 (2005) 16794–16800.

[126] B. J. Minder, T. Malla, K. Pickel, K. Steiner, A. Baiker, Enantioselective hydrogenation of ethyl pyruvate in supercritical fluids, Catal Lett 34 (1995) 1.

[127] D. Xu, R. G. Carbonell, D. J. Kiserow, G. W. Roberts, Hydrogenation of polystyrene in CO_2-expanded solvents: Catalyst poisoning, Ind. Eng. Chem. Res. 44 (2005) 6164–6170.

[128] T. Gu, W. K. Lee, J. V. Zee, Appl. Catal. B: Gen. 56 (2005) 43.

[129] A. Sun, Z. Qin, S. Chen, J. Wang, J. Mol. Catal. A : Chem. 210 (2004) 189.

[130] B. M. Bhanage, Y. Ikushima, M. Shirai, M. Arai, The selective formation of unsaturated alcohols by hydrogenation of α,β-unsaturated aldehydes in supercritical carbon dioxide using unpromoted Pt/Al_2O_3 catalyst, Catalysis Letters 62 (1999) 175–177.

[131] F. Zhao, S.-I. Fujita, J. Sun, Y. Ikushima, M. Arai, Hydrogenation of nitro compounds with supported platinum catalyst in supercritical carbon dioxide, Catalysis Today 98 (2004) 523–528.

[132] F. Zhao, Y. Ikushima, M. Arai, Hydrogenation of nitrobenzene with supported platinum catalysts in supercritical carbon dioxide: effects of pressure, solvent, and metal particle size, Journal of Catalysis 224 (2004) 479–483.

[133] D. Ferri, T. Burgi, A. Baiker, Probing boundary sites on a Pt/Al_2O_3 model catalyst by CO_2 hydrogenation and in situ ATR-IR spectroscopy of catalytic solid-liquid interfaces, Phys. Chem. Chem. Phys. 4 (2002) 2667–2672.

[134] A. Maméde, J.-M. Giraudon, A. Lófberg, L. Leclercq, G. Leclercq, Hydrogenation of toluene over β-Mo_2C in the presence of thiophene, Applied Catalysis A: General 227 (2002) 73–82.

[135] R. I. Slioor, J. M. Kanervo, A. O. I. Krause, Temperature programmed hydrogenation of toluene, Catal Lett (2008) 121 (2008) 24–32.

[136] D. Hoge, M. Tueshaus, A. M. B. Shaw, Surface Science 207 (1988) L935.

[137] O. Levenspiel, Chemical Reaction Engineering, 3rd Edition, John Wiley & sons, inc., 1999.

[138] W. Rachmady, M. A. Vannice, Acetic acid hydrogenation over supported platinum catalysts, Journal of Catalysis 192 (2000) 322–334.

[139] Y. Akutsu, D.-Y. Lee, Y.-Y. Li, T. Noike, Hydrogen production potentials and fermentative characteristics of various substrates with different heat-pretreated natural microflora, International Journal of Hydrogen Energy 34 (2009) 5365–5372.

[140] C. Dinamarca, R. Bakke, Apparent hydrogen consumption in acid reactors: observations and implications, Water Science & Technology 59(7) (2009) 1441–1447.

[141] S.-K. Han, H.-S. Shin, Biohydrogen production by anaerobic fermentation of food waste, International Journal of HydrogenEnergy 29 (2004) 569–577.

[142] Z. Wu, S.-T. Yang, Extractive fermentation for butyric acid production from glucose by clostridium tyrobutyricum, Biotechnol. Bioeng. 82 (2003) 93–102.

[143] D. J. Miller, Kirk-Othmer Encyclopedia of Chemical Technology, 4th Edition, Wiley, New York, 1991.

[144] R. Pestman, R. M. Koster, A. van Duijne, J. A. Z. Pieterse, V. Ponec, Reactions of carboxylic acids on oxides. 2. bimolecular reaction of aliphatic acids to ketones, Journal of Catalysis 168 (1997) 265–272.

[145] R. Pestman, R. M. Koster, J. A. Z. Pieterse, V. Ponec, Reactions of carboxylic acids on oxides 1. selective hydrogenation of acetic acid to acetaldehyde, Journal of Catalysis 168 (1997) 255–264.

[146] E. J. Grootendorst, R. Pestman, R. M. Koster, V. Ponec, Selective reduction of acetic acid to acetaldehyde on iron oxides, Journal of Catalysis 148 (1994) 261–269.

[147] W. Rachmady, M. A. Vannice, Acetic acid reduction to acetaldehyde over iron catalysts i. kinetic behavior, Journal of Catalysis 208 (2002) 158–169.

[148] T. Yokoyama, N. Yamagata, Hydrogenation of carboxylic acids to the corresponding aldehydes, Applied Catalysis A: General 221 (2001) 227–239.

[149] W. Rachmady, M. A. Vannice, Acetic acid reduction by H_2 over supported Pt catalysts: A DRIFTS and TPD/TPR study, Journal of Catalysis 207 (2002) 317–330.

[150] A. Demirbass, Biodiesel fuels from vegetable oils via catalytic and non-catalytic supercritical alcohol transesterification and other methods: a survey, Energy Conversion and Management 44 (2003) 2093–2109.

[151] E. Karimi, A. Gomez, S. W. Kycia, M. Schlaf, Thermal decomposition of acetic and formic acid catalyzed by red mud-implications for the potential use of red mud as a pyrolysis bio-oil upgrading catalyst., Energy Fuels 24 (2010) 2747–2757.

[152] R. Pestman, R. M. Koster, E. Boellaard, A. M. van der Kraan, V. Ponec, Identification of the active sites in the selective hydrogenation of acetic acid to acetaldehyde on iron oxide catalysts, Journal of Catalysis 174 (1998) 142–152.

[153] H. A. Wittcoff, B. G. Reuben, Industrial Organic Chemicals, Jhon Wiley & Sons, INC., 1996.

[154] C. Nordhei, K. Mathisen, O. Safonova, W. V. Beek, D. G. Nicholson, Decomposition of carbon dioxide at 500 °C over reduced iron, cobalt, nickel, and zinc ferrites: A combined XANES-XRD study, J. Phys. Chem. C 113 (2009) 19568–19577.

[155] N. Calvar, A. Dominguez, J. Tojo, Vapor-liquid equilibria for the quaternary reactive system ethyl acetate + ethanol + water + acetic acid and some of the constituent binary systems at 101.3 kPa, Fluid Phase Equilibria 235 (2005) 215–222.

[156] [link].
URL http://www1.eere.energy.gov/industry/chemicals/pdfs/acetic_acid.pdf

[157] B. Urbas, Recovery of acetic acid from a fermentation broth, US Patent 4,405,717.

[158] Y. K. Hong, W. H. Hong, Removal of acetic acid from aqueous solutions containing succinic acid and acetic acid by tri-n-octylamine, Separation and Purification Technology 42 (2005) 151–157.

[159] S. K. C. Lin, C. Du, A. C. Blaga, M. Camarut, C. Webb, C. V. Stevens, W. Soetaert, Novel resin-based vacuum distillation-crystallisation method for recovery of succinic acid crystals from fermentation broths, Green Chem., 2010 12 (2010) 666–671.

[160] M. D. K. H. A. Barker, B. T. Bornstein (Eds.), The Synthesis of Butyric and Caproic Acids from Ethanol and Acetic Acid by Clostridium kluyveri, Proceedings of the National Academy of Sciences of the United States of America, Vol. 31, No. 12 (Dec. 15, 1945), pp. 373-381.

A
EXPERIMENTAL BENCH

A.1 BENCH SETUP
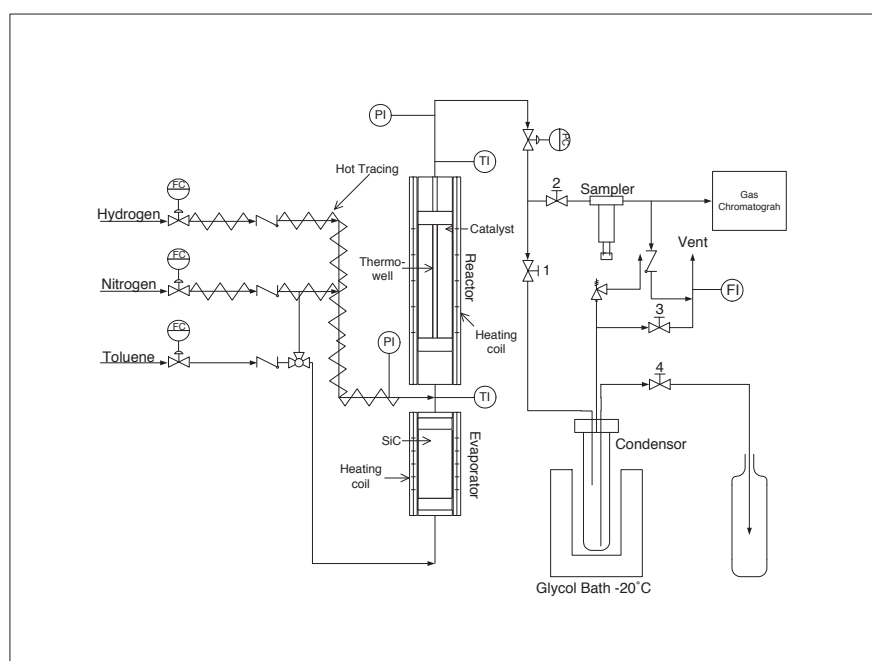
Figure A.1: Experiment bench for toluene hydrogenation - Process Flow Diagram

The bench consists of a packed bed reactor. It is 5 cm in height and 0.5 cm in diameter. Reactor is filled by 2 g of catalyst between 5 mm of quartz layers and is coupled with toluene evaporator working at vapour pressure point temperature with respect to the composition. Reactor and evaporator are coil heated while, the center tube is hot traced to maintain

desired temperature. Toluene is injected, at the bottom of the evaporator, via a dosing pump (HAVARD APPARTAUS PHD-4400). There are three checks available with the bench to ensure exact quantity of toluene vapour entering into the reactor i) dosing pump meter, ii) level indicator across the evaporator i.e. a simple transparent Teflon tube is added across the vertical reactor and evaporator to determine the exact level of liquid in the system; this should remain constant during the test run, and iii) physical weight balance for the sampler. Schematic of experimental setup is shown in figure C.1. In case of octanoic acid same equipment is used while for acetic acid condensers are bypassed and all the lines are hot traced to keep the acid and its products in gas form.

A.2 BENCH OPERATION

All experiments are performed in approximately 8 h day shift. Operation was continuous with certain time always left for transition period both at startup and shutdown.

A.2.1 EVAPORATOR

In fact there is no pumping system available that is without pulsation. Even the smoothest system does have a micro level of inherited perturbation. This pulsation is multiplied by the factor of vaporization of hydrocarbons, which is above 400. So automatically this enhanced effect will result in huge disturbances in the flow through reactor. These perturbations would remain there, until this evaporator is converted to a saturator i.e. a natural equilibrium is established between the concentration of the liquid in the reactor at much lower temperature corresponding to the vapour pressure of the respective component. In other words vapour pressure of liquid is so adjusted that resulting partial pressure of the hydrocarbon becomes equal to the desired molar composition in the final mixture. This methodology however, only works with pure liquids or with azeotropes.

A.2.2 REACTOR

Reaction starts with the entrance of reaction mixture in the reactor. Reactor is always pressurised with hydrogen and liquid is turned off through liquid cut-off valve, when not in use. Reactor is de-pressurised when start up sequence is initiated slowly to the desired pressure. After opening liquid cut-off valve the temperature of evaporator is gradually increased to set point and liquid injection started. Once temperature is achieved the gas is bubbled through the liquid via gas change over valve. In this way required mixtures enters into the reactor for conversion. Total care is taken to curtail any ingression of oxygen into the setup as catalyst deterioration is rapid especially reduced iron oxide is highly pyrophoric .

A.2.3 PRESSURE REGULATOR/ FLOW CONTROLLERS

To determine the effect of pressure on reaction a pressure regulator is provided. This regulator is placed at the downstream of the recator, as system stability is strongly dependent on equilibrium which is controlled by pressure also; so any sharp change in pressure will result in disturbed equilibrium of liquid and hence the level. Therefore sometimes, it is observed that whole of the saturator get emptied or over flowed because of uncontrolled pressure.

Hence this pressure regulator should be precise enough to ensure smooth continuous operation of this experiment bench. Five gas flow controllers manufactured by ANALYT of capacities between 100 ml/min to 500 ml/min are used to control the flow of ingoing gases.

A.2.4 REFRIGERATION/HEATING SYSTEM

Refrigeration setup is composed of a chillier and a glycol bath to maintain the temperature as minimum as -25 °C. This is low enough to condense almost all of the products form the reactor. The sampler and condenser remain in the bath, thus ensuring complete condensation.

On the other hand in case of acetic acids all products are analysed in gas phase. Keeping acetone and acetic acid in gaseous form, sample line must be heated to avoid any condensation. For heating purpose the water bath is used with temperature of 90°C. This temperature is high enough to keep 5% mixture of acetic acid and its products in gas form.

A.2.5 LABVIEW

For the sake of automatic control programming by LabVIEW software is used. This is preferred because of its virtual graphical programming environment and easiness to debug. LabVIEW is a graphical dataflow language and block diagram approach which naturally represents the flow of data and thus easy to understand and program.

A.2.6 PRESSURE TEST

After each catalyst replacement, setup is pressure checked at the pressure of 3 bar absolute. The bench was pressurized by nitrogen for 16 hours. If there is no leakage then experiments are conducted otherwise leaks are detected with the help of soap solutions and eliminated.

A.2.7 START UP

i) cooling system is started to achieve desired temperature for sampler.

ii) reactor is de-pressurised to the desired pressure.

iii) liquid cut off valve is opened and set point to the temperature controller for reactor, evaporator and heating coil are given. Set point for hot tracing is 0 - 5 °C above that of evaporator depending upon the past hit and trial experience of enhanced stability. This stability is determined through the flow meter at exit. Usually setup is considered stable if the perturbations are within ±3ml/min.

iv) dosing pump is started to inject liquid. Keep gas entrance at the downstream of gas changeover until the evaporator is heated to the desired temperature.

v) when desired temperature for evaporator is achieved, then gas is bubbled through the liquid via gas changeover valve. Wait until equilibrium is established between gas and vapours. This is indicated by the level indicator present across the reactor. Level should remain constant during the normal run.

A.2.8 SAMPLE COLLECTION

i) during transition run sample is collected in a one condenser while, for sample collection second condenser is used.

ii) valve opening and closure is done accordingly to collect sample. Sampling time change subject to sufficient amount collected.

iii) first sample after stabilisation is always rejected to avoid any contamination by unsteady state product.

iv) after sample collection sampler is always thoroughly rinsed by acetone and dried under air flow.

A.2.9 SHUT DOWN

i) cut off the power to heating elements.

ii) stop the dosing pump.

iii) change gas entrance from upstream to downstream of gas change over valve and close the liquid isolation valve.

iv) keep reactor under the flow of hydrogen to remove any liquid in reactor for 15min.

v) pressurised the reactor to sufficient pressure to avoid any entrainment of liquid or air.

A.3 EMERGENCY SAFETY SHEET

Numéro de la fiche : F106-1-ATA

lgpc	**Responsable :C de Bellefon**	**Sujet : Hydrogénation**	
Laboratoire : F106		**N° de sorbonne :1**	**Date d'émission : 23/04/09**
Emetteur : Aqeel Ahmad TAIMOOR		**Tél :**	
Personnes habilitées à manipuler : Aqeel Ahmad TAIMOOR ATA, FBO (31760)			

Substances/ Risques Chimiques	**RNCAS**	**Quantité**	**Pictogrammes**
Acide Octanoic	127-07-2	1 lit	
Acide Acétique	64-19-7	1 lit	
Hydrogène	1333-74-0	100ml/min	
Azote	7727-37-9	100ml/min	
CO2	124-38-9	100ml/min	
Methane	74-82-8	100ml/min	
CO	630-08-0	0.312 kg Bouteille d'étalonnage utilisation ponctuelle	

Autres risques	**Descriptif**	**Danger**	**Pictogrammes**
Température	Chauffage	Brûlures	

Protections individuelles	**Consignes de sécurité**	**En cas d'urgence**	**Personnes à contacter**
	Garder la sorbonne fermée.	Arrêt Urgence , couper les gaz, arrêtez le pousse seringue.	**La Direction : C de Bellefon** **L'ACMO : S Pallier** **POMPIERS : 0-18**

NE PAS ARRETER : Le bain cryogénique

Visa :Emetteur   **Visa : Direction/ ACMO**

Fiche de poste   *ACMO-S Pallier*   *17/03/09*
                         Version 01.02

Figure A.2: Safety data sheet and emergency protocole

B

CATALYST CHARACTERISATION

B.1   Pt/Al$_2$O$_3$

The catalyst consists of γ-alumina particles impregnated by Pt/ acetyl-acetonate. Size of supported alumina provided by Sasol Chemie was found between 150 -250 mm with an effective specific surface area of 145 - 165 m^2·g^{-1}. 150 g of alumina powder was mixed with 200 ml toluene and 3.13 g of Platinum Acetyl-acetonate. The mixture was stirred for 3 h at 60 °C. The solvent was then removed by evaporation at 80 °C under reduced pressure. The resulted powder was then dried at 120 °C for one night. This catalyst was then calcined with air at 500 °C for 4 h with an average temperature ramp of 3 °C·min^{-1}. After impregnation and drying platinum content on Alumina are about 0.88 % and overall dispersion is about 54 % measured through hydrogen chemisorption. Nitrogen adsorption reveals BET = 147 m^2·g^{-1} with pore diameter and pore volume equal to 12.3 nm and 0.45 cm^3·g^{-1} respectively.

B.2   Pt/SiO$_2$

10 g of SiO$_2$ having particle size of 150 - 250 mm are mixed with 50 ml of Toluene and then impregnated by 0.2057 g (0.1 g Pt) of Pt/ acetyl-acetonate. The mixture was stirred for 5 h while temperature was adjusted to 70 °C followed by vacuum evaporation for 2h at 80 °C. The resulting solid was placed in oven for one night at 120 °C then dried in air at 150 °C for 2 h; temperature was increased with the ramp of 10 °C·min^{-1}. For calcination, temperature was programmed to increase at the rate of 4 °C·min^{-1} up till 500 °C thereafter catalyst was kept for 4 h at same temperature. The platinum content is about 0.91 wt % and overall dispersion below 5 %.

B.3   Pt/TiO$_2$-SiO$_2$

In order to prepare bi-support catalyst the two supports (20 g each) were mixed together in 80 ml water. Mixture was heated to 70 °C for 4 h before vacuum evaporation at 80 °C

for 2 h. The resulting mass remained in oven for 2 days at $120\,^{\circ}$C before calcination at $500\,^{\circ}$C ($@4\,^{\circ}$C·min^{-1}) for 4 h. 20 g of SiO$_2$-TiO$_2$ was mixed with 30 ml of Toluene and then impregnated by 0.403 g (0.2 g Pt) of Pt/ acetyl-acetonate. The mixture was stirred for 4 hrs while temperature was adjusted to $70\,^{\circ}$C followed by vacuum evaporation for 2 h at $80\,^{\circ}$C. The resulting solid was placed in oven for one night at $120\,^{\circ}$C. For calcination, temperature was programmed to increase at the rate of $4\,^{\circ}$C·min^{-1} uptill $450\,^{\circ}$C thereafter catalyst was kept for 4 h at same temperature. The platinum contents and dispersion measured for this catalyst is 1 wt.% and 63.4 % respectively.

B.4 FeO

Iron oxide in FeO form is directly purchased from Sigma Aldrich with 99.98% purity level (Ref No. 203513). It is available in form of powder and small chunks. For FeO the ratio of ferrous in this sample varies between Fe$_{0.84}$O to Fe$_{0.95}$O. Size of particles vary but are smaller than 10 mesh.

C
CHROMATOGRAPHY

C.1 TOLUENE/MCH

AGILENT TECHNOLOGIES series 6890N NETWORK SYSTEM Gas chromatograph is used for analysis. The column HP-PONA Methyl Siloxane 50 m in length and 200 μm in diameter is installed to separate hydrocarbons. Helium is used as gas vector and its flow and pressure are maintained at $0.9\text{ml} \cdot \text{min}^{-1}$ and 2.093 bar respectively. Before the sample injection of $1\mu l$, oven is heated to $50\,^{\circ}\text{C}$. After injection temperature is increased to $140\,^{\circ}\text{C}$ with a ramp of $10\,^{\circ}\text{C} \cdot \text{min}^{-1}$ then to $220\,^{\circ}\text{C}$ with $20\,^{\circ}\text{C} \cdot \text{min}^{-1}$ ramp. Column is maintained under the same conditions for 2 min thus making a total of 15 min run for each sample analysis. A Flame Ignition Detector (FID) is used to differentiate between different components emerging from the column, provided with $40\text{ ml} \cdot \text{min}^{-1}$ of hydrogen and 400 $\text{ml} \cdot \text{min}^{-1}$ of air flow to support flame at $300\,^{\circ}\text{C}$.

C.2 $CO_2/N_2/CH_4/CO$

12/06

VARIAN

APPLICATION NOTE

Permant gases and CO2

Application 2050 GC

Fast analysis of permanent gases and CO2 using a tandem of PLOT columns

A parallel setup of 2 PLOT columns is tuned for separation of permanent gases in short time. The sample is injected via a normal injection port and is splitted into the parallel setup of 2 columns. (A short CP-Molsieve is used to separate the inert gases (helium, oxygen nitrogen, methane and CO) before the first peak(composite peak of all inert gases) elutes from the CP-PoraBOND Q PLOT column. After the first peak the methane and CO2 elute from the CP-PoraBOND Q column. (if water is present, we will see that also on the CP-PoraBond).
This analysis is done isothermally and can be speeded up significantly. The CO2 and eventually water that enters the Molsieve column will be adsorbed. If the amount of CO2 or water accumulated on the CP-Molsieve causes a shift of the retention time of the inert gases out of the integration window, the Select Permanent gases/CO2 column can be regenerated by 30 minutes at 300°C. Practically we found that CO2 and water adsorption has very little impact on the retention and many analysis can be done before regeneration is required. As methane elutes from both systems the split ratio between the columns can be calculated by the ratio of the methane peaks. If heavier compounds are injected on the CP-Molsieve, they will elute later between the peaks that elute from the CP-PoraBOND Q.

Technique	: GC				
Column	: Fused Silica, Select Permanent gases/CO2				
	Part nr. CP7429				
Temperature	: 45°C				
Carrier Gas	: H2, 60 kPa				
Injector	: Split 50 ml/min				
Detector	: µ-TCD		1	He	(from ms-5A)
Sample Size	: 10 µl		2	O2	(from ms-5A)
Concentration range	: % level		3	N2	(from ms-5A)
			4	Methane	(from ms-5A)
Courtesy	: C. Duvekot, Varian Application laboratory,		5	CO	(from ms-5A)
	Middelburg, The Netherlands		6	He	(from PBQ)
			7	N2 +O2 +CO	(from PBQ)
			8	Methane	(from PBQ)
			9	CO2	(from PBQ)

Figure C.1:

C.3   OCTANOIC/ACETIC & PRODUCTS

Analysis for this section of thesis are conducted by 6890 N series of chromatograph provided by Agilent Technologies. DB-5 is used to separate the products. Initial oven temperature is adjusted to 50 °C for octanoic acid and its products; subsequently increases to 200 °C at a ramp rate of 50 °C/min. Oven is held for 3min at same conditions thus making total analysis time of 6 min. 0.1 μl of sample in liquid phase is injected with injector temperature maintained at 300 °C. Helium is used as carrier gas with its pressure and flow maintained at 2.642 bar and 0.4 ml/min respectively. FID at 250 °C is used to detect the outgoing components.

Acetic acid and its respective products are detected in a on-line chromatograph as sample cannot be cooled to liquefy all products. Same on-line gas chromatograph as used for gas analysis is integrated with a third column of DB 5, with same procedure as described previously. However the product from the added column is detected by FID.

D

DRIFT SETUP

D.1 CELL

The DRIFTS (from Spectra-Tech$^{\textcircled{R}}$) cell was used in this study. The reactor of the DRIFT cell (as shown in figure D.1) was modified to ensure that no catalyst bed by-pass took place, contrary to the case of the as-received cell. The original crucible was replaced by a hollow ceramic to decrease the reactor pressure drop, while the gap between the ceramic and the metal base support was sealed with Teflon. Quartz was used to support the catalyst. The original cell only allowed a partial conversion (i.e., ca. 20%) of CO over a Pt/SiO_2 in the presence of excess oxygen between 473 and 600 K, while total conversion in CO oxidation could be obtained at 473 K using the modified cell. The system average residence time, which was measured during a step change between a mixture of Ar + Kr to pure Ar, was ca. 6 s. No CO oxidation activity was recorded over a cell loaded with SiC.

D.2 OPERATING PROCEDURE

The DRIFTS assembly was fitted in a Nicolet Magna 550 FTIR spectrometer and a MCT detector cooled with liquid nitrogen was used. Gases (i.e. high purity Ar, O_2, CO_2 and H_2 from Air Liquide) were fed through low volume heated stainless-steel lines to the cell. Toluene was introduced via a saturator kept at $25\,^{\circ}\mathrm{C}$. The feed composition was different from that used in the kinetic setup and consisted of 1.6% toluene + 40% H_2 + 2 or 40% CO_2 (if present) in Ar. A low partial pressure of toluene was used here to prevent condensation on the DRIFTS cells walls, which were held at around room temperature. The tests were made at atmospheric pressure and at a total flow rate of 25 ml·min^{-1}. The contribution of gas-phase toluene and cyclohexane were subtracted from the surface DRIFTS signal. The DRIFTS data are reported as $\log(1/R)$, where R is the sample reflectance. The pseudo-absorbance $\log 1/R$ gives a better linear representation of the band intensity against sample surface coverage than that given by the Kubelka-Munk function for strongly absorbing media such as those based on alumina.

The reaction cell crucible was filled first with a layer of SiC and then topped with 19 mg
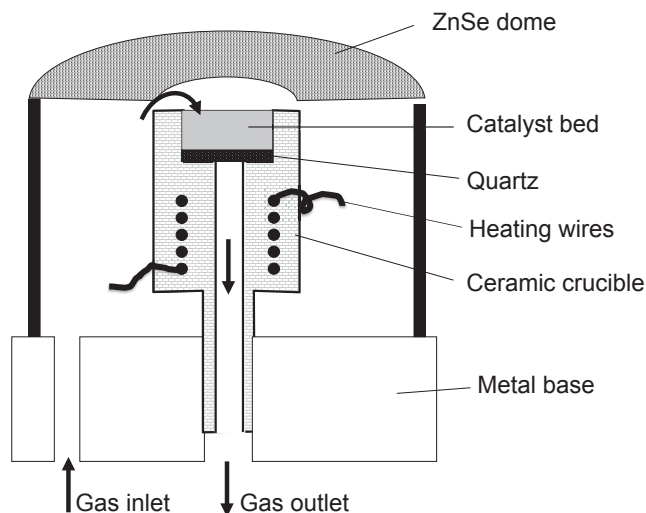
Figure D.1: DRIFT reactor setup

of catalyst powder. The corresponding residence time was about 1.04 kgcat·mol^{-1}·sec. The cell thermocouple was located at the interface between the SiC and catalyst layers. The sample was first oxidized at 350 °C under 20 % O_2 in Ar before being reduced for 30 min under 40% H_2 in Ar at the same temperature (heating ramp was about 30 °C·min^{-1}). The reference backgrounds were collected at 75 °C over the activated sample using 128 scans at a 4 cm^{-1} resolution. A background using a totally reflecting aluminium mirror was also recorded. 8, 16 or 32 scans were collected during the operando analysis, depending on the time resolution sought.

Toluene and methylcyclohexane gas-phase concentrations were measured after the DRIFTS cell using an IR gas-cell, the optical pathway of which was about 27 cm. Toluene conversion was calculated on the basis of the concentrations of toluene and methylcyclohexane measured, assuming that no other reaction product was formed. This assumption was reasonable since the gas-phase IR spectra could be accurately decomposed using the spectra of pure toluene and methylcyclohexane only.

The DRIFTS cell loaded with inert SiC presented a non-negligible activity for toluene hydrogenation to methylcyclohexane (about 4% conversion at 75 °C in the absence of CO_2 and 3.6 % in the presence of CO_2). Most of the exposed naked heating wires that were present in the original cell were covered with a ceramic coating, but with no improvements. The observed activity could possibly due to a reaction occurring on remaining exposed heating wires and/or the thermocouple guide. The conversion due to the cell (i.e. 4 %) was subtracted from that measured with the catalyst when calculating TOF number.

E

MODEL VBA CODE

Attribute VBA-ModuleType=VBAModule

```
Sub Module1
Sub Macro1()
'
Macro1 Macro
% Macro recorded 2/19/2009 by Taimoor
%constant values
kkh2=2.1
Range("A2").Select
ActiveCell.FormulaR1C1="kkh2"
Cells(2, 2)=kkh2
ct=0.0244
Range("A3").Select
ActiveCell.FormulaR1C1="ct"
Cells(3, 2)=ct
k=0.00045
Range("A4").Select
ActiveCell.FormulaR1C1="k"
Cells(4, 2)=k
alpha=0.5
Range("A5").Select
ActiveCell.FormulaR1C1="alpha"
Cells(5, 2)=alpha
beta=0
Range("A6").Select
ActiveCell.FormulaR1C1="beta"
Cells(6, 2)=beta
kktol=6.8e-07
Range("A7").Select
ActiveCell.FormulaR1C1="kktol"
```

```
Cells(7, 2)=kktol
ktol=kktol/(5705·(0.659·k·35154^{alpha}+kktol+0.22·kkh2))
Range("A8").Select
ActiveCell.FormulaR1C1="ktol"
Cells(8, 2)=ktol
kh2=(1-ktol·5705/(35154^{0.5})
Range("A1").Select
ActiveCell.FormulaR1C1="kh2"
Cells(1, 2)=kh2
Range("D1").Select
ActiveCell.FormulaR1C1="n"
Range("D2").Select
ActiveCell.FormulaR1C1="a"
Range("E1").Select
ActiveCell.FormulaR1C1="X"
Range("F1").Select
ActiveCell.FormulaR1C1="nH2"
Range("G1").Select
ActiveCell.FormulaR1C1="nTol"
Range("H1").Select
ActiveCell.FormulaR1C1="nN2"
Range("I1").Select
ActiveCell.FormulaR1C1="nMCH"
Range("J1").Select
ActiveCell.FormulaR1C1="nt"
Range("K1").Select
ActiveCell.FormulaR1C1="PH2"
Range("L1").Select
ActiveCell.FormulaR1C1="PTol"
Range("M1").Select
ActiveCell.FormulaR1C1="PN2"
Range("N1").Select
ActiveCell.FormulaR1C1="PMCH"
Range("O1").Select
ActiveCell.FormulaR1C1="Pt"
Range("P1").Select
ActiveCell.FormulaR1C1="Gamma"
Range("Q1").Select
ActiveCell.FormulaR1C1="CÂř"
Range("R1").Select
ActiveCell.FormulaR1C1="f(x)"
Range("T1").Select
ActiveCell.FormulaR1C1="Time"
Range("T2:T12").Select
Selection.Merge
ActiveCell.FormulaR1C1="CÂř"
Range("T2:T12").Select
With Selection
```

```
.HorizontalAlignment=xlCenter
.VerticalAlignment=xlCenter
.WrapText=False
.Orientation=0
.AddIndent=False
.ShrinkToFit=False
.MergeCells=True
End With
Range("a2").Select
tf=536400
dt=5364
t=dt
counter=22
Do
Cells(1,counter)=t
x=0
Do
nf=50
n=1
xo=0
Cells(2,5)=xo
nh2o=1.8e-05
Cells(2,6)=nh2o
ntolo=4e-06
Cells(2,7)=ntolo
nn2o=1.8e-05
Cells(2,8)=nn2o
nmcho=0
Cells(2,9)=nmcho
nto=nh2o+ntolo+nn2o+nmcho
Cells(2,10)=nto
pt=101300
Cells(2,11)=Cells(2,6)/Cells(2,10)·pt
Cells(2,12)=Cells(2,7)/Cells(2,10)·pt
Cells(2,13)=Cells(2,8)/Cells(2,10)·pt
Cells(2,14)=Cells(2,9)/Cells(2,10)·pt
Cells(2,15)=Cells(2,11)+Cells(2,12)+Cells(2,13)+Cells(2,14)
Cells(2,21)=0
Cells(2,17)=Cells(2,counter-1)
```

thetao=3·k·Cells(2,11)^{alpha}·(ct-Cells(2,17))+kktol· Cells(2,17) + kkh2·(ct-Cells(2,17))

fo=3·k·Cells(2,11)^{alpha} ·(ct-Cells(2,17)) · (ktol·Cells(2,12) ·thetao-kktol·Cells(2,17))/(ktol·Cells(2,12) ·thetao-kktol·Cells(2,17)+kh2·Cells(2,11)$^{0.5}$·thetao-kkh2 ·(ct-Cells(2,17)))

theta1 = 3 · k · Cells(2, 11) ^{alpha} · (ct - (Cells(2, 17) + dt / 2 · fo)) + kktol · (Cells(2, 17) + dt / 2 · fo) + kkh2 · (ct - (Cells(2, 17) + dt / 2 · fo))

f1 = 3 · k · Cells(2, 11) ^{alpha} · (ct - (Cells(2, 17) + dt / 2 · fo)) · (ktol · Cells(2, 12) · theta1 - kktol · (Cells(2, 17) + dt / 2 · fo)) / (ktol · Cells(2, 12) · theta1 - kktol · (Cells(2, 17) + dt / 2 · fo) + kh2 · Cells(2, 11) $^{0.5}$ · theta1 - kkh2 · (ct - (Cells(2, 17) + dt / 2 · fo)))

theta2 = 3 · k · Cells(2, 11) ^{alpha} · (ct - (Cells(2, 17) + dt / 2 · f1)) + kktol · (Cells(2, 17) + dt / 2 · f1) + kkh2 · (ct - (Cells(2, 17) + dt / 2 · f1))

f2 = 3 · k · Cells(2, 11) ^{alpha} · (ct - (Cells(2, 17) + dt / 2 · f1)) · (ktol · Cells(2, 12) · theta2 - kktol · (Cells(2, 17) + dt / 2 · f1)) / (ktol · Cells(2, 12) · theta2 - kktol · (Cells(2, 17) + dt / 2 · f1) + kh2 · Cells(2, 11) $^{0.5}$ · theta2 - kkh2 · (ct - (Cells(2, 17) + dt / 2 · f1)))

theta3 = 3 · k · Cells(2, 11) ^{alpha} · (ct - (Cells(2, 17) + dt · f2)) + kktol · (Cells(2, 17) + dt · f2) + kkh2 · (ct - (Cells(2, 17) + dt · f2))

f3 = 3 · k · Cells(2, 11) ^{alpha} · (ct - (Cells(2, 17) + dt · f2)) · (ktol · Cells(2, 12) · theta3 - kktol · (Cells(2, 17) + dt · f2)) / (ktol · Cells(2, 12) · theta3 - kktol · (Cells(2, 17) + dt · f2) + kh2 · Cells(2, 11) $^{0.5}$ · theta3 - kkh2 · (ct - (Cells(2, 17) + dt · f2)))

Cells(2, counter) = Cells(2, counter - 1) + dt / 6 · (fo + 2 · f1 + 2 · f2 + f3)

Cells(2, 16) = (ktol · Cells(2, 12) - kktol · Cells(2, 17)) / ((ktol · Cells(2, 12) - kktol · Cells(2, 17)) + (kh2 · Cells(2, 11) - kkh2 · (ct - Cells(2, 17))))

Cells(2, 18) = Cells(2, 7) / (k · Cells(2, 11) ^{alpha} · Cells(2, 12) ^{beta} · (ct - Cells(2, 17)))

Do

Cells(nf + 2, 5) = x

Cells(n + 2, 4) = n

Cells(n + 2, 5) = (Cells(nf + 2, 5) - xo) / nf · Cells(n + 2, 4)

Cells(n + 2, 7) = ntolo - Cells(n + 2, 5) / 100 · ntolo

Cells(n + 2, 6) = nh2o - 3 · (ntolo - Cells(n + 2, 7))

Cells(n + 2, 8) = nn2o

Cells(n + 2, 9) = nmcho + ntolo - Cells(n + 2, 7)

Cells(n + 2, 10) = Cells(n + 2, 6) + Cells(n + 2, 7) + Cells(n + 2, 8) + Cells(n + 2, 9)

Cells(n + 2, 11) = Cells(n + 2, 6) / Cells(n + 2, 10) · pt

Cells(n + 2, 12) = Cells(n + 2, 7) / Cells(n + 2, 10) · pt

Cells(n + 2, 13) = Cells(n + 2, 8) / Cells(n + 2, 10) · pt

Cells(n + 2, 14) = Cells(n + 2, 9) / Cells(n + 2, 10) · pt

Cells(n + 2, 15) = Cells(n + 2, 11) + Cells(n + 2, 12) + Cells(n + 2, 13) + Cells(n + 2, 14)

Cells(n + 2, 21) = 0

Cells(n + 2, 17) = Cells(n + 2, counter - 1)

thetao = 3 · k · Cells(n + 2, 11) ^{alpha} · (ct - Cells(n + 2, 17)) + kktol · Cells(n + 2, 17) + kkh2 · (ct - Cells(n + 2, 17))

fo = 3 · k · Cells(n + 2, 11) ^{alpha} · (ct - Cells(n + 2, 17)) · (ktol · Cells(n + 2, 12) · thetao - kktol · Cells(n + 2, 17)) / (ktol · Cells(n + 2, 12) · thetao - kktol · Cells(n + 2, 17) + kh2 · Cells(n + 2, 11) $^{0.5}$ · thetao - kkh2 · (ct - Cells(n + 2, 17)))

theta1 = 3 · k · Cells(n + 2, 11) ^{alpha} · (ct - (Cells(n + 2, 17) + dt / 2 · fo)) + kktol · (Cells(n + 2, 17) + dt / 2 · fo) + kkh2 · (ct - (Cells(n + 2, 17) + dt / 2 · fo))

f1 = 3 · k · Cells(n + 2, 11) ^{alpha} · (ct - (Cells(n + 2, 17) + dt / 2 · fo)) · (ktol · Cells(n + 2, 12) · theta1 - kktol · (Cells(n + 2, 17) + dt / 2 · fo)) / (ktol · Cells(n + 2, 12) · theta1 - kktol · (Cells(n + 2, 17) + dt / 2 · fo) + kh2 · Cells(n + 2, 11) $^{0.5}$ · theta1 - kkh2 · (ct - (Cells(n + 2, 17) + dt / 2 · fo)))

theta2 = 3 · k · Cells(n + 2, 11) ^{alpha} · (ct - (Cells(n + 2, 17) + dt / 2 · f1)) + kktol · (Cells(n + 2, 17) + dt / 2 · f1) + kkh2 · (ct - (Cells(n + 2, 17) + dt / 2 · f1))

f2 = 3 · k · Cells(n + 2, 11) ^{alpha} · (ct - (Cells(n + 2, 17) + dt / 2 · f1)) · (ktol · Cells(n + 2, 12) · theta2 - kktol · (Cells(n + 2, 17) + dt / 2 · f1)) / (ktol · Cells(n + 2, 12) · theta2

```
    - kktol · (Cells(n + 2, 17) + dt / 2 · f1) + kh2 · Cells(n + 2, 11) 0.5 · theta2 - kkh2 · (ct -
    (Cells(n + 2, 17) + dt / 2 · f1)))
        theta3 = 3 · k · Cells(n + 2, 11) alpha · (ct - (Cells(n + 2, 17) + dt · f2)) + kktol ·
    (Cells(n + 2, 17) + dt · f2) + kkh2 · (ct - (Cells(n + 2, 17) + dt · f2))
        f3 = 3 · k · Cells(n + 2, 11) alpha · (ct - (Cells(n + 2, 17) + dt · f2)) · (ktol · Cells(n
    + 2, 12) · theta3 - kktol · (Cells(n + 2, 17) + dt · f2)) / (ktol · Cells(n + 2, 12) · theta3
    - kktol · (Cells(n + 2, 17) + dt · f2) + kh2 · Cells(n + 2, 11) 0.5 · theta3 - kkh2 · (ct -
    (Cells(n + 2, 17) + dt · f2)))
        Cells(n + 2, counter) = Cells(n + 2, counter - 1) + dt / 6 · (fo + 2 · f1 + 2 · f2 + f3)
        Cells(n + 2, 16) = ktol · Cells(n + 2, 12) / (ktol · Cells(n + 2, 12) + kh2 · Cells(n +
    2, 11))
        Cells(n + 2, 18) = Cells(2, 7) / (k · Cells(n + 2, 11) alpha · Cells(n + 2, 12) beta · (ct -
    Cells(n + 2, 17)))
      n = n + 1
      Loop Until n = nf
      Cells(n + 2, 4) = nf
      Cells(n + 2, 7) = ntolo - Cells(n + 2, 5) / 100 · ntolo
      Cells(n + 2, 6) = nh2o - 3 · (ntolo - Cells(n + 2, 7))
      Cells(n + 2, 8) = nn2o
      Cells(n + 2, 9) = nmcho + ntolo - Cells(n + 2, 7)
      Cells(n + 2, 10) = Cells(n + 2, 6) + Cells(n + 2, 7) + Cells(n + 2, 8) + Cells(n + 2,
    9)
      Cells(n + 2, 11) = Cells(n + 2, 6) / Cells(n + 2, 10) · pt
      Cells(n + 2, 12) = Cells(n + 2, 7) / Cells(n + 2, 10) · pt
      Cells(n + 2, 13) = Cells(n + 2, 8) / Cells(n + 2, 10) · pt
      Cells(n + 2, 14) = Cells(n + 2, 9) / Cells(n + 2, 10) · pt
      Cells(n + 2, 15) = Cells(n + 2, 11) + Cells(n + 2, 12) + Cells(n + 2, 13) + Cells(n +
    2, 14)
      Cells(n + 2, 21) = 0
      Cells(n + 2, 17) = Cells(n + 2, counter - 1)
        thetao = 3 · k · Cells(n + 2, 11) alpha · (ct - (Cells(n + 2, 17) + dt · f2)) + kktol ·
    Cells(n + 2, 17) + kkh2 · (ct - Cells(n + 2, 17))
        fo = 3 · k · Cells(n + 2, 11) alpha · (ct - (Cells(n + 2, 17) + dt · f2)) · (ktol · Cells(n +
    2, 12) · thetao - kktol · Cells(n + 2, 17)) / (ktol · Cells(n + 2, 12) · thetao - kktol · Cells(n
    + 2, 17) + kh2 · Cells(n + 2, 11) 0.5 · thetao - kkh2 · (ct - Cells(n + 2, 17)))
        theta1 = 3 · k · Cells(n + 2, 11) alpha · (ct - (Cells(n + 2, 17) + dt / 2 · fo)) + kktol ·
    (Cells(n + 2, 17) + dt / 2 · fo) + kkh2 · (ct - (Cells(n + 2, 17) + dt / 2 · fo))
        f1 = 3 · k · Cells(n + 2, 11) alpha · (ct - (Cells(n + 2, 17) + dt / 2 · fo)) · (ktol · Cells(n
    + 2, 12) · theta1 - kktol · (Cells(n + 2, 17) + dt / 2 · fo)) / (ktol · Cells(n + 2, 12) · theta1
    - kktol · (Cells(n + 2, 17) + dt / 2 · fo) + kh2 · Cells(n + 2, 11) 0.5 · theta1 - kkh2 · (ct -
    (Cells(n + 2, 17) + dt / 2 · fo)))
        theta2 = 3 · k · Cells(n + 2, 11) alpha · (ct - (Cells(n + 2, 17) + dt / 2 · f1)) + kktol ·
    (Cells(n + 2, 17) + dt / 2 · f1) + kkh2 · (ct - (Cells(n + 2, 17) + dt / 2 · f1))
        f2 = 3 · k · Cells(n + 2, 11) alpha · (ct - (Cells(n + 2, 17) + dt / 2 · f1)) · (ktol · Cells(n
    + 2, 12) · theta2 - kktol · (Cells(n + 2, 17) + dt / 2 · f1)) / (ktol · Cells(n + 2, 12) · theta2
    - kktol · (Cells(n + 2, 17) + dt / 2 · f1) + kh2 · Cells(n + 2, 11) 0.5 · theta2 - kkh2 · (ct -
    (Cells(n + 2, 17) + dt / 2 · f1)))
```

theta3 = 3 · k · Cells(n + 2, 11) ^{alpha} · (ct - (Cells(n + 2, 17) + dt · f2)) + kktol · (Cells(n + 2, 17) + dt · f2) + kkh2 · (ct - (Cells(n + 2, 17) + dt · f2))

f3 = 3 · k · Cells(n + 2, 11) ^{alpha} · (ct - (Cells(n + 2, 17) + dt · f2)) · (ktol · Cells(n + 2, 12) · theta3 - kktol · (Cells(n + 2, 17) + dt · f2)) / (ktol · Cells(n + 2, 12) · theta3 - kktol · (Cells(n + 2, 17) + dt · f2) + kh2 · Cells(n + 2, 11) $^{0.5}$ · theta3 - kkh2 · (ct - (Cells(n + 2, 17) + dt · f2)))

Cells(n + 2, counter) = Cells(n + 2, counter - 1) + dt / 6 · (fo + 2 · f1 + 2 · f2 + f3)

Cells(n + 2, 16) = ktol · Cells(n + 2, 12) / (ktol · Cells(n + 2, 12) + kh2 · Cells(n + 2, 11))

Cells(n + 2, 18) = Cells(2, 7) / (k · Cells(n + 2, 11) ^{alpha} · Cells(n + 2, 12) ^{beta} · (ct - Cells(n + 2, 17)))

counterodd = 3

countereven = 4

odds = 0

evens = 0

Do

odds = Cells(counterodd, 18) + odds

evens = Cells(countereven, 18) + evens

counterodd = counterodd + 2

counterteven = countereven + 2

Loop Until counterodd >= n

Cells(n + 3, 18) = (Cells(n + 2, 5) - Cells(2, 5)) / (100 · 3 · n) · Cells(2, 18) + Cells(n + 2, 18) + 4 · odds + 2 · evens)

Cells(n + 3, counter) = x

x = x + 1

Loop Until Cells(n + 3, 18) >= 0.002 Or x = 100

t = t + dt

counter = counter + 1

Loop Until t = tf + dt

End Sub

End Sub

F

MASS AND ENERGY BALANCE FOR PROCESS SIMULATION

Stream	Temp.	Press.	Flow	Heat flow	H$_2$	H$_2$O	CO$_2$	acid	Acetone
	°C	kPa	kgmole·h^{-1}/kg·h^{-1}	kJ·h^{-1} ×10^5			mol frac / mass frac		
1	23	101	34.3/716	61.5	0.53/0.05	0.03/0.02	0.44/0.92	0	0
2	40	513	34.3/716	61.6	0.53/0.05	0.03/0.02	0.44/0.92	0	0
3	5	446	34.3/716	62.2	0.53/0.05	0.03/0.02	0.44/0.92	0	0
4	5	446	0.9/16.2	2.57	0	1/0.99	0/0.01	0	0
5	5	446	33.4/700	59.6	0.55/0.05	0.19/0.17	0.45/0.95	0	0
6	-3.5	446	51.7/1117	2.6	0.53/0.05	0	0.46/0.94	0	0
7	116	377	51.7/1117	93.1	0.53/0.05	0	0.46/0.94	0	0
8	300	308	51.7/1117	89.7	0.53/0.05	0	0.46/0.94	0	0
9	300	308	57.3/1458	113	.048/0.04	0	0.42/0.72	0.1/0.23	0
10	300	308	60.2/1458	113	0.46/0.04	0.05/0.04	0.45/0.81	0	0.05/0.12
11	210	239	60.2/1458	115	0.46/0.04	0.05/0.04	0.45/0.81	0	0.05/0.12
12	120	170	60.2/1458	117	0.46/0.04	0.05/0.04	0.45/0.81	0	0.05/0.12
13	40	101	60.2/1458	119	0.46/0.04	0.05/0.04	0.45/0.81	0	0.05/0.12
14	215	513	60.2/1458	59.3	0.46/0.04	0.05/0.04	0.45/0.81	0	0.05/0.12
15	40	517	60.2/1458	120	0.46/0.04	0.05/0.04	0.45/0.81	0	0.05/0.12
16	-20	448	60.2/1458	122	0.46/0.04	0.05/0.04	0.45/0.81	0	0.05/0.12
17	-23	101	5.8/218	16.1	0	0.5/0.24	0.04/0.04	0	0.46/0.71
18	25	101	0.5/14.4	0			Air - N$_2$ = 0.79, O$_2$ = 0.21		
19	-24	101	5.6/209	15.4	0	0.52/25	0/0.6	0	0.47/0.73
20	-24	101	0.69/22.9	0.73	0	N$_2$ = 0.48	0.34/0.26	O$_2$ = 0.15	0.03/0.02
21	-20	448	54/1240	106	0.51/0.04	0	0.49/0.94	0	0.01/0.01
22	-20	448	36/824	70.5	0.51/0.04	0	0.49/0.94	0	0.01/0.01
23	-20	448	18.3/417	35.6	0.51/0.04	0	0.49/0.94	0	0.01/0.01
24	25	101	5.7/342	26.2	0	0	0	1	0
25	25	446	5.7/342	24	0	0	0	1	0
26	190	377	5.7/342	26.2	0	0	0	1	0
27	300	308	5.7/342	23.4	0	0	0	1	0
28	100	101	2.7/48.5	7.5	0	1	1	0	0
29	15	35	2.9/158	0	0.08/0.03	0	0	Ethanal = 0.02/0.01	0.9/0.96
30	15	35	0.01/2.54	0.145	0	0.02/0.01	0.42/0.36	Ethanal = 0.03/0.03	0.52/0.6

Table F.1: Mass and energy balance at 10% acetic acid entering the reactor

RESUME en français

La production de l'hydrogène à partir de biomasse est actuellement à l'étude mais la méthode de valorisation du biogaz (mélange H_2/CO_2) par réactions catalytiques, autres que la simple combustion, n'a pas encore été retenue. Par conséquent, le principal objectif de ce travail est d'explorer les autres voies. L'effet du CO_2 sur le système catalytique est mal connu et seulement un effet négatif sur la dissociation de l'hydrogène a été mentionné. L'hydrogénation du toluène sur un catalyseur Pt a d'abord été étudiée sans CO_2 pour suivre son comportement et éventuellement sa perte d'activité. En présence de CO_2, l'inactivité complète du catalyseur pour l'hydrogénation du toluène a été mis en évidence. La modification de la surface du catalyseur par le CO_2 est quantifiée par DRIFT et un mécanisme à deux sites a été montré. La réaction de Reverse Water Gas Shift produisant du CO se trouve être la principale cause de la désactivation de la surface de catalyseur avec le CO_2. Donc la compétition d'adsorption entre le CO et des acides carboxyliques a été mise à profit pour favoriser sélectivement la conversion des acides. Pour l'alumine, elle est polluée par des carbonates complexes venant du CO_2. La silice étant aussi connue pour promouvoir la décomposition, ces supports ont été rejetés. L'oxyde de titane a été utilisé pour catalyser une autre gamme de produits. Sur ce catalyseur, le changement de sélectivité entre le RWGS et la conversion de l'acide a été observé. Quant à l'oxyde de fer (catalyseur moins actif), il n'est pas capable de produire du CO à partir du CO_2. La chimie de surface de l'oxyde de fer joue un rôle important sur la sélectivité du produit parmi les cétones et les aldéhydes. Un mécanisme à deux sites peut re utilisé pour l'oxyde de fer, montrant qu'un fonctionnement stable peut être trouvé si la réduction par l'hydrogène est continue. Si l'oxyde de fer est totalement oxydé par le CO_2, produit de réaction, la production des cétones cesse. Énergiquement, le procédé de production d'acétone peut être autosuffisant et l'acétone peut être utilisée comme une molécule de stockage d'énergie. Le procédé va aussi compenser le nouveau procédé de production de phénol qui ne produit pas l'acétone.

TITRE en anglais
BIOGAS VALORIZATION FOR CHEMICAL INDUSTRIES VIA CATALYTIC PROCESS

RESUME en anglais :

Hydrogen potential from biomass is currently being studied but ways of valorization of such biogas (H_2/CO_2 mix) via catalytic reaction, other than simply burning has not yet been considered. Thus the main objective of this work is the exploration of such methods. Effect of CO_2 over catalytic system was not well known and only hydrogen dissociation inhibition is reported. Toluene hydrogenation over Pt catalyst is studied and activity loss transition behavior is observed with no CO_2 where as complete catalyst inactivity for toluene hydrogenation is found in presence of CO_2. Catalyst surface change by CO_2 is quantified by DRIFT analysis and two-site mechanism is found to prevail. Reverse water gas shift reaction producing CO is found to be the main cause behind such catalyst surface response to CO_2. Adsorption competition between CO and carboxylic acids is exploited for selectivity shift in favor of acids conversion. Alumina support is fouled by carbonates complexes with CO_2 while silica is reported to promote decomposition, thus both were rejected and titanium oxide is used instead with a range of products produced. The required selectivity shift between reverse water gas shift and acid conversion is thus observed. Less active iron oxide catalyst further suppresses CO_2 conversion. Iron oxide surface chemistry plays an important role over product selectivity among ketones and aldehydes. Two sites mechanism still prevails over iron and stable continuous operation requires simultaneous iron reduction via hydrogen, if totally oxidized by CO_2–a reaction product, will cease to produce ketones. Energetically the process devised for acetone production is self sufficient and acetone not only act as an energy storage molecule but can also compensate new phenol production process producing no acetone.

DISCIPLINE : CATALYTIC PROCESS ENGINEERING

MOTS-CLES: BIOGAS, TOLUENE HYDROGENATION, PLATINUM, CARBON DIOXIDE, REVERSE WATER GAS SHIFT REACTION, IRON OXIDE, CARBOXYLIC ACID, ACETONE